

Fate Modeling of Xenobiotic Organic Compounds (XOCs) in Wastewater Treatment Plants

by

Rosita Ghalajkhani

A thesis

presented to the University of Waterloo

in fulfillment of the

thesis requirement for the degree of

Master of Applied Science

in

Civil Engineering

Waterloo, Ontario, Canada, 2013

© Rosita Ghalajkhani 2013

I hereby declare that I am the sole author of this thesis. This is a true copy of the thesis, including any required final revisions, as accepted by my examiners.

I understand that my thesis may be made electronically available to the public.

Abstract

Xenobiotic Organic Compounds (XOCs) are present in wastewater and wastewater-impacted environmental systems. Pharmaceuticals and personal care products are a broad and varied category of chemicals that are included among these compounds. Although, these compounds have been detected at low levels in surface water, concerns that these compounds may have an impact on human health and aquatic life, have led to increased interest in how XOCs are removed during wastewater treatment. Recognizing specific mechanisms in recent literature and simulating those mechanisms responsible for the removal of XOCs is the main objective of this study. Conventional models, such as the popular activated sludge models (ASM1, ASM2, etc), do not sufficiently address the removal processes; therefore, a fate model is created to provide a means of predicting and simulating removal mechanisms along with experimental analyses.

GPS-X is a multi-purpose modeling tool for the simulation of municipal and industrial wastewater treatment plants. This software package includes conventional models as built-in libraries, which can be used as bases on which new models can be created. In this thesis, the removal mechanisms of XOCs are recognized and investigated; a new library for GPS-X is also created to include XOCs.

As a first step the uncalibrated fate model, which includes all mechanisms of interest with their process rates and state variables, is developed using in GPS-X software. A modified ASM1 (Mantis model) is used as a basis for developing the fate model. Since only a group of mechanisms is responsible for the removal of each compound the mechanisms are categorized in three different case studies as the next step. Thus, one submodel is associated with each case study. The model developer toolbar in GPS-X software is used to develop the model for these case studies. The first case study involves the removal of antibiotics, such as Sulfamethoxazole. The removal mechanisms used in this case are biodegradation, sorption, and parent compound formation, with co-metabolism and competitive inhibition effects being inserted into the structure of the model. Secondly, the removal of nonylphenol ethoxylates (NPEOs) occurs through abiotic oxidative cleavage, hydrolysis, and biodegradation. The third case study includes removal mechanisms of biodegradation and sorption for neutral and ionized compounds.

In the calibration process, model parameters are tuned such that the model can best simulate the experimental data using optimization methods. A common error criterion is Sum of Squared Errors

(SSE) between the simulated results and the measured data. By minimizing SSE, optimal values of parameters of interest can be estimated. In each case study different data sets were used for the validation process.

To validate the calibrated model, simulated results are compared against experimental data in each case study. The experimental data set used in the validation process is different from that used for calibrating the model, which means the validation process data set was obtained from the different literature. By looking at the validation results, it is concluded that the proposed model successfully simulates removal of XOCs.

Since the operating parameters of wastewater treatment plants, such as Solids Retention Time (SRT) and Hydraulic Retention Time (HRT) are crucial for the fate of XOC's, a sensitivity analysis is carried out to investigate the effect of those parameters. Moreover, the pH effect is studied because it relates to the ionized XOCs. Sensitivity analysis results show that the fate model is more sensitive to model parameters i.e. biodegradation rate constant (kb) than the operational parameters, i.e. SRT and HRT. Furthermore, the responses showed sensitivity to pH, whereby acidic conditions provide a better environment for removing neutral forms and alkaline conditions were suitable for removing ionized forms, according to the ionized compound fate model.

Acknowledgements

I would like to thank my supervisor at the University of Waterloo, Professor Wayne J. Parker, who has provided me with his precious insight and kind support during the course of my MAsc. degree. I am forever grateful for your constant support and kind encouragement which enabled me to take on new challenging tasks.

I would like to express my sincere appreciation to my families and friends for their valuable support and guidance throughout my life.

Dedication

To my family...

Table of Contents

List of Figures	x
List of Tables.....	xiv
Nomenclature	xvi
CHAPTER 1.....	1
INTRODUCTION.....	1
1.1 Background	1
1.2 Objective	2
CHAPTER 2.....	4
LITERATURE BACKGROUND	4
2.1 Objectives of literature review	4
2.2 Removal mechanisms.....	4
2.2.1Physical chemical processes.....	5
2.2.2 Biodegradation	11
2.3 Review and comparison of existing fate models.....	19
2.3.1 Sorption processes in fate models	21
2.3.2 Biodegradation processes in fate models.....	22
2.4 Development of an ASM-based contaminant fate model.....	29
CHAPTER 3.....	30
MODELING IN GPS-X.....	30
3.1 Introduction	30
3.2 Fate model description	30
3.2.1 GPS-X state variable libraries	31

3.2.3 Activated sludge biological models	31
3.2.4 XOC removal mechanisms	32
3.3 Integration of fate model in GPS-X	33
3.3.1 Model developer (MD)	33
3.3.2 Model calibration and validation	35
3.4 Case study descriptions	38
3.4.1 Selection of target compounds	38
3.4.2 Case study 1	41
3.4.5 Case study 2	44
3.4.6 Case study 3	46
CHAPTER 4	50
SIMULATION RESULTS AND DISCUSSION	50
4.1 Introduction	50
4.2 Model calibration and validation	50
4.2.1 Case study 1	50
4.2.2 Case study 2	56
4.2.3 Case study 3	60
4.3 Sensitivity analysis of the fate model	65
4.3.1 Effect of solid retention time	65
4.3.2 Effect of hydraulic retention time	83
4.3.3 Effect of pH-case study 3	96
4.3.4 Chapter summary	99
CHAPTER 5	100
CONCLUSIONS AND RECOMMENDATIONS	100
5.1 Summary	100
5.2 Recommendations	102
Bibliography	103

APPENDICES.....	118
A: Uncalibrated Model.....	119
B: ASM1 model.....	123
C: Mantis model.....	127
D: Case study 1 Matrix.....	129
E: Case study 2 Matrix.....	136
F: Case Study 3 Matrix.....	139
G: Different XOCs including some parameter variables and experimental data.....	142
H: Degradation rate constant K_{bio} observed in batch experiments with activated sludge.....	149
I: The process variables and the compound parameters for case study 1.....	151
J: The process variables and the compound parameters for case study 2.....	156
K: The process variables and the compound parameters for case study 3.....	160
L: Types of Libraries within the GPS-X.....	165

List of Figures

Figure 2.1 Nonylphenol polyethoxylates and their metabolites in aerobic condition

Figure 2.2 Sorption model for batch experiments Taken from [40]

Figure 2.3 Correlation between K_{ow} and k_p in the cases of (a) pH at 6.7 and (b) pH at 5.6. Taken from [41]

Figure 2.4 Representation of the three-compartment model of micropollutants in sludge. Taken from [1]

Figure 2.5 Water/sediment experiment on SMX transformation under denitrifying conditions, chart (a): concentrations of SMX (biotic and sterile control), desamino-SMX and 4-nitro-SMX. Chart (b): concentrations of nitrate and nitrite. Mean values of two batches per time point, error bars represent the respective concentration range of duplicates plus the analytical error, Taken from [77].

Figure 3.1 Schematic modeling process flow chart of this thesis

Figure 3.2 Plant configuration for the removal of SMX

Figure 3.3 Plant configuration for the removal of NPEOs

Figure 3.4: schematic of general model for ionized compound fate model

Figure 3.5 Plant configuration for the removal of Ibuprofen

Figure 4.1 Simulated against the target concentrations in the calibration of case 1 model.

Figure 4.2 Simulated against the target concentrations in the calibration of case 2 model.

Figure 4.3 Results of Case 3 calibration. (a) Bisphenol-A, (b) Ibuprofen

Figure 4.4 (a) Active heterotrophic biomass (x_{bh}), (b) Total suspended solid (TSS) in aeration, HRT=10.8hr

Figure 4.5 (a) Soluble SMX conc. in the effluent (S_{zf}) with respect to kd in constant kb (b) Soluble SMX in effluent (S_{zf}) with respect to kb in constant kd , Influent concentration of $S_{zf}= 210$ ng/l, HRT=10.8hr

Figure 4.6 (a) Particulate SMX conc. in wastage flow (X_{za}) with respect to kd in constant kb (b) Particulate SMX conc. in wastage flow (X_{za}) with respect to kb in constant kd , Influent concentration of $X_{za}=0$, HRT=10.8hr

Figure 4.7 (a) S_{zg} conc. (b) and biodegradation rate for S_{zg} , Influent concentration of $S_{zg}= 467$ ng/l, HRT=10.8hr

Figure 4.8 (a) Biodegradation rate for SMX with respect to kd in constant kb and (b) Biodegradation rate for SMX with respect to kb in constant kd , HRT=10.8hr

Figure 4.9 (a) Net sorption rate for SMX with respect to kd in constant kb and (b) Net sorption rate for SMX with respect to kb in constant kd versus SRT, HRT=10.8hr

Figure 4.10 (a) Filtered COD (soluble COD), (b) Active heterotrophic biomass (x_{bh}), (c) Total suspended solid (TSS) in aeration

Figure 4.11 (a) $CNPEO$ (S_{za}) (NPEO in the bulk liquid $CNPEO$), (b) $SS,NPEO$ (S_{zb}) (readily biodegradable substrate portion of NPEO), (c) $SH,NPEO$ (S_{zc}) (slowly biodegradable portion of NPEO) and (d) Biodegradation of NPEO with respect to different kb

Figure 4.12 (a) Active heterotrophic biomass (x_{bh}), (b) Total suspended solid (TSS) in aeration, HRT=12hr

Figure 4.13 (a) Soluble Ibuprofen (neutral form) in effluent (S_{zh}) with respect to kd in constant kb , (b) Soluble Ibuprofen (neutral form) in effluent (S_{zh}) with respect to kb in constant kd , (c) Soluble Ibuprofen (ionized form) in effluent (S_{zi}) with respect to kd in constant kb , and (d) Soluble Ibuprofen (ionized form) in effluent (S_{zi}) with respect to kb in constant kd , Influent conc. of $S_{zh}= 24000$ ng/l, $S_{zi}= 4.3673E6$ ng/l, HRT=12hr

Figure 4.14 (a) Particulate Ibuprofen (neutral form) in effluent (X_{zb}) with respect to kd in constant kb , (b) Particulate Ibuprofen (neutral form) in effluent (X_{zb}) with respect to kb in constant kd , (c) Particulate Ibuprofen (ionized form) in effluent (X_{zc}) with respect to kd in constant kb , and (d) Particulate Ibuprofen (ionized form) in effluent (X_{zc}) with respect to kb in constant kd , Influent conc. of $X_{zc}=X_{zd}=0$, HRT=12hr

Figure 4.15 (a) Biodegradation rate for Ibuprofen (neutral form) with respect to kd in constant kb , (b) Biodegradation rate for Ibuprofen (neutral form) with respect to kb in constant kd , (c) Biodegradation rate for Ibuprofen (ionized form) with respect to kd in constant kb , and (d) Biodegradation rate for Ibuprofen (ionized form) with respect to kb in constant kd , HRT=12hr

Figure 4.16 (a) Net sorption rate for Ibuprofen (neutral form) with respect to kd in constant kb , (b) Net sorption rate for Ibuprofen (neutral form) with respect to kb in constant kd , (c) Net sorption rate for Ibuprofen (ionized form) with respect to kd in constant kb , and (d) Net sorption rate for Ibuprofen (ionized form) with respect to kb in constant kd , HRT=12hr

Figure 4.17 (a) Active heterotrophic biomass (x_{bh}), (b) Total suspended solid (TSS) in aeration, SRT=16d

Figure 4.18 (a) Soluble SMX in effluent (S_{zf}) with respect to kd in constant kb and (b) Soluble SMX in effluent (S_{zf}) with respect to kb in constant kd , Influent concentration of S_{zf} = 210 ng/l, SRT=16d

Figure 4.19 (a) S_{zg} and (b) Biodegradation rate for S_{zg} , SRT=16d

Figure 4.20 (a) Particulate SMX in wastage flow (X_{za}) with respect to kd in constant kb and Particulate SMX in wastage flow (X_{za}) with respect to kb in constant kd , Influent conc. of X_{za} =0, SRT=16d

Figure 4.21 (a) Biodegradation rate for SMX with respect to kd in constant kb and (b) Biodegradation rate for SMX with respect to kb in constant kd , SRT=16d

Figure 4.22 (a) Net sorption rate for SMX with respect to kd in constant kb and (b) Net sorption rate for SMX with respect to kb in constant kd , SRT=16d

Figure 4.23 (a) Filtered COD (soluble COD), (b) Active heterotrophic biomass (x_{bh}), (c) Total suspended solid (TSS) in aeration, SRT=15d

Figure 4.24 (a) CNPEO (S_{za}) (NPEO in the bulk liquid CNPEO), (b) $SS,NPEO$ (S_{zb}) (readily biodegradable substrate portion of NPEO), (c) $SH,NPEO$ (S_{zc}) (slowly biodegradable portion of NPEO) and (d) Biodegradation rate of NPEO with respect to different kb , Influent conc. of S_{za} = 114mg/l, SRT=15d

Figure 4.25 (a) Active heterotrophic biomass (x_{bh}), (b) Total suspended solid (TSS) in aeration, SRT=15d

Figure 4.26 (a) Soluble Ibuprofen (neutral form) in effluent (S_{zh}) with respect to kd in constant kb , (b) Soluble Ibuprofen (neutral form) in effluent (S_{zh}) with respect to kb in constant kd , (c) Soluble Ibuprofen (ionized form) in effluent (S_{zi}) with respect to kd in constant kb , and (d) Soluble Ibuprofen (ionized form) in effluent (S_{zi}) with respect to kb in constant kd , Influent conc. of S_{zh} = 24000ng/l, S_{zi} = 4.3673E6ng/l, SRT=15d

Figure 4.27 (a) Particulate Ibuprofen (neutral form) in effluent (X_{zb}) with respect to kd in constant kb , (b) Particulate Ibuprofen (neutral form) in effluent (X_{zb}) with respect to kb in constant kd , (c) Particulate Ibuprofen (ionized form) in effluent (X_{zc}) with respect to kd in constant kb , and (d) Particulate Ibuprofen (ionized form) in effluent (X_{zc}) with respect to kb in constant kd , Influent conc. of X_{zb} = X_{zc} =0, SRT=15d

Figure 4.28 (a) Biodegradation rate for Ibuprofen (neutral form) with respect to kd in constant kb , (b) Biodegradation rate for Ibuprofen (neutral form) with respect to kb in constant kd , (c) Biodegradation rate for Ibuprofen (ionized form) with respect to kd in constant kb , and (d) Biodegradation rate for Ibuprofen (ionized form) with respect to kb in constant kd , SRT=15d

Figure 4.29 (a) Net sorption rate for Ibuprofen (neutral form) with respect to kd in constant kb , (b) Net sorption rate for Ibuprofen (neutral form) with respect to kb in constant kd , (c) Net sorption rate for Ibuprofen (ionized form) with respect to kd in constant kb , and (d) Net sorption rate for Ibuprofen (ionized form) with respect to kb in constant kd , SRT=15d

Figure 4.30 (a) Szh , (b) Szi , (c) Xzb , (d) Xzc in effluent flow versus pH, Influent conc. of $Szh=24000\text{ng/l}$, $Szi= 4.3673\text{E}6\text{ng/l}$, $Xzb=Xzc=0$, HRT=12 hr, SRT=15 d

Figure 4.31 (a,b) Biodegradation and (c,d) Net sorption rate versus pH, HRT=12 hr, SRT=15 d

List of Tables

Table 2.1 Solid liquid partitioning coefficient K_d for pharmaceuticals and polycyclic musk fragrances in contact with primary and secondary sludge [10, 23, 27, 29, 40, 44, 58, 87, 90].

Table 2.2 Structures, P_{Ka} and $\log K_{OW}$ values

Table 2.3 Models describing XOC fate in activated sludge processes, with indication of mechanism type and biomass estimation in each fate models

Table 2.4 Stoichiometry and process kinetics for growth on a primary substrate and degradation of a non-volatile Specific Organic Compound (SOC) in a completely mixed reactor [105]

Table 2.5 Stoichiometric matrix of Lindbolm et al. 2009 [25] model

Table 2.6 Stoichiometric matrix of Plosz et al. 2010 [30] model

Table 3.1 Case studies for fate modeling of XOCs

Table 3.2 Target compound chemical properties

Table 3.3 process matrix of SMX and its metabolite

Table 3.4 WWTP Physical and Operational Parameters

Table 3.5 process matrix of NPEO

Table 3.6 WWTP physical and operational parameters

Table 3.7 process matrix of Ibuprofen

Table 3.8 process matrix of Bisphenol-A

Table 3.9 WWTP Physical and Operational Parameters for Case Study 3-Ibuprofen

Table 3.10 WWTP Physical and Operational Parameters for Case Study 3-Bisphenol-A

Table 4.1 Calibration results for case study 1

Table 4.2: Simulation results of case study 1, Considering aerobic and anoxic parent compound transformations

Table 4.3 Characteristics and the plant operating conditions used for validation of SMX removal in wastewater treatment

Table 4.4 Calibration results for case study 2

Table 4.5 Simulation results of case study 2

Table 4.6 Characteristics and the plant operation condition for prediction of NPEO removal in Wastewater Treatment

Table 4.7 Calibration results for case study 3-ionized compound

Table 4.8 Calibration results for case study 3-Neutral compound

Table 4.9 Simulation results of case study 3 (Neutral compound)

Table 4.10 continued: Simulation results of case study 3 (Ionized compound)

Table 4.11 Characteristics and the plant operation condition for prediction of Bisphenol-A removal in Wastewater Treatment

Table 4.12 Characteristics and the plant operation condition for prediction of Ibuprofen removal in Wastewater Treatment

Table 4.13 Quantified effects of kd on percentage of removed, biotransformed and wasted SMX

Table 4.14 Quantified effects of kb on percentage of removed, biotransformed and wasted SMX

Table 4.15 Variation of removed, biotransformed and wasted percentage of SMX at constant kb and kd , $kb=1.529E-3$, $kd=2.914E-4$, versus SRT, HRT=10.8hr

Table 4.16 Variation of removed, biotransformed and wasted percentage of Ibuprofen at constant kb with respect to kd , SRT= 15 days, HRT=12 hr

Table 4.17 Variation of removed, biotransformed and wasted percentage of Ibuprofen at constant kd with respect to kb , SRT= 15 days, HRT=12 hr

Table 4.18 Variation of removed, biotransformed and wasted percentage of Ibuprofe at constant kb and kd , $kb=0.1943$, $kd1=3.24E-4$, $kd2=1.96E-5$, versus SRT, HRT=12

Table L1 Carbon – Nitrogen – Industrial Pollutant Library (CNIPLIB)

Table L2 Nomenclature for the Jacobsen et al. 1996 [105] matrix model

Nomenclature

Q_{air}	air applied per volume of reactor and time	$L_{air}d^{-1}$
Q_{in}	influent flow rate	Ld^{-1}
Q_{out}	effluent flow rate	Ld^{-1}
Q_w	wastage flow rate	Ld^{-1}
V	reactor volume	$L_{reactor}$
SRT	sludge retention time	d
C	total compound concentration	mgL^{-1}
S	soluble concentration of trace compound	mgL^{-1}
K_H	Henry or air water partitioning coefficient	-
θ_h	hydraulic retention time of a plug flow reactor	$1/d$
F_{gas}	compound load stripped into the air	$mgL_{wastewater}^{-1}$
X	concentration sorbed into sludge per unit reactor volume	mgL^{-1}
fCOD	soluble COD in effluent flow	$g\ COD / m^3$
X_{part}	concentration sorbed, per amount of sludge dry matter	$mg \cdot gSS^{-1}$
M_{sp}	compound load withdrawn with the excess sludge, per unit of treated wastewater	mgL^{-1}
M_{in}	influent compound load	mgL^{-1}
SP	sludge production soluble, per unit of treated wastewater	$gSSL^{-1}$

k_p	water–sludge partition coefficient	$LgSS^{-1}$
$\eta_{stripped}$	stripping efficiency	-
R_{strip}	relative amount stripped	-
K_{sor}	rate constant for sorption	$LgSS^{-1}d^{-1}$
K_d	solid-liquid partitioning coefficient	$LgSS^{-1}$
K_{ow}	Octanol-water partitioning coefficient	$LgSSL^{-1}$
r_b	biodegradation rate	mgd^{-1}
μ_m	maximum specific growth rate	1/d
Y	maximum yield coefficient	gCOD/gVss
K_{bio}	pseudo-first order biodegradation constant	$LgSS^{-1}d^{-1}$
T_{ref}	reference temperature	$^{\circ}C$
K_T	temperature coefficient	-
K_1	first-order biodegradation kinetics	1/d
K_{Dec}	parent compound formation reaction rate coefficient	$LgSS^{-1}d^{-1}$
<i>STP</i>	Sludge Treatment Plant	
<i>DCM</i>	dissolved/colloidal matter	
K_{DCM}	equilibrium constant of compound sorption to DCM	Lg_{DCM}^{-1}
K_{part}	equilibrium constant of compound sorption to particles	Lg_{part}^{-1}
μ_{mh} (μ_{mH})	heterotrophic maximum specific growth rate	1/d
μ_{ma} (μ_{mA})	autotrophic maximum specific growth rate	1/d
x_{bh}	active heterotrophic biomass	g COD / m^3
ϵ_{tag}	anoxic growth factor	-

bh	heterotrophic decay rate	1/d
kh	maximum specific hydrolysis rate	1/d
ka	ammonification rate	m ³ /g COD/d
ba	autotrophic decay rate	1/d
xba	active autotrophic biomass	g COD / m ³
fp	Fraction of decay biomass that produces (forms) endogenous residue	
i _{XB} (ibhn)	N content of active biomass	g N / g COD
i _{XP} (iuhn)	N content of endogenous/inert mass	g N / g COD
η _g	Fraction of heterotrophs capable of using nitrate as EA (electron acceptor)	-
η _h (etah)	anoxic hydrolysis factor	-
ka	ammonification rate	m ³ /g COD/d
fuh	heterotrophic endogenous fraction	gCOD/gCOD
fua	autotrophic endogenous fraction	gCOD/gCOD
yh	heterotrophic yield	gCOD/gCOD
ya	autotrophic yield	gCOD/gCOD
xu	unbiodegradable particulate matter from cell decay	g COD / m ³
xs	slowly biodegradable substrate	g COD / m ³
xi	particulate inert organic material	g COD / m ³
xnd	particulate biodegradable organic nitrogen	g N / m ³
ss	readily biodegradable substrate	g COD / m ³
snh	free and ionized ammonia	g N / m ³
snd	soluble biodegradable organic nitrogen	g N / m ³

sno	nitrate and nitrite nitrogen	$\text{g N} / \text{m}^3$
si	soluble inert organic material	$\text{g COD} / \text{m}^3$
so	dissolved oxygen	$\text{g O}_2 / \text{m}^3$
snn	dissolved dinitrogen	$\text{g N} / \text{m}^3$
salk	alkalinity	mole / m^3
xii	inert inorganic suspended solids	g / m^3
X_{SS}	suspended solids concentration in raw wastewater or production of suspended solids in primary and/or	gss / m^3
TSS in AR	total suspended solid (TSS) production in aeration	gss / m^3
TSS	TSS in wastage flow	gss / m^3
Sz_{a_i}	Influent NPEO's in bulk liquid concentration	g / m^3
$Sz_{a(C_{\text{NPEO}})}$	NPEO concentration in bulk liquid	g / m^3
$Sz_b(S_{\text{S,NPEO}})$	readily biodegradable substrate of NPEO	g / m^3
$Sz_c(S_{\text{H,NPEO}})$	slowly biodegradable portion of NPEO	g / m^3
$Sz_d(S_{\text{I,NPEO}})$	non biodegradable portion of NPEO	g / m^3
$Sz_f(C_{\text{LI}})$	concentration of soluble substrate in effluent	g / m^3
Sz_{f_i}	Influent soluble concentration	g / m^3
$Sz_g(C_{\text{CI}})$	concentration of substrates biotransformed via the parent compound	g / m^3
Sz_h	neutral soluble concentration form of ionized compound (HA)	g / m^3
Sz_{h_i}	Influent soluble concentration of neutral form of ionized compound (Ibuprofen)	g / m^3
Sz_i	ionized soluble concentration form of ionized compound (Ibuprofen) (A^-)	g / m^3
Sz_{i_i}	Influent soluble concentration of ionized form of ionized compound	
Sz_j	soluble concentration of neutral compound	g / m^3

Sz _j	Influent soluble concentration of neutral compound Bisphenol A	g / m ³
X _{za}	concentration of particulate substrate in wastage flow	g / m ³
X _{zb}	neutral particulate concentration form of ionized compound in wastage flow	g / m ³
X _{zc}	ionized particulate concentration form of ionized compound in wastage flow	g / m ³
X _{zd}	particulate concentration of neutral compound in wastage flow	g / m ³
f _{i,NPEO}	non-biodegradable fraction of NPEO	g COD/g COD
α	readily biodegradable fraction of NPEO produced through adsorption/oxidative cleavage,	g COD/g COD
K _{OCL}	first-order adsorption/oxidative cleavage coefficient	1/d
K _{h,NPEO}	hydrolysis rate coefficient of NPEO	1/d
K _{X,NPEO}	half-saturation coefficient for the hydrolysis of NPEO	g COD/g COD
K _{bio, NPEO}	Biodegradation rate coefficient of NPEO	m ³ /gbiomass/d
k _{oh}	aerobic oxygen half saturation coefficient	g O ₂ / m ³
K _{1BioOx}	SMX aerobic biotransformation rate for C _{LI}	m ³ /gbiomass/d
K _S	half-saturation coefficient for ss	g/m ³
η _{Bio}	correction factor for ss inhibition on S biodegradation	-
η _{1Dec}	correction factor for ss inhibition on s formation	-
K _{1DecOx}	SMX aerobic biotransformation rate coefficient for C _{CJ}	m ³ /gbiomass/d
K _{Des}	rate constant for desorption	1/d
K _{1DOx}	SMX aerobic solid-liquid sorption coefficient	m ³ /gbiomass
K _{1BioAx}	SMX anoxic biotransformation rate for C _{LI}	m ³ /gbiomass/d
K _{1DecAx}	SMX anoxic biotransformation rate coefficient for C _{CJ}	m ³ /gbiomass/d
K _{1DAx}	SMX anoxic solid-liquid sorption coefficient	m ³ /gbiomass

K_{1Des}	desorption rate coefficient for neutral form of ionized compound	1/d
K_{2Des}	desorption rate coefficient for ionized form of ionized compound	1/d
K_{3Des}	desorption rate coefficient for neutral compound	1/d
K_{bio1}	aerobic biotransformation rate for neutral form of ionized compound	$m^3/gbiomass/d$
K_{bio2}	aerobic biotransformation rate for ionized form of ionized compound	$m^3/gbiomass/d$
K_{bio3}	aerobic biotransformation rate for neutral compound	$m^3/gbiomass/d$
K_{D1}	solid-liquid partitioning coefficient for neutral form of ionized compound	$m^3/gbiomass$
K_{D2}	solid-liquid partitioning coefficient for ionized form of ionized compound	$m^3/gbiomass$
K_{D3}	solid-liquid partitioning coefficient for neutral compound	$m^3/gbiomass$

CHAPTER 1

INTRODUCTION

1.1 Background

Municipal wastewater contains a complex mixture of Xenobiotic Organic Compounds (XOCs) originating from personal care products, pharmaceuticals, excreted hormones, household and industrial chemicals, and so on. Press-Kristensen et al., 2007 [31] have estimated that wastewater could contain many types of XOCs.

Wastewater treatment plants (WWTPs) remove XOCs from the water mainly by sorption, biological and/or chemical degradation, volatilization, and/or stripping. Conventional wastewater treatment is not directly designed for removing XOCs but reduces concentration of several key XOCs [156, 157, 158]. However, particular XOCs are frequently reported in WWTP effluents in potentially toxic concentrations [160] that are known to cause toxic effects in different recipients and species. In addition, these chemicals may cause long-term changes in aquatic ecosystems [161]. Feminisation of male fish in different species is a well-known effect observed in recipients loaded with treated wastewater. Experiments with caged fish have confirmed that wastewater containing Endocrine Disrupting Compounds (EDC) have the capability to cause feminization. EDCs originate from several sources, such as natural and pharmaceutical hormones and industrial chemicals. Furthermore, XOCs in freshwater have been observed and may constitute a risk on human health and aquatic life [67].

Improved wastewater treatment may be an efficient way to reduce XOCs pollution. Several studies have identified the biodegradation of XOCs as a vital elimination process in WWTPs [156, 159]. However, our ability to utilize and control the parameters and processes governing the biodegradation of XOCs in activated sludge systems remains a challenge. Therefore, models developed and calibrated from the experiments with carefully selected model pollutants should be constructed to support scientists to reveal and realize optimal treatment levels.

1.2 Objective

The objective of this thesis is to develop and critically evaluate an enhanced fate model for **XOCs** in wastewater treatment plants. Major mechanisms that are responsible for the removal of XOCs in wastewater treatment were identified and integrated with an ASM1 model to create an uncalibrated fate model. Activated sludge models (ASM) can differentiate between viable and non-viable biomass, so it was expected that ASM-based integrated fate models should be able to provide more accurate predictions of XOC fate over a range of operating conditions. Hence the development of an integrated fate and ASM model was employed in this research to have an improved estimate of the viable biomass.

The fate modeling will address the following categories of fate mechanisms:

- 1- Physical chemical processes
 - Abiotic cleavage process
 - Abiotic hydrolysis
 - Stripping and volatilization
 - Sorption-desorption of neutral and ionized compound process
- 2- Biodegradation
 - Biotic hydrolysis
 - Aerobic and anoxic biotransformation
 - Aerobic and anoxic parent compound formation
 - Co-metabolism
 - Competitive inhibition

These mechanisms will initially be incorporated into the GPS-X process simulator to create the uncalibrated fate model of this thesis. Since only a group of mechanisms is responsible for the removal of each compound the mechanisms are categorized in three different case studies as the next step. Each case study will be calibrated and validated individually using corresponding data from the literature.

The combined enhanced model will be critically evaluated by conducting a sensitivity analysis that will evaluate the impact of operational and modeling parameters, such as Solid Retention Time (SRT), biodegradation and partitioning coefficients, and pH on contaminant fate.

CHAPTER 2

LITERATURE BACKGROUND

2.1 Objectives of literature review

Most households regularly use products containing trace organic compounds (TOrcs), including suspected endocrine disrupting compounds (EDCs), pharmaceutically active compounds (PhACs), personal care products (PCPs), and household chemicals (HHCs) that ultimately end up in municipal wastewater treatment systems. These anthropogenic TOrcs are of concern due to the increasing number of reports of reproductive disorders in aquatic wildlife residing below wastewater outfalls. The objective of the literature review for this thesis is to initially identify the major mechanisms that are responsible for the removal of Xenobiotic Organic Compounds (XOCs) in wastewater treatment to support the creation of a model that can describe the fate of these compounds in wastewater treatment systems. The other aim of this review is to gather experimental data sets on the removal of XOCs that can be used to calibrate and validate the various models developed. The literature review includes major findings and research gaps related to modeling.

2.2 Removal mechanisms

The objective of this work is to develop a model that can be used to better understand and optimize the removal of Xenobiotic Organic Compounds (XOCs) in combination with removal of traditional pollutants in wastewater treatment plants. Therefore, accurate predictions of the removal of these compounds, requires appropriate recognition of removal mechanisms. XOC removal processes are categorized in two major groups: 1) physical-chemical processes such as sorption and volatilization, and 2) biological degradation. For a number of XOCs, biodegradation is recognized as the dominant removal process, whereas for some others, sorption is the most effective process. For antibiotics, that form a large group of XOCs, biodegradation and sorption are the major processes for removal, while volatilization and hydrolysis are negligible. For most micropollutants, volatilization is not significant since these compounds tend to partition into liquid phase more than into the gas phase [10, 60, 40, 75, 83].

Under these two main categories, the following sub-mechanisms have been identified and will be subsequently described:

1- Physical chemical processes

- Abiotic cleavage process
- Sorption-desorption of neutral and ionized compound process

2- Biodegradation

- Biotic hydrolysis
- Aerobic and anoxic biotransformation
- Aerobic and anoxic parent compound transformation
- Co-metabolism
- Competitive inhibition

2.2.1 Physical chemical processes

Physical chemical processes can occur at any scale, and can be considered as the changes in the conditions of chemical compounds that are not mediated by bacteria [19, 72, 73, 74].

2.2.1.1 Abiotic cleavage process

In this process a complex molecule is cleaved into molecules that may be more available for biodegradation. The rate of this process is typically described by the following equation:

$$r_{AC} = k_{AC} \cdot a \quad (2.1)$$

Where k_{AC} , is the first-order abiotic cleavage coefficient (d^{-1}) and a is the complex molecule concentration (g/m^3) [19, 73, 74].

A class of compounds that are transformed by this mechanism are the Nonylphenol Ethoxylates (NPEOs) [19]. In aerobic systems, the major pathway of biodegradation for NPEO has been shown to be the stepwise oxidation and cleavage of the polyoxyethylene chain either by hydrolysis or an oxidative hydrolytic mechanism before biodegradation of this compound. In aerobic conditions, the oxidative cleavage process converts the NPEOs to nonylphenoxy acetic acid (NPE1C), and to nonylphenoxyethoxy acetic acid (NPE2C) [78, 79, 80, 81]. The structures of the NPEOs and their metabolites are shown in Figure 2.1.

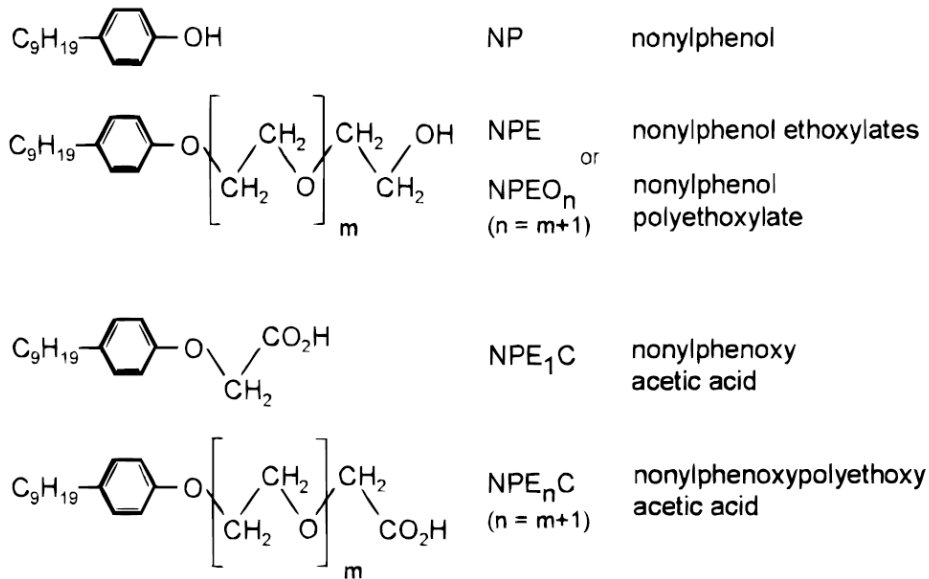


Figure 2.1 Nonylphenol polyethoxylates and their metabolites in aerobic condition.

2.2.1.2 Sorption-desorption of neutral and ionized compound process

Sorption is one of the major mechanisms of XOC removal within activated sludge processes. The sorption process can be considered as the net result of two reactions, sorption from the liquid to the solid phase and desorption from the solid to the liquid phases. In a number of studies [25, 30, 40], the model employed for sorption of XOCs is described in Figure 2.2:

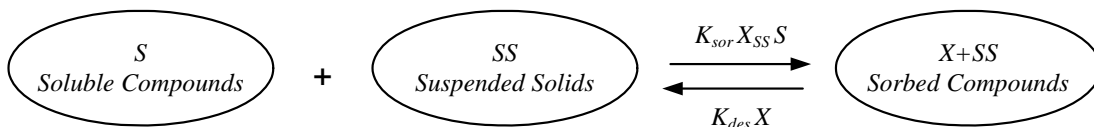


Figure 2.2 Sorption model for batch experiments Taken from [40]

Assuming sorption from the liquid phase to the particulate matter and desorption from the particulate matter are independent, a dynamic model of sorption can be stated as per equations 2.2-2.3: (parameters are also defined in nomenclature.)

$$\frac{dS}{dt} = -K_{sor} \cdot X_{SS} \cdot S + K_{des} \cdot X \quad (2.2)$$

$$\frac{dX}{dt} = K_{sor} \cdot X_{SS} \cdot S - K_{des} \cdot X \quad (2.3)$$

K_{sor} : rate constant for sorption, $LgSS^{-1}d^{-1}$

X_{SS} : suspended solids concentration in raw wastewater or production of suspended solids in primary and/or secondary treatment per L of wastewater, gss/ m³

K_{Des} : rate constant for desorption, 1/d

S : soluble concentration of trace compound, mgL^{-1}

Sorption equilibrium occurs when the rates of sorption and desorption are equal. An equilibrium sorption coefficient, K_d can be employed to describe the equilibrium partitioning characteristics of a compound. Under equilibrium conditions, the concentration sorbed to sludge is often assumed to be linearly proportional to the concentration in solution [39, 75].

$$K_d = \frac{X_{part}}{S} = \frac{X}{X_{SS} \cdot S} = \frac{K_{sor}}{K_{des}} \quad (2.4)$$

$$C = X + S \quad (2.5)$$

$$C = S \cdot (1 + X_{SS} \cdot K_d) \quad (2.6)$$

The total compound concentration in a sample, C , can be defined as per equation 2.5 and under equilibrium conditions this expression can be written as per equation 2.6. These equations are typically employed for neutral organic compounds.

The pH of the wastewater can play a crucial role in the sorption of weak acids. The Sorption of acidic pharmaceuticals has been reported to increase with decreasing pH [41]. In acidic conditions (i.e pH \ll pKa), the K_d of an ionizing compound has a linear relation with $\log(K_{ow})$; in other words, the sorption tendency of pharmaceuticals can be estimated by their corresponding $\log(K_{ow})$ because the acidic compounds in acidic conditions are electrically neutral solutes. Figure 2.3a shows the relationship between $\log K_{ow}$ and $\log k_p$ for selected compounds. This figure shows a strong correlation for E₂, EE₂, BPA, E1, BZP, PPZ and CBZ, which do not have a hydrophilic carboxyl functional group. Unlike these electrically neutral substances, a linear relationship was not found for acidic pharmaceutical compounds like CA, GFZ, IBP, FEP, KEP, NPX, DCF and IDM. This is because these acidic pharmaceuticals are ionized at neutral pH conditions and hence have little tendency to adsorb in the sludge. Figure 2.3.b shows that the k_p values of the target compounds were

correlated linearly with $\log K_{ow}$ in the acidic pH condition. Comparing Figure 2.3.b with Figure 2.3.a, the k_p of CA, GFZ, IBP, FEP, KEP, NPX, DCF and IDM increased in the acidic condition while the effect of pH on k_p was small for E₂, EE₂, BPA, E1, BZP, PPZ and CBZ, which do not have a hydrophilic carboxyl functional group. These results demonstrate that the acidic pharmaceuticals are electrically neutral solutes in the acidic condition and the increased tendency of adsorption can be predicted by $\log K_{ow}$. So according to Figure 2.3, for removal of acidic pharmaceuticals, acidic condition provides a better environment [41].

For weak organic acids with only one acidic group the compound may be partially dissociated depending upon the pH. The partitioning of the neutral and ionized forms of the compounds to the solids phase will differ and hence the overall partitioning can be described as:

$$D_{ow} = \frac{[HA]_{oc} + [A^-]_{oc}}{[HA]_w + [A^-]_w} \quad (2.7)$$

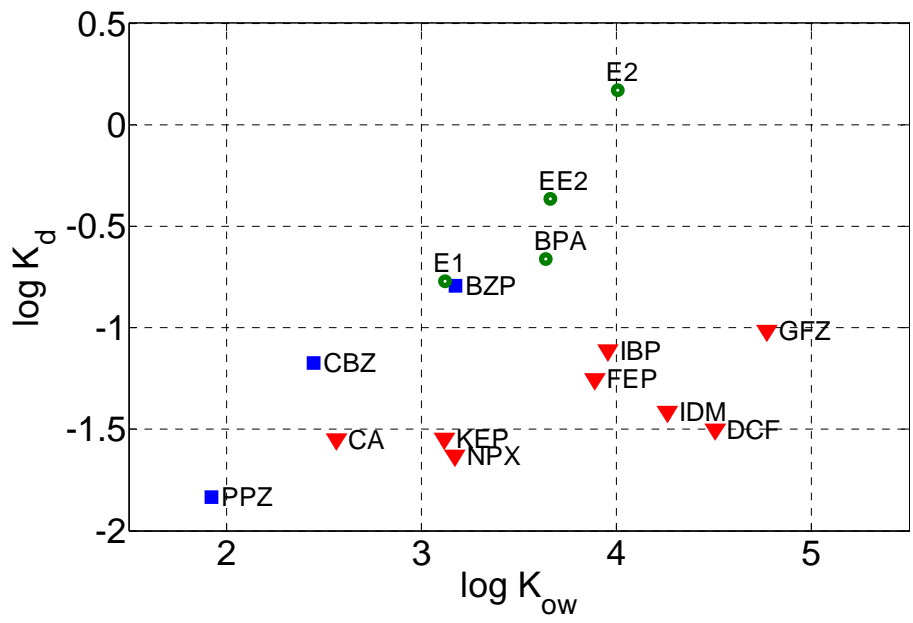
Where oc , represent the concentration in solid phase and w represents the concentration in water phase. For neutral compounds the value of D_{ow} equals K_d .

$$K_a = \frac{[H^+] \times [A^-]}{[HA]_w} \quad (2.8)$$

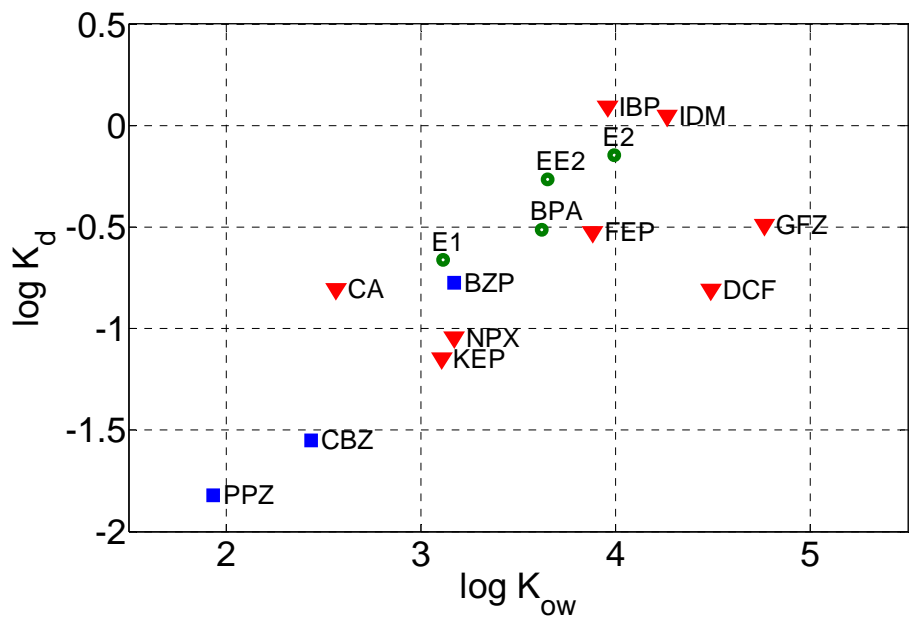
$$\log D_{ow} = \log K_{ow} + \log \frac{1}{1 + 10^{(pk_a - pH)}} \quad (2.9)$$

Equilibrium dissociation of the acid can be described by equation 2.8, and hence for acidic compounds equation 2.9 can be used to derive an expression for $\log D_{ow}$ [45, 46].

The removal by sorption in municipal sewage treatment plants (STP) without biological degradation, for compounds with $K_d \leq 0.3 \text{ LgSS}^{-1}$ has been reported to be minimal [20, 39, 41]. As the K_d of most pharmaceuticals lies in $K_d \leq 0.3 \text{ LgSS}^{-1}$, sorption is typically not considered to be a dominant removal mechanism for them. Values of K_d for musk fragrances are however greater than those of pharmaceuticals and thus sorption mechanism can be a dominant process for the removal of these types of compounds (Table 2.1).



(a)



(b)

Figure 2.3 Correlation between K_{ow} and k_p in the cases of (a) pH at 6.7 and (b) pH at 5.6 [41]

Table 2.1 Solid liquid partitioning coefficient K_d for pharmaceuticals and polycyclic musk fragrances in contact with primary and secondary sludge [10, 23, 27, 29, 40, 44, 58, 87, 90].

Group	Compound	K_d primary sludge [LgSS ⁻¹]	K_d secondary sludge [LgSS ⁻¹]	pKa	
Antibiotics	Azithromycin		0.38±0.09	8.7-9.5	
	Clarithromycin		0.26±0.01	8.9-9.0	
	Ciprofloxacin	2.6±1.6	26±7.3	6.0-8.8	
	Anhydroerythromycin		0.165	8.9	
	Norfloxacin	2.5±1.5	37±13	6.3-8.4	
	Sulfamethoxazole		0.26±0.17	1.8-5.6	
	Drugs	Carbamazepine	≤0.02	0.0012±0.0005	--
Clofibric acid		≤0.03	0.005±0.0025	3.0	
Cyclophosphamide		0.055±0.02	0.0024±0.0005	--	
Diazepam		0.044±0.026	0.02±0.008	3.3	
Diclofenac		0.46±0.03	0.016±0.003	4.2	
Fenoprofen			0.026	4.5	
Gemfibrozil			0.075	4.8	
Ibuprofen		≤0.02	0.007±0.002	4.5-5.2	
Ifosfamide		0.022±0.014	0.0014±0.0004	--	
Indomethacin			0.028	4.5	
Naproxen			0.013 ^[27]	4.2 ^[27]	
Paracetamol			≤0.001	9.5	
Contrast Media		Iopromide	≤0.005	0.011±0.001	9.9
Fragrances		AHTN	4.9±2.1	1.8±0.5	--
	HHCB	5.3±1.9	2.4±1.0	--	
Hormones	17α-Ethinylestradiol	0.28±0.005	0.35±0.04	10.5	

In most sorption models, the sludge is considered to be a two-compartment system in which XOCs are partitioned between liquid and sludge phases. However, in recent models [1], the sludge is described as a three-compartment matrix in which XOCs are present in three states: freely dissolved,

sorbed to particles, and sorbed to dissolved and colloidal matter (DCM), as depicted schematically in Figure 2.4.

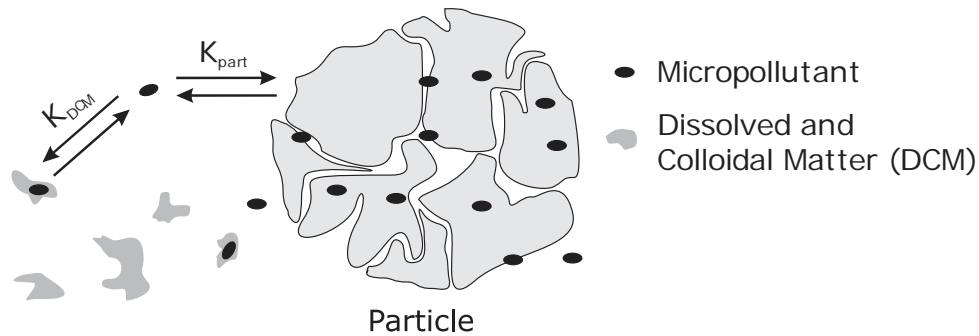


Figure 2.4 Representation of the three-compartment model of micropollutants in sludge [1]

The sorption model depicted in Figure 2.2 can be extended for this condition, with the assumption of equilibrium conditions, and sorption of XOCs to sludge is described by two different equilibrium relationships (equations 2.10-2.11):

$$K_{DCM} : \text{Equilibrium constant of compound sorption to DCM } (Lg_{DCM}^{-1}) = \frac{C_{DCM}}{C_{free}} \quad (2.10)$$

$$K_{part} : \text{Equilibrium constant of compound sorption to particles } (Lg_{part}^{-1}) = \frac{C_{part}}{C_{free}} \quad (2.11)$$

Since the measurement of C_{free} is practically difficult, a new relevant quantity C_{aqu} is defined which is much easier to measure. This variable is obtained by summing the freely dissolved and sorbed to DCM concentrations and afterwards K_{global} has been defined as per equation 2.12 (Barret et al. 2010 [1]):

$$K_{global} = \frac{C_{part}}{C_{aqu}} = \frac{K_{part} \cdot C_{free}}{K_{DCM} \cdot C_{free} \cdot [DCM] + C_{free}} = \frac{K_{part}}{K_{DCM} \cdot [DCM] + 1} \quad (2.12)$$

Overall, the description of XOC sorption in a three-compartment matrix may lead to more accurate results for the fate of these compounds; however studies, such as [1], have shown that the affinity of XOCs for particles is stronger than colloids and thus in most cases it can be excluded from models.

2.2.2 Biodegradation

Biological degradation plays an important role in removal of XOCs in wastewater treatment. Current models available in the literature which describe the biodegradation phenomenon, consist of either

simple structures such as pseudo-first order kinetic (or first order) models, or more complex models in which inhibition kinetics and metabolic models are also included [3, 25, 19, 30].

The pseudo-first order kinetic model is:

$$\frac{dC}{dt} = -K_{bio} \cdot X_{SS} \cdot S \quad (2.13)$$

And the first order kinetic model is:

$$\frac{dC}{dt} = -K'_{bio} \cdot S \quad (2.14)$$

Batch experiments have indicated that in the absence of activated sludge, no removal is observed in the clean water systems [40]. Thus, the removal of XOCs occurs as a result of interactions between the XOCs and the sludge. Therefore, equation 2.13 is typically deemed to be more appropriate for describing biodegradation rates. In some reports it is assumed that the sorption and desorption processes are fast relative to the biodegradation process and equation 2.13 is re-written as equation 2.15:

$$\frac{dS}{dt} = \frac{-K_{bio}}{1 + K_d \cdot X_{SS}} \cdot X_{SS} \cdot S \quad (2.15)$$

In some models such as TOXCHEM⁺, the suspended growth biodegradation process is described by the Monod model [76]:

$$r_b = \frac{\mu_m}{Y} \left(\frac{C}{K_s + C} \right) X \quad (2.16)$$

Rearranging equation 2.16, yields the following equation:

$$r_b = K_{bio}^* \left(\frac{C}{1 + C / K_s} \right) X \quad (2.17)$$

where $K_{bio}^* = \frac{\mu_m}{Y \cdot K_s}$.

In cases where the compound concentration is low relative to K_s , which is the case for XOCs, equation 2.17 is simplified to equation 2.18:

$$\text{if } C \ll K_s \rightarrow r_b = K_{bio} \cdot C \cdot X \quad (2.18)$$

In many models, K_{bio} , is expressed per unit of sludge dry matter, and hence this constant depends not only on the degradability characteristics of compounds but also on the sludge composition [75]. However, it would be expected that the following properties are will influence the biodegradation process:

- biodiversity of the active biomass
- fraction of active biomass within the total suspended solids
- availability of the co-substrate

Sludge retention time (*SRT*) is one of the crucial parameters in the biodegradation process. Increasing the *SRT* has been reported to result in an increase in the biodiversity of the activated sludge [5, 110, 112], as in equation 2.18'. In COD removal plants with $SRT \leq 4d$, the removal of trace compounds has been observed to be reduced whereas for plants with $SRT \geq 10d$, a larger number of compounds are biologically transformed [9, 52, 75].

$$X_m = \left(\frac{SRT}{HRT}\right) \left[\frac{Y(S_0 - S)}{1 + kd \cdot SRT}\right] \quad (2.18')$$

X_m : Viable biomass concentration

Y : Yield coefficient

S_0 : Influent concentration of soluble biodegradable COD

S : Effluent concentration of soluble biodegradable COD

kd ; Decay coefficient

In most fate models, the active biomass is not measurable experimentally; thus, in practice it is assumed to be equal to the Mixed Liquor Suspended Solid (MLSS) or the Mixed Liquor Volatile Suspended Solid MLVSS [30, 83, 84]. Activated sludge models (ASM) [153], however can differentiate between viable and non-viable biomass, so it would be expected that ASM based integrated fate models, should be able to provide more accurate predictions of XOC fate over a range of operating conditions. Hence in this research the development of an integrated fate and ASM model will be employed to have an improved estimate of the viable biomass.

Temperature is a significant factor affecting the rate of biodegradation [24]. In many of the models presented for biodegradation (Schwarzenbach et al. 2005 [32], Lindblom et al. 2009 [25]) temperature effects on biodegradation rate coefficients are based on the Arrhenius equation:

$$K_{bio,T_{ref}} = K_{bio,T} \cdot e^{K_T(T_{ref}-T)} \quad (2.19)$$

where the temperature coefficient K_T lies between 0.03-0.09 [38]. Consequently, considering a seasonal temperature variation of 10 °C for municipal wastewater, the temperature effect on $K_{bio,T}$ would be a multiplier of 2.4 which could be significant when considering the fate of XOCs in wastewater treatment.

The availability of electron acceptors (i.e. the redox potential in the reactor) can also affect the value of K_{bio} . The values of K_{bio} for estrone (E1), 17 α -ethinylstradiol (EE2), ibuprofen, ketoprofen, naproxen and sulfamethoxazole, have been reported to be significantly higher if these compounds were degraded in the presence of oxygen rather than other electron acceptors like nitrate which have lower redox potential (Joss et al. 2004 [15], Zabczynski et al. 2009 [42]). In Appendix F, K_{bio} for several XOCs are presented. In the following subsections various biodegradation processes in different conditions related to different electron acceptors will be discussed.

2.2.2.1 Aerobic and anoxic biotransformation

Depending upon the wastewater treatment plant configuration, biodegradation may occur in either aerobic or anoxic conditions. The differences between these two conditions are the oxygen availability and the bacteria that are responsible for biomass growth. In aerobic conditions, oxygen is available for biodegradation and the bacteria that are responsible for biomass growth are heterotrophs (X_{bh}). In anoxic conditions, oxygen is not available and the bacteria are facultative heterotrophs (X_{bh}) using different electron acceptor like nitrate for growing biomass [19, 30, 42, 71, 75].

2.2.2.2 Biotic hydrolysis

Biotic hydrolysis is mediated by bacteria, and hence can only occur in the presence of biomass. In this process the slowly biodegradable portion of a compound is assumed to be converted to a readily biodegradable substrate. A wide range of conventional compounds and some XOCs can be employed as examples of this transformation. The kinetics of this phenomenon has been described by the following rate expressions [153]:

$$\frac{dX_s}{dt} = -k_h \left[\frac{X_s / X_{BH}}{K_X + (X_s / X_{BH})} \right] \left[\left(\frac{S_O}{K_{O,H} + S_O} \right) + \eta \left(\frac{K_{O,H}}{K_{O,H} + S_O} \right) \left(\frac{S_{NO}}{K_{NO} + S_{NO}} \right) \right] X_{BH} \quad (2.20)$$

$$\frac{dS_s}{dt} = k_h \left[\frac{X_s / X_{BH}}{K_X + (X_s / X_{BH})} \right] \left[\left(\frac{S_O}{K_{O,H} + S_O} \right) + \eta \left(\frac{K_{O,H}}{K_{O,H} + S_O} \right) \left(\frac{S_{NO}}{K_{NO} + S_{NO}} \right) \right] X_{BH} \quad (2.21)$$

In equations 2.20 and 2.21, the slowly biodegradable organic compound, X_s is converted to the readily biodegradable compound S_s [19, 71, 72]. The stoichiometry between reactants and products is 1:1 and the units typically have a COD basis. There are switching functions in the structure of process rate expressions such that the rate is influence by the availability of oxygen and nitrate (aerobic and anoxic).

2.2.2.3 Aerobic and anoxic parent compound transformation

The formation of parent compounds (PCF) from conjugated versions of the compounds has been identified relatively recently and introduced into predictive fate models. In the absence of this phenomenon, fate models have been observed to deviate from experimental data [30]. In these processes the metabolites of pharmaceuticals are transformed back to the parent compound as a result of enzyme-catalyzed reactions [61]. Plosz et al. (2010) [30] proposed equations 2.22-2.23 to describe biodegradation and formation of a selection of antibiotics. Equation 2.22 describes the biodegradation of the parent compounds, equations 2.23 and 2.24 provides the biotransformation of conjugate and parent compound respectively, which means the conjugate form is converted backe to the parent compound.

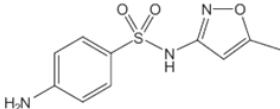
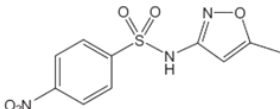
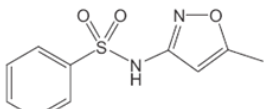
$$\frac{dC_{LI}}{dt} = -K_{bio} \cdot X_{SS} \cdot C_{LI} \quad (2.22)$$

$$\frac{dC_{CJ}}{dt} = -K_{Dec} \cdot X_{SS} \cdot C_{CJ} \quad (2.23)$$

$$\frac{dC_{LI}}{dt} = K_{Dec} \cdot X_{SS} \cdot C_{CJ} \quad (2.24)$$

Evidence for this phenomenon has been provided by Nodler et al., 2012 [77]. The antibiotic sulfamethoxazole (SMX) which is extensively used in both human and veterinary medicine was studied. Since it cannot be completely eliminated by the typical wastewater treatment technology, it is frequently detected in the water cycle. Two transformation products (TPs) of SMX (4-nitro-N-(5-methylisoxazol-3-yl)-benzenesulfonamide (4-nitro-SMX), and N-(5-methylisoxazol-3-yl)-benzenesulfonamide (desamino-SMX)) were identified and these could be produced under denitrifying conditions. The chemical structure and properties of these compounds is shown in Table 2.2 Hence, in this case the parent compound is SMX and the daughter compounds are 4-nitro-SMX and desamino-SMX.

Table 2.2 Structures, pK_a and $\log K_{OW}$ values

Compound (CAS)	Structure	pK_a^a	$\log K_{ow}^a$	Quantifier (CE) ^d	Qualifier (CE) ^d
Sulfamethoxazole, SMX (723-46-6)		5.81 ± 0.5^b 1.4 ± 0.1^c	0.66 ± 0.41	252 → 154 (13.5 V)	252 → 106 (17.5 V)
4-nitro-SMX (29699-89-6)		5.65 ± 0.4	1.27 ± 0.41	282 → 138 (20.5 V)	282 → 186 (13.0 V)
Desamino-SMX (13053-79-7)		6.92 ± 0.5	1.34 ± 0.40	237 → 141 (13.0 V)	237 → 77 (25.5 V)

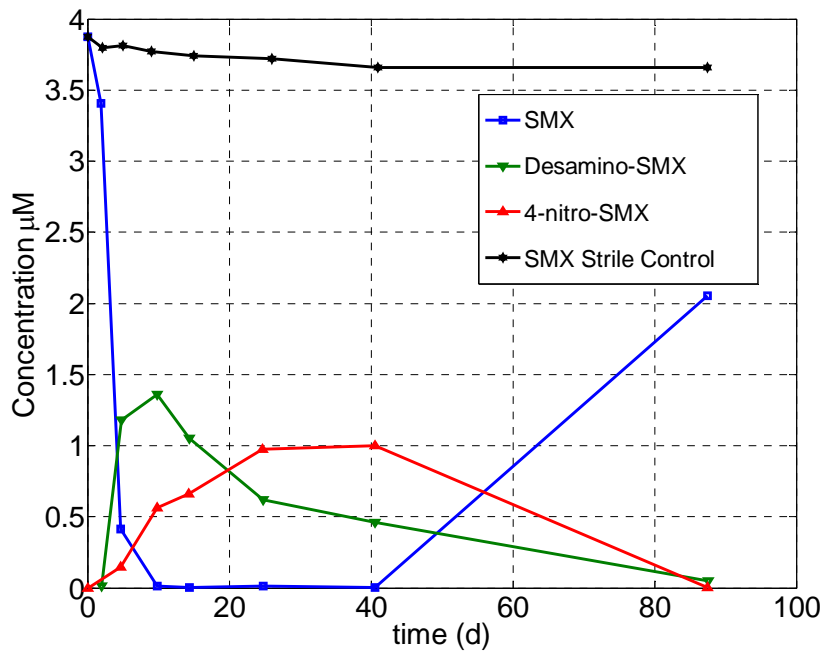
a Scifinder predicted values.

b pK_a of the secondary amine.

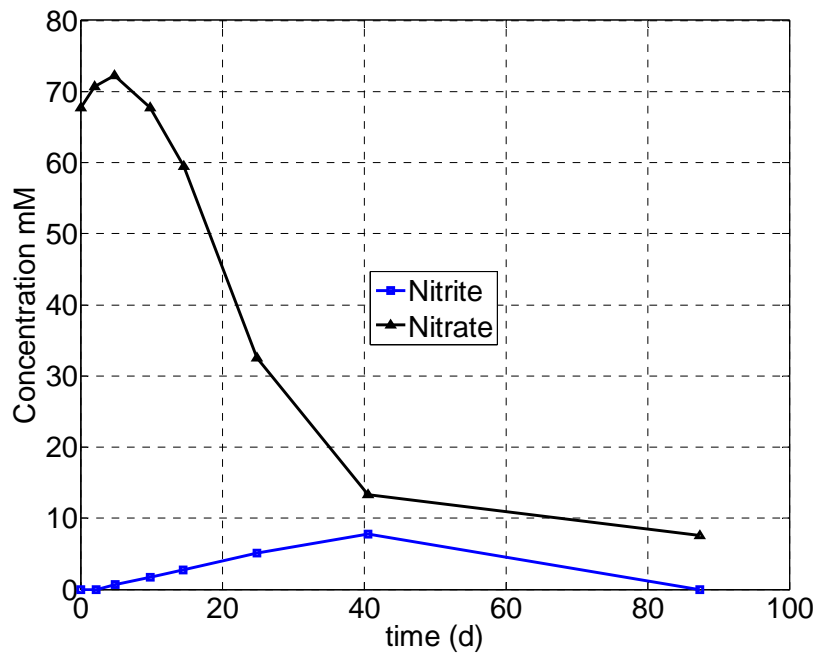
c pK_a of the primary amine (conjugate acid).

d Collision energy.

In a denitrifying degradation experiment SMX was not detected after 10 days whereas increasing concentrations of the two TPs were observed. However, after 87 days the SMX concentration recovered to $53 \pm 16\%$ of the initial concentration after most of the nitrate was consumed. The transformation of 4-nitro-SMX to SMX was confirmed in an anoxic water/sediment test in the absence of nitrate as electron acceptor. Figure 2.5 demonstrates this phenomenon that includes converting of SMX to the two different compounds and then reconverting them to SMX. In wastewater systems it is possible that the conjugates (4-nitro-SMX and desamino-SMX) could enter the wastewater treatment plant in the raw wastewater and then be transformed to form the parent compound in the plant [30].



(a)



(b)

Figure 2.5. Water/sediment experiment on SMX transformation under denitrifying conditions, chart (a): concentrations of SMX (biotic and sterile control), desamino-SMX and 4-nitro-SMX. Chart (b): concentrations of nitrate and nitrite [77].

2.2.2.4 Co-metabolism and competitive inhibition

In some cases the biotransformation of a target compound can be impacted by the presence of other substances. Co-metabolism is defined as the degradation of two compounds simultaneously, in which the degradation of the secondary substrate depends on the presence of the primary substrate [62]. Competitive inhibition is a form of enzyme inhibition where the binding of the inhibitor to the active site on the enzyme prevents the binding of the substrate and vice versa. Therefore, competitive inhibitors bind reversibly to the active site of the enzyme; however, an enzyme may bind either the inhibitor or the substrate but never both at the same time [63, 64].

Both co-metabolism and competitive inhibition have been recently included in predictive fate models [30]. The simultaneous degradation of the co-substrate and the micropollutant is linked to the capacity of the enzymes to degrade many substrates [134]. For example, methanotrophic bacteria are known to co-oxidise PAHs, alkanes and aromatic compounds [85]. When a co-substrate is present, direct biodegradation and cometabolism can occur simultaneously. Alvarez-Cohen and Speitel (2001) [86] and Plosz et al. (2010) [30], described cometabolism of a micropollutant as a competitive inhibition of the direct biodegradation due to the presence of a co-substrate. The integration of cometabolism in models requires that both macropollutants and micropollutant fate be modelled simultaneously. This approach has been validated in recent models [30] and [96] and has been implemented through modification of equations 2.22-2.24 [62, 82, 86, 89, 96]. When the uptake of readily biodegradable growth substrates (S_s) occurs, through cometabolism, the uptake of S_s can affect the transformation of cometabolic substrates, causing competitive inhibition on micropollutant biotransformation processes. By inserting $\frac{K_{S_s} \cdot \eta_{Bio}}{K_{S_s} \cdot \eta_{Bio} + S_s}$ and $\frac{K_{S_s} \cdot \eta_{Dec}}{K_{S_s} \cdot \eta_{Dec} + S_s}$ in equations 2.22 and 2.23 respectively, the modified equations are presented as follows:

$$\frac{dC_{LL}}{dt} = -K_{bio} \cdot \frac{C_{LL}}{1 + \frac{S_s}{K_{S_s} \cdot \eta_{Bio}}} \cdot X_{SS} \quad (2.25)$$

$$\frac{dC_{CJ}}{dt} = -K_{Dec} \cdot \frac{C_{CJ}}{1 + \frac{S_s}{K_{S_s} \cdot \eta_{Dec}}} \cdot X_{SS} \quad (2.26)$$

2.3 Review and comparison of existing fate models

In this section a review of the fate models that have been reported in the literature and an assessment of their ability to describe XOC removal in activated sludge processes are presented. The review identified seven different fate models. Four references were to commercial software including SimpleTreat (Struijs et al., 1991 [135]), WWTreat (Cowan et al., 1993 [95]), TOXCHEM+ (Melcer et al., 1994 [132]; Parker et al., 1994 [122]; Kemp et al., 2002 [153]), and WEST (Cloutier et al., 2008 [130]; Plosz et al., 2010 [30]) (Table 2.3). Among the models, it was deemed important to differentiate between steady-state and dynamic models (Table 2.3). Both model types use the same mass balance equations, but steady-state models only simulate conditions that are constant with time. By design, dynamic models can account for temporal variations of micropollutants concentrations in the WWTP inlet.

As previously discussed, the removal of micropollutants within activated sludge systems can be attributed to two main mechanisms: sorption to the sludge and biological conversion (biodegradation). Each of them can contribute to a change in micropollutant concentration in the dissolved and solid compartments. Sorption consists of a transfer of the micropollutant between the two compartments (dissolved-solid compartments), whereas biodegradation typically implies an elimination of the micropollutant from the dissolved compartment.

In the following sections, the theoretical and modelling tools proposed in the literature to describe these two major removal mechanisms are reviewed.

Table 2.3 Models describing XOC fate in activated sludge processes, with indication of mechanism type and biomass estimation in each fate models

Mechanisms	Struijs et al. (1991)—SimpleTreat [135]	Cowan et al.(1993) — WWTreat [95]	Jacobsen and Arvin (1996) [105]	Kemp et al. (2002)—TOXCHEM+™ [153]	Urase and Kikuta (2005) [41]	Lindblom et al. (2009) [25]	Plosz et al. (2010)—WEST [30]
Aerobic growth of XOC	×	×	×	×	×	×	×
Anoxic growth of XOC							×
Instantaneous Sorption	×	×					
Sorption			×	×	×	×	×
Desorption			×				×
Decay of XOC			×			×	
Parent compound transformation							×
Co-Metabolism							×
Competitive inhibition							×
Abiotic hydrolysis							
Biotic hydrolysis							
Abiotic cleavage process							
Biomass prediction for XOC degradation	MLSS	MLVSS	*	MLVSS	MLSS	*	MLSS
ASM based model			×			×	×
Dynamic			×	×	×	×	×
Static	×	×					

* Active specific biomass for XOC degradation

2.3.1 Sorption processes in fate models

As described in section 2.2, two compartments are usually defined for sorption: the aqueous compartment which is the dissolved phase, and the solid phase of the sludge or mixed liquor (that can be considered as a biosorbent). When an XOC is distributed between these two compartments under non-equilibrium conditions, sorption and desorption can occur simultaneously, as described in equation 2.28.

$$\left(\frac{dS_{XOC}}{dt}\right)_{sorption} = -k_{sor} \times S_{XOC} \times MLSS + k_{des} \times X_{XOC} \quad (2.28)$$

k_{sor} : sorption kinetic constant (l/gss/d)

k_{des} : desorption kinetic constant (1/d)

$MLSS$: liquor suspended solids concentration (mg/L)

In the literature, empirical models with a limited number of parameters have frequently been employed to describe sorption. The common models used to describe sorption isotherms are the Langmuir model, the Freundlich model and the linear model. At low concentrations of micropollutants (e.g., $S_{XOC} < 1 \mu\text{g/L}$), the linear model is typically employed [114].

$$k_d = \frac{k_{sor}}{k_{des}} = \frac{X_{XOC}}{S_{XOC} \times MLSS} \quad (2.29)$$

In the steady state models that were reviewed sorption was assumed to be instantaneous, on the basis of it being more rapid than biodegradation and also because of the extended HRT employed in the activated sludge process (typically 6–24 h) [122]. Moreover, desorption was typically assumed to be significantly slower than sorption. According to Table 2.3, the two model were mentioned which were used instantaneous sorption concept for the sorption model. The first one is a spread sheet box fate model [135] and the second one is the fate model developed by Cowan et al. 1993 [95]. In the dynamic models (5 out of 7), a kinetic parameter (k_{sor}) was integrated to simulate sorption [25, 30, 41, 105, 153]

2.3.2 Biodegradation processes in fate models

In the literature biodegradation modelling commonly includes a biokinetic parameter, the dissolved XOC concentration (the substrate; S_{XOC}), and the concentration of biomass that is able to convert this substrate. Usually, a first order biodegradation reaction is shown as equation 2.30 and a pseudo first order kinetic is written as equation 2.31 [83, 91, 95, 131, 132, 118].

$$\left(\frac{dS_{XOC}}{dt}\right)_{biodegradation} = -k_{bio} \times S_{XOC}(t) \times X_{active} \quad (2.30)$$

$$\left(\frac{dS_{XOC}}{dt}\right)_{biodegradation} = -k'_{bio} \times S_{XOC}(t) \quad (2.31)$$

k_{bio} : biodegradation kinetic constant ($LgSS^{-1}d^{-1}$)

k'_{bio} : biodegradation kinetic constant (d^{-1})

X_{active} : active biomass (mg/L), defined as a fraction of MLSS

In practice, the active biomass is not measurable experimentally; thus, it is often assumed that the MLSS or MLVSS can represent the active biomass ([83, 84]). According to Table 2.3, the fate model presented by [30, 41, 135] inserted the MLSS instead of active biomass in biodegradation rate equations and the fat models by [95 and 153] used the MLVSS in biodegradation rate equation and the rest of them [25 and 105] considered specific active biomass that were responsible for the removal of the XOC. Using this assumption, the influence of the operating conditions and local conditions (for example: oxygen, carbon, nitrogen or phosphorus concentrations) on biodegradation kinetics is not taken into account. Moreover, first order kinetics depends on S_{XOC} at all XOC concentrations, while Monod-type kinetics vary with S_{XOC} concentration only at low concentrations. Equations using Monod-type kinetics with oxygen limitation for instance (equation 2.32), consider XOC biodegradation as a growth process, integrate variables like the dissolved oxygen concentration (SO) and the substrate limitation (S_{XOC}). Hence, they require additional parameters [128, 25, 30].

$$\left(\frac{dS_{XOC}}{dt}\right)_{biodegradation} = \frac{1}{Y_{XOC}} \times \mu_{max,XOC} \times \left(\frac{S_O(t)}{K_{O,XOC}(t) + S_O(t)}\right) \times \left(\frac{S_{XOC}(t)}{K_{XOC}(t) + S_{XOC}(t)}\right) \times X_{active} \quad (2.32)$$

Y_{xoc} : yield coefficient

$\mu_{max,xoc}$: maximum growth rate (1/d)

S_O : oxygen concentration (mg/l)

$K_{O,xoc}$: oxygen half saturation coefficient (mg/l)

K_{XOC} : XOC half saturation coefficient (mg/l)

X_{active} : active biomass (mg/l), defined as a fraction of MLSS

Other than using different structures and biomass estimation for biodegradation rate equations, in developed fate models, different approaches were applied to describe biodegradation process. The reviewed models addressed whether dissolved and sorbed compounds are considered to be subject to biodegradation. Among the 7 models, 2 different concepts have been proposed:

- only dissolved XOC (S_{XOC}) are biodegraded (Govind et al., 1991[13]; Struijs et al., 1991[135]; Melcer et al., 1994 [132]; Monteith et al., 1995[105]; Kemp et al., 2002 [153]; Rittmann et al., 2003 [129]; Lindblom et al., 2009 [25]; Plosz et al., 2010 [30]);
- Dissolved and sorbed micropollutants are biodegraded simultaneously and with separate rates (Cowan et al., 1993 [95]; Lee et al., 1998 [113]; Byrns, 2001[83]).

The direct biodegradation of solid-phase substances is not commonly accepted however, Larson and Yashon (1983) and Shimp and Young (1988) observed biodegradation of a group of cationic surfactants when more than 99% of the compounds were in the sorbed phase. Cowan et al. (1993) [95] also observed that several classes of consumer product chemicals were biodegraded when they were nearly 100% associated with the solids. These observations suggest that direct biodegradation of target compounds in the sorbed phase could be a mechanism contributing to the total biodegradation of the compound [148]. This hypothesis seems most plausible for systems like activated sludge, in which the target compounds are sorbed onto biomass. Thus, adsorption to the solid phase may not decrease the compound's biodegradability when the sorbing surface is the biomass itself.

Although the hypothesis of utilization of a sorbed compound remains to be experimentally verified, modeling analyses indicate that direct sorbed-phase biodegradation can significantly alter the fate of the target compound during activated-sludge treatment if the adsorbed compound is indeed bioavailable [148]. In general, direct biodegradation of sorbed increases the amount of biodegradation

and decreases the amount of target compound leaving in the effluent and/or sludge. Therefore, sorbed-phase degradation is incorporated to the model to account for the loss of sorbed compound through bacterial metabolism.

In the WW-TREAT fate model [95], biodegradation was described using equations 2.33 and 2.34. The biodegradation rate contains two terms. The first term represents the biodegradation of the compound in the solution phase and is assumed to have a degradation rate, k_1 , and a reactor residence time equal to the hydraulic residence time (HRT). The second term represents the biodegradation of the chemical which is associated with the solids and is assumed to have a biodegradation rate, k_2 and a reactor residence time equal to the sludge or solids residence time (SRT). This algorithm differs from other models of the fate of xenobiotic chemicals in activated sludge plants [135] by including biodegradation of the sorbed chemical in addition to biodegradation of the dissolved portion.

$$C_r = C_i / (1 + k_b) \quad (2.33)$$

$$k_b = k_1 HRT [1 - (k_d MLSS / (1 + k_d MLSS))] + k_2 SRT [k_d MLSS / (1 + k_d MLSS)] \quad (2.34)$$

C_r : Concentration of compound in the reactor

C_i : Concentration of compound in the influent

k_b : overall biodegradation rate

k_1 : biodegradation rate for the dissolved compound

k_2 : biodegradation rate for the sorbed compound

Further work is needed to better establish the most appropriate biodegradation kinetic relationship for each XOC. Prior researchers have adapted the biodegradation equations to their needs and hence the hypothesis, formalisms and parameters are different for each model.

2.3.2.1 Parent compound transformation in fate models

Considering the fate of an XOC without its parent compounds and/ or by-products of biodegradation is often a simplification. This assumption could hide important aspects of compounds behaviour; for example a by-product may be more toxic than the studied micropollutant. By-product analysis in wastewater will likely be a point of interest in the forthcoming years. Plosz et al. (2010) [30] proposed the parent compound concept to describe the production of micropollutants in the biological

reactor of an activated sludge system. The Plosz model describes the production of the dissolved form (S_{XOC}) of a compound from several possible chemical conjugate forms for which the studied XOC is a metabolite (e.g., sulfamethoxazole, tetracycline and ciprofloxacin). However, in practice the relationship between parent compounds and metabolites is often unknown for many micropollutants, as biodegradation pathways have not been established. The possibility of the presence of XOC transformations during biological treatment is often detected when removal efficiencies are found to be negative [133].

2.3.2.2 *Cometabolism in fate models*

In some cases micropollutants are not a source of carbon or energy for the biomass and hence a co-substrate (i.e. readily biodegradable COD or ammonium) is required to serve as a growth substrate. The simultaneous degradation of the co-substrate and the XOC is linked to the capacity of the enzymes to degrade many substrates [134]. For example, methanotrophic bacteria are known to co-oxidise PAHs, alkanes and aromatic compounds [85]. When a co-substrate is present, direct biodegradation and cometabolism occur simultaneously. Alvarez-Cohen and Speitel (2001) [86] and Plosz et al. (2010) [30] described cometabolism of a XOC as a competitive inhibition of the direct biodegradation due to the presence of a co-substrate. The integration of cometabolism in models requires concurrent modeling of the co-substrate and XOC fate. This approach to describing biodegradation reactions has been validated in recent models [30] and [96].

2.3.2.3 *ASM-based fate models*

Activated sludge models such as ASM1 (by International Water Association (IWA)) were developed for design and operation of biological wastewater treatment plants and removal of conventional contaminants; however, these models were not designed to predict the fate and transport of XOCs. Recent models introduced for removal of XOCs have been based on the ASM models and modifications have been made to optimize and better describe the removal of XOCs [19, 25, 30, and 105]. Those models were presented in Table 2.3. One of the major modifications in these fate models was that the biomass estimation is integrated in the structure of biodegradation process. The biomass estimation comes from the ASM part of the whole model.

In ASM-based fate model developed by Jacobsen and Arvin 1996 [105] and Lindblom et al. 2009 [25], the modeller consider specific biomass growth rate that were responsible for the biodegradation of XOC. The Peterson matrix of [105] is presented in Table 2.4. The structure of this fate model was based on the ASM1 model except for the sorption model that is kinetic based and is similar to that

presented section 2.4.1.1. For the biodegradation of the specific SOC, the Monod model was employed and for the biomass growth and, specific active biomass that was responsible for the biodegradation of SOC (X1) was included. The biomass growth on conventional compounds was based on ASM1 model calculation. The nomenclature for the Jacobsen et al. 1996 [105] was presented in Appendix L. Lindblom et al. 2009 [25], describes the aerobic growth of specific organisms on XOC and decay of specific organisms, similar to those in ASM1 model with two processes, sorption and desorption of XOC have been added on top of ASM1. Stoichiometric matrix representation of the fate model developed in this reference is shown in Table 2.5 In biodegradation and decay process rate, the specific biomass $X_{B,XOC}$ was expressed.

In another model introduced by Plosz et al. 2010 [30], model matrix is analogous to that in ASM1 except sorption and desorption mechanisms are added to the base model and also some modifications on the biodegradation mechanism are done. The corresponding modified model matrix is presented in Table 2.6. In the structure of this model, some correction was done in biodegradation process rate that are included parent compound transformation, co-metabolism and competitive inhibition. These mechanisms were widely discussed in sections 2.2.2.3 and 2.2.2.4

Table 2.4 Stoichiometry and process kinetics for growth on a primary substrate and degradation of a non-volatile Specific Organic Compound (SOC) in a completely mixed reactor [105]

Process Compound → ↓	X_A	X_I	X_S	$X1$	X_{SI}	SI	S	S_{O_2}/k_{La}	Process rate
Growth, X_A	1						$-1/Y_{XA}$	$1-1/Y_{XA}$	$\mu_{m,X_A} \times X_A \times \frac{S}{k_{S,X_A} + S}$
Hydrolysis, X_S			-1				1		$k_{hyd} \times \frac{X_s}{X_s / X_A + k_x}$
Decay, X_A	-1	f_i	$1-f_i$						$b_{X_A} \times X_A$
Growth, $X1$				1			$-1/Y_{X1}$	$1-1/Y_{X1}$	$\mu_{m,X1} \times X1 \times \frac{S}{k_{S,X1,S} + S}$
Biodegradation, SI						-1			$k_{bio,m,SI} \times X1 \times \frac{SI}{k_{S,X1,S} + SI}$
Decay, $X1$		f_i	$1-f_i$	-1					$b_{X1} \times X1$

Sorption, SI					1	-1			$k_{sor} \times SI \times (X_A + X_I + X_S + XI)$
Desorption, SI					-1	1			$k_{des} \times X_{SI}$
Aeration								1	$k_L a \times (S_{O_2, sat} - S_{O_2, set})$

Table 2.5 Stoichiometric matrix of Lindbolm et al. 2009 [25] model

i Component → j Process ↓	1 S _O	2 S _{XOC}	3 X _{XOC}	4 X _{B,XOC}	Process rate ↓
1 Aerobic growth of specific organisms on XOC	$-\frac{1 - Y_{XOC}}{Y_{XOC}}$	$-\frac{1}{Y_{XOC}}$		1	$\hat{\mu}_{XOC} \cdot \left(\frac{S_O}{K_{O,XOC} + S_O} \right) \cdot \left(\frac{S_{XOC}}{K_{XOC} + S_{XOC}} \right) \cdot X_{B,XOC}$
2 Decay of specific organisms				-1 ^a	$b_{XOC} \cdot X_{B,XOC}$
3 Sorption of XOC		-1	1		$k_{sor} \cdot S_{XOC} \cdot VSS$
4 Desorption of XOC		1	-1		$k_{des} \cdot X_{XOC}$
	Oxygen [g -COD m ⁻³]	Soluble XOC [g COD m ⁻³]	Sorbed XOC [g COD m ⁻³]	Specific XOC degraders [g COD m ⁻³]	Kinetic parameters: $\hat{\mu}_{XOC}$, b_{XOC} , $K_{O,XOC}$, K_{XOC} , k_{sor} , k_{des}
					Stoichiometric parameter: Y_{XOC}
a Decay of specific XOC degraders produces X _S and X _P (in ASM1).					

Table 2.6 Stoichiometric matrix of Plosz et al. 2010 [30] model

component → j process ↓	1 C _{LI}	2 C _{CJ}	3 C _{SL}	process rate
desorption	1		-1	$k_{Des} \cdot C_{SL}$
aerobic processes				
sorption	-1		1	$k_{Des} \cdot K_{D,Ox} \cdot C_{LI} \frac{S_O}{K_O + S_O} X_{SS}$
parent compound formation	1	-1		$k_{Dec,Ox} \cdot C_{CJ} \frac{K_S \cdot \eta_{Dec}}{K_S \cdot \eta_{Dec} + S_S K_O + S_O} X_{SS}$
biodegradation	-1			$k_{Bio,Ox} \cdot C_{LI} \frac{K_S \cdot \eta_{Bio}}{K_S \cdot \eta_{Bio} + S_S K_O + S_O} X_{SS}$
anoxic processes				
sorption	-1		1	$k_{Des} \cdot K_{D,Ax} \cdot C_{LI} \frac{K_O}{K_O + S_O} X_{SS}$
parent compound formation	1	-1		$k_{Dec,Ax} \cdot C_{CJ} \frac{K_S \cdot \eta_{Dec}}{K_S \cdot \eta_{Dec} + S_S K_O + S_O} X_{SS}$
biodegradation	-1			$k_{Bio,Ax} \cdot C_{LI} \frac{K_S \cdot \eta_{Bio}}{K_S \cdot \eta_{Bio} + S_S K_O + S_O} X_{SS}$

2.4 Development of an ASM-based contaminant fate model

The previous section presented a review of existing fate models and the removal mechanisms employed in each of them. Most of the existing models describe the fate of XOC without including more complex mechanisms such as parent compound transformation, co-metabolism, etc. Only a few models have considered biodegradation in aerobic and anoxic conditions [15, 30, 37, 136]. Characterising biodegradation in anoxic conditions will improve accuracy of models in treatment plants that employ denitrification. In addition, isolating the role of heterotrophic biomass from that of autotrophic biomass (nitrifiers) in aerobic modeling would also be beneficial. The sorption mechanism can be complex and still remains not sufficiently documented. For example it is not clear whether it is beneficial to have 3 compartment to reflect the impact of colloids on contaminant fate [1]. In addition sorption is a physicochemical process and consequently, weak acid partitioning may be dependent on pH conditions.

Considering these discrepancies, it is proposed to develop a fate model that will include complex mechanisms such as parent compound transformation, co-metabolism, etc as a general model capable of describing the fate of XOCs. An important aspect in fate modeling is the estimation of biomass that is responsible for the biodegradation of XOCs. In most fate models, the volatile fraction of total biomass has been employed in the biokinetic rate equations. In the model developed in the current study heterotrophic biomass will be separated to describe their role in the fate of XOCs more precisely. The fate model will be integrated with an ASM-based model that is able to describe the removal of conventional compounds and XOCs simultaneously.

CHAPTER 3

MODELING IN GPS-X

3.1 Introduction

Based on the literature review that was conducted for this research, specific removal mechanisms that should be recognized and included in models to obtain accurate predictions of the fate of XOCs were identified. The mechanisms were identified in the literature review as a starting point for model development and application. Operating parameters such as SRT, HRT and pH have major effect on fate of these compounds; therefore, a sensitivity analysis was carried out as part of this research.

GPS-X is a multi-purpose modeling tool that can be employed for the simulation of municipal and industrial wastewater treatment plants. This software package provides conventional models as built-in libraries that can be used as a basis on which new models can be created. A description of the new fate model that is integrated with the ASM model into the GPS-X will be provided. Hence, the new model is an ASM-based model for better prediction of viable biomass that is believed to be responsible for removing trace compounds. This ASM-based model is able to be employed for predicting removal of conventional and trace compounds simultaneously. Selected case studies have been developed and modeled to evaluate specific aspects of the model. These case studies are detailed and discussed in this chapter.

3.2 Fate model description

In this section, the development of the fate model, including removal mechanisms and the selection of representative compounds is explained. The fate model is depicted using a Peterson matrix that includes the rates of the removal processes (mechanisms) in the rows and compound species (the model variables), such as particulate and soluble species in the columns. This section also includes a description of the GPS-X software that was used as the modeling platform in this research. The source of parameter values, including GPS-X, literature review, and calibration process optimal outputs are described. Since the new fate model is integrated with the conventional activated sludge models (ASM) in GPS-X, the description of GPS-X state variable libraries, that consist of conventional and industrial state variables (fate model variables), ASM1 and Mantis Model are explained in the following sections.

3.2.1 GPS-X state variable libraries

A library in GPS-X is a list of wastewater process models using a set of basic wastewater components or state variables. The term state variable refers to the basic variables that are continuously integrated over time. The composite variables are those variables that are calculated from (or composed of) the state variables. The relationships between the state and composite variables are calculated at every connection point of the plant layout. Details of the different types of libraries in the GPS-X software can be found in Appendix L.

In this thesis, the Industrial Pollutant Variables Library (CNIPLIB) was used. This library includes forty-six state variables: sixteen are predefined and thirty are user defined (15 soluble, 15 particulate). In this research, these state variables are used for fate model variables. For example, for Bisphenol-A in the solid phase, is described by Xzd while the soluble species is described by Szj .

3.2.3 Activated sludge biological models

3.2.3.1 ASM1

The International Association on Water Pollution Research and Control (IAWPRC) task group realized that due to the long solids retention times and low growth rates of bacteria, the actual effluent substrate concentrations between different activated sludge treatment plants did not vary greatly. What significantly differed was the levels of MLSS and electron acceptor (oxygen or nitrate). Thus the focus of the Activated Sludge Model No.1 (ASM1) is the prediction of the solids generation and electron acceptor consumption. In this research, this model was employed to predict the viable biomass in the activated sludge process (heterotroph biomass). More details about the ASM1 model within the GPS-X software and ASM1 Petersen matrix can be found in Appendix B. This approach differs from that employed in recent models where either the MLSS or MLVSS were employed to reflect biomass production in the structure of the fate model [30, 41, 75]. It should be noted that, instead of using X_{ss} to describe the biomass concentration (as is traditionally employed in fate modeling) xbh was employed to take advantage of the integration of the fate model with the ASM based model.

3.2.3.2 Mantis

The Mantis model is identical to IAWPRC Activated Sludge No.1 (ASM1), except for the following modifications:

- 1- Two additional growth processes are introduced, one for autotrophic organisms and one for the heterotrophic organisms
- 2- The kinetic parameters are temperature dependant
- 3- Aerobic denitrification is introduced

The additional growth processes account for the observed growth of organisms during conditions of low ammonia and high nitrate. Under these conditions, the organisms can uptake nitrate as a nutrient source. The Petersen Matrix for the Mantis model can be found in Appendix C. In this research, the Mantis model was employed as the basis model for conventional pollutant modeling and the fate model was built upon it.

3.2.4 XOC removal mechanisms

As mentioned in section 2.1, XOC removal mechanisms have been categorized into two major groups with sub-mechanisms that are mentioned below:

- 1- Physical chemical processes
 - Abiotic cleavage process
 - Sorption-desorption of neutral and ionized compound process
- 2- Biodegradation
 - Biotic hydrolysis
 - Aerobic and anoxic biotransformation
 - Aerobic and anoxic parent compound formation
 - Co-metabolism
 - Competitive inhibition

A detailed description of these mechanisms was provided in section 2.2. These mechanisms, with corresponding process rates, were added to the base Mantis model to create an uncalibrated model. Subsequently the kinetic and stoichiometric coefficients were extracted from the literature (see Appendix A). For the process rates of the conventional compounds, the default matrix of Mantis model within the GPS-X software was used.

3.3 Integration of fate model in GPS-X

In this section, the integration of the fate model into GPS-X is explained. The integrated fate model employs an ASM-based (Mantis) model for prediction of viable biomass that is subsequently responsible for removal and transformation of trace compounds. Hence, the model is able to be employed for predicting the removal of conventional and trace compounds simultaneously. The “model developer”, which is a software tool developed by Hydromantis was used to generate the ASM based fate model and is subsequently described.

3.3.1 Model developer (MD)

To create the new model in GPS-X, the model developer that included the Mantis model matrix as the basis and the CNIPLIB library was used. The CNIPLIB was selected as it has the capacity to employ a number of pre-defined states for industrial customized components that in this research consisted of the target XOC's (See Appendix L). The model developer contains several spread sheets with the first spread sheet containing the fate model matrix. The second sheet includes the composite variables vector for GPS-X. The third sheet contains the fate model parameters and coefficients, such as state variables, composite variables, and the stoichiometric and kinetic parameters, for both the conventional and the trace compounds. The last sheet contains the list of the GPS-X library state variables. The model developer converts the matrix components to a language that can be read by the GPS-X software.

Since specific groups of mechanisms were identified to be responsible for the removal of selected compounds, three different case studies were created for three different groups of compounds. Hence, three different submodels were created within the fate model. Each submodel was generated in the GPS-X software separately. To achieve this goal, compounds that were not included in a specific submodel, were omitted by inserting zero values in the corresponding rows and columns. For example for Case Study 1 that was created for removal of SMX process rates and compounds that were not related to SMX fate were zeroed (See Appendix D for more details). The three different submodels were calibrated separately using relevant literature data for both the conventional and trace compounds, and the optimal parameters were obtained and inserted in the corresponding sheet of the model developer (third sheet). After this step, each submodel was generated in the GPS-X software by using the model developer tool, and the simulation results were reported. Figure 3.1 depicts the work flow for the modeling process.

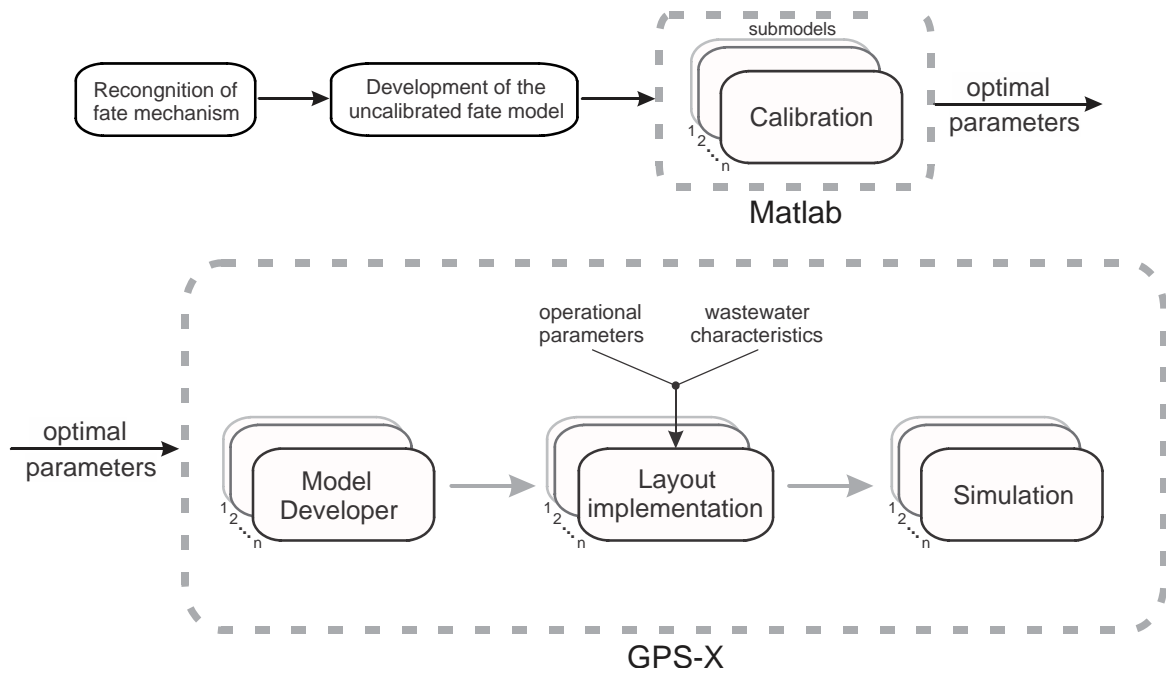


Figure 3.1. Schematic modeling process flow chart of this thesis

3.3.2 Model calibration and validation

3.3.2.1 Calibration

Models that are employed to simulate XOC fate in WWTP systems include a number of kinetic and stoichiometric parameters. Without accurate values for these parameters, the equations in the model merely describe a general shape or pattern of the real behaviour of the system. In the calibration process, using optimization methods, model parameters can be ‘tuned’ such that the model can best follow the experimental data. A common error metric is Sum of Squared Errors (SSE) between the simulated results and measured data, optimal values of parameters of interest were found. Equation 3.1 shows the objective function for the calibration:

$$SSE = \sum_{i=1}^n SSE_i \quad \text{with} \quad SSE_i = \left(\frac{y_i^{sim} - y_i^{exp}}{y_i^{exp}} \right)^2 \quad (3.1)$$

where y_i^{sim} and y_i^{exp} are the simulated and measured values of the response variable y (usually effluent substrate concentration), respectively. Index i refers to the i^{th} data point where the total number of data points is n in the experimental process.

Although using optimized parameter values, the model can best describe the system behaviour, in some cases, these parameter values are infeasible [25]. Hence in the optimization problem, lower and upper bounds were added to the model parameters to avoid infeasible values for parameters.

Therefore, the calibration process formulation was written as:

$$\begin{aligned} \min \quad & SSE(t, P) \\ & LB_j \leq P_j \leq UB_j \end{aligned} \quad (3.2)$$

where SSE is a function of time and vector of parameters P , LB and UB are the lower bounds and upper bounds on the parameter, and index j refers to the j^{th} parameter.

In this research, minimum and maximum values that were obtained from the literature were adopted as LB and UB . In Appendix G, a list of references from which the ranges of parameter values were obtained are presented. The details of the procedure and convergence study on the optimal design parameters are subsequently described. For each calibration, parameters were obtained by solving the optimization problem using the Genetic Algorithm (GA) in MATLAB. To assure the optimality of the parameter values, GA was run for three times, and then the parameters corresponding to the least objective function were put into the Pattern Search function as a Direct Search (DS) routine until the

change in the objective function and constraint violation values were less than 1E-6. At this point the resulting values were accepted to provide the global optimum.

The uncertainties involved in the calibration process are computed by means of a numerical method explained in Draper and Smith, 1981 [154]; Smith et al., 1998 [155]. In a general case, the objective function J can be multi-objective, and defined as:

$$J = \sum_{i=1}^n J_i \text{ with } J_i = \mu_1 \left(\frac{y_{i1}^{sim} - y_{i1}^{exp}}{y_{i1}^{exp}} \right)^2 + \mu_2 \left(\frac{y_{i2}^{sim} - y_{i2}^{exp}}{y_{i2}^{exp}} \right)^2 + \dots \quad (3.3)$$

where μ_1, μ_2, \dots are the weights of different terms in the objective function and y_{i1}, y_{i2}, \dots are i^{th} values of the multiple responses. Assuming a linear behaviour for the response, this approach approximates the mean square error for each parameter from the sensitivity of the objective function to each parameter and a variance defined as follows:

$$\sigma^2 = \frac{\hat{J}}{n - p} \quad (3.4)$$

where \hat{J} is the objective function value at the optimal point, n is the number of observations, and p is the number of calibration parameters.

Additionally, the sensitivity can be approximated in discrete form as follows:

$$\frac{\partial J_i}{\partial P_j} \approx \frac{J_i(\hat{P}_j + \Delta P_j) - J_i(\hat{P}_j)}{\Delta P_j} \quad (3.5)$$

where \hat{P}_j is the optimal estimate of parameter P , index i refers to the i^{th} data point, index j refers to the j^{th} parameter, $\hat{P}_j + \Delta P_j$ is the perturbed parameter, $J_i(\hat{P}_j + \Delta P_j)$ is the objective function at the perturbed parameter value, and $J_i(\hat{P}_j)$ is the objective function value at the optimal parameter estimate. Note that J_i is equal to the SSE_i in case the objective function is single objective, as defined in equation 3.1. Then the sensitivity matrix can be formed as follows:

$$S = \begin{bmatrix} S_{11} & S_{12} & \cdots & S_{1p} \\ S_{21} & S_{22} & \cdots & S_{2p} \\ \vdots & \vdots & S_{MN} & \vdots \\ S_{p1} & S_{p2} & \cdots & S_{pp} \end{bmatrix} \quad (3.6)$$

The sensitivity matrix is a symmetric square matrix ($p \times p$) that includes the sensitivity of the objective function with respect to all calibration parameters. Each component is defined as:

$$S_{MN} = \sum_{i=1}^n \frac{\partial J_i}{\partial P_M} \frac{\partial J_i}{\partial P_N} \quad \text{with } M, N \in \{1, 2, \dots, p\} \quad (3.7)$$

Then the 95% confidence interval for each parameter is acquired as:

$$\hat{P}_j \pm 1.96 \sqrt{V_{jj}} \quad \text{with } V = \sigma^2 S^{-1} \quad (3.8)$$

where equation 3.8 calculates the interval for the j^{th} estimated parameter with 95% confidence.

The described calibration process was employed to initially calibrate the fate model for the trace compounds; however, calibration of the conventional parameters was also deemed to be important. The viable biomass production that is predicted by the conventional part of the model also required calibration. Therefore, the wastewater characteristics, such as the ratio of inert particulate COD to biodegradable COD and influent VSS were established from the literature data. However in some cases this data was not available and hence the default values for municipal wastewater characteristics were chosen within the typical range. In addition steady state mixed liquor suspended solid production in the bioreactor (MLSS) and operational parameters including SRT and HRT, were determined from the literature data. The plant layout for the plant under study was built for the calibration process along with operational parameters. The MLSS production in steady state condition in the calibrated model was tuned with the MLSS production of that plant in steady state condition by trial and error within the GPS-X software. The results of the calibration process for each case study are explained in chapter 4.

3.3.2.2 Validation

Once the model was calibrated, it was able to describe the experimental data used in the calibration process; however its ability to predict results under other conditions was not verified. Therefore the model was validated using different data sets. The validation process assures more reliability of the model under desired conditions. In this thesis, for each case study, different data sets were used for the validation. In the validation procedure, the plant operating condition was matched to the case used for the validation, but parameters that obtained from the calibration process were not changed. As will be subsequently discussed in some cases, the calibrated model could not describe that additional data set well. Potential causes of the poor validation will be discussed in chapter 4.

3.4 Case study descriptions

Since only selected mechanisms are responsible for the removal of a specific compound, three different case studies (three sub models) were developed in this study. Each case study addressed a specific group of compounds. The case studies are described in Table 3.1.

Table 3.1 Case studies for fate modeling of XOCs

	Compound	Mechanism
Case study 1	Sulfamethoxazole (SMX)	<ol style="list-style-type: none"> 1. Aerobic and anoxic biodegradation 2. Parent compound formation 3. Co-metabolism and competitive inhibition 4. Aerobic and anoxic sorption
Case study 2	Nonylphenol ethoxylates (NPEOs)	<ol style="list-style-type: none"> 1. Abiotic oxidative cleavage 2. Biotic hydrolysis 3. Aerobic biodegradation
Case study 3	Ibuprofen and Bisphenol-A	<ol style="list-style-type: none"> 1. Aerobic biodegradation of ionized and neutral compounds 2. Sorption of ionized and neutral compounds

3.4.1 Selection of target compounds

In this study, the selection of compounds was motivated by the following criteria: (1) the presence of the compounds in Canadian municipal wastewater effluent at relatively high concentrations; (2) high usage of the selected pharmaceuticals by the Canadian population; (3) and most importantly, they are impacted by specific removal mechanisms which were recognized recently in the literature. The considered XOCs were: ibuprofen, sulfamethoxazole, Nonylphenol ethoxylates, and Bisphenol-A. Table 3.2 displays a list of the selected compounds and some of their general properties, including therapeutic classes, molecular weights, octanol-water and sludge-water partitioning coefficients, and pKa (acid dissociation constant). Further details on the chemical and physical properties of the compounds are provided in the following sections.

Table 3.2 Target compound chemical properties

Compound	Therapeutic Class	Molar Mass (g/mol)	Log K _{ow}	Kd (l/gss)	Pka
Sulfamethoxazole (Case study 1)	Antibiotic	253.279 (C ₁₀ H ₁₁ N ₃ O ₃ S)	0.89	0.26±0.17 ^[40]	5.7
Nonylphenol (NPEO) (Case study 2)	Nonionic detergent metabolite	220.35 (C ₁₅ H ₂₄ O)	4.48	15 ^[152]	10.7
Bisphenol-A (Case study 3)		228.29 (CH ₃) ₂ C(C ₆ H ₄ OH) ₂	3.05	0.071-1 ^[25]	9.78
Ibuprofen (Case study 3)	Anti-inflammatory	206.28 (C ₁₃ H ₁₈ O ₂)	3.5	0.007±0.002 ^[40, 45]	4.74

3.4.1.1 Sulfamethoxazole (SMX)

Sulfamethoxazole (SMX) is an antibiotic that is used for the treatment of infectious diseases in humans. A wide range of removal efficiencies, even negative in some cases have been reported for this compound in WWTP and this has been attributed to the potential presence of conjugated metabolites of SMX [151]. Biodegradation and sorption are the two main processes for removal of this compound, although some specific mechanisms, such as co-metabolism and parent compound transformation, and competitive inhibition, have been reported to affect the removal of this substance [30, 37]. The value of the solid/liquid partition coefficient (K_d) for SMX in the literature has been reported to be in the range of $0.26 \pm 0.17 \text{ LgSS}^{-1}$ [40]. The Henry's law constant for SMX has been reported to be $6.42 \text{E-}13$; and hence SMX is considered as non-volatile in WWTPs.

3.4.1.2 NPEOs

Nonylphenol and its ethoxylates (NPEOs) are widely used surfactants found in soaps, detergents, and similar cleaning products. More than half of the NP found in the environment is as a result of individual consumer use of products containing NPEOs. Concern about the endocrine disrupting properties of NPEOs led Environment Canada to introduce national regulations and restrictions on the manufacture and importation of NPEOs. Consequently, annual NPEO production has reduced from 3.35 million kg in 2003 to 1.03 million kg in 2006.

Removal efficiencies of NPEOs in wastewater treatment plants have been reported to be between 60 and 97%, depending on the type of treatment [51, 52, 66, 68, and 69]. Nonetheless, concentrations of NPEOs in the microgram per litre range have been observed in various surface waters [65, 67, and 69]. Biodegradation has been reported to be the dominant process for removal of these compounds [19].

3.4.1.3 Bisphenol-A

Bisphenol-A (BPA) is referred to as a neutral compound with a pKa of 9.78. The solid/liquid partition coefficient (K_d) for BPA has been reported in the literature to range from 0.07 L gSS^{-1} [59] to 1 L gSS^{-1} ; [25] The Henry's law constant for BPA is $1.7 \text{ E-}9$ [59] and hence BPA is considered as non-volatile in WWTPs. BPA has been deemed to be readily biodegradable under aerobic conditions and biodegradation under anoxic and anaerobic conditions is unlikely [60].

3.4.1.4 Ibuprofen

Ibuprofen is a non-prescription antiphlogistic drug that is used for relieving symptoms of arthritis, primary dysmenorrhea, fever, and pain. Excretion rates for non-metabolized ibuprofen have been estimated to be 7 and 23% via urine and feces, respectively [48]. The removal of ibuprofen in wastewater treatment has been reported to exceed 90% in numerous studies [49-54]. Given sufficient hydraulic residence time (i.e. at least 6 hours), virtually complete removal can be achieved [22]. In wastewater treatment, removal may occur via biodegradation and sorption [55, 50]. Acidic pharmaceuticals, such as ibuprofen, have been reported to have low sorption capacity in natural systems [88].

3.4.2 Case study 1

This case study was created to address the biodegradation and sorption of SMX along with biodegradation (conversion) of its metabolite to the parent compound (SMX). In developing Case Study 1, all process rates and compound species that were not related to the SMX and its metabolite removal were omitted from the fate model matrix by inserting zeros in the relevant rows and columns. The submodel for this case was a Mantis based model that addressed the removal of SMX and its metabolite along with the conventional compounds (see Appendix D for the relevant matrix). The removal mechanisms responsible for the removal of SMX and its metabolite were presented in Table 3.1, and the Matrix for the SMX and its metabolite was presented in Table 3.3.

Two major mechanisms are responsible for removal of SMX: biodegradation and sorption. For fate modeling of this compound, the impact of aerobic and anoxic conditions was considered for both biodegradation and sorption mechanisms. The biodegradation of its metabolite (daughter compound, *Szg*) was also considered in this model. The metabolite that was present in the raw wastewater during the biodegradation process was converted to the parent compound (SMX). The expressions for the process rates of aerobic/anoxic biodegradation, and aerobic/anoxic parent and daughter compounds transformation contain modifying terms $\frac{(K_s \cdot \eta_{bio})}{(K_s \cdot \eta_{bio} + S_s)}$ and $\frac{(K_s \cdot \eta_{1DEC})}{(K_s \cdot \eta_{1DEC} + S_s)}$ respectively that reduce the rates in the presence of readily biodegradable COD. The uptake of readily biodegradable COD (S_s) has been reported to cause competitive inhibition of micropollutant biotransformation processes [30].

Plosz et al. (2010) [30] observed an increase in the concentration of SMX, through wastewater treatment with negative or low removal efficiencies observed for this compound. Hence it was concluded that other mechanisms should be taken into account during the removal of this compound [30, 151]. In activated sludge, the presence of metabolites of pharmaceuticals that can be transformed back to the parent compound as a result of enzyme-catalyzed reactions has been reported [30]. It is possible for certain pharmaceuticals that the conjugated form may be present in the raw wastewater at concentrations greater than of the parent. Hence a mechanism referred to as parent compound transformation was added. Equations 3.10 and 3.12 describe the process rates for the aforementioned phenomenon.

Table 3.3 process matrix of SMX and its metabolite

SMX and its metabolite components			Process rate	Process rate description	
Szf	Szg	Xza			
-1			$k_{1BioOx} \cdot Szf \cdot \frac{(K_s \cdot \eta_{bio})}{(K_s \cdot \eta_{bio} + S_s)} \cdot \frac{S_o}{(K_o + S_o)} \cdot xbh$	Aerobic biotransformation of Szf	(3.9)
1	-1		$k_{1DecOx} \cdot Szg \cdot \frac{(K_s \cdot \eta_{1DEC})}{(K_s \cdot \eta_{1DEC} + S_s)} \cdot \frac{S_o}{(K_o + S_o)} \cdot xbh$	Aerobic parent compound transformation	(3.10)
-1			$k_{1BioAx} \cdot Szf \cdot \frac{(K_s \cdot \eta_{bio})}{(K_s \cdot \eta_{bio} + S_s)} \cdot \frac{S_o}{(K_o + S_o)} \cdot xbh$	Anoxic biotransformation of Szf	(3.11)
1	-1		$k_{1DecAx} \cdot Szg \cdot \frac{(K_s \cdot \eta_{1DEC})}{(K_s \cdot \eta_{1DEC} + S_s)} \cdot \frac{S_o}{(K_o + S_o)} \cdot xbh$	Anoxic parent compound transformation	(3.12)
1		-1	$K_{Des} \cdot Xza \cdot \frac{S_o}{(K_o + S_o)}$	Aerobic desorption of Szf	(3.13)
-1		1	$K_{Des} \cdot K_{1DOx} \cdot Szf \cdot \frac{S_o}{(K_o + S_o)} \cdot X_{ss}$	Aerobic sorption of Szf	(3.14)
1		-1	$K_{Des} \cdot Xza \cdot \frac{K_o}{(K_o + S_o)}$	Anoxic desorption of Szf	(3.15)
-1		1	$K_{Des} \cdot K_{1DAx} \cdot Szf \cdot \frac{K_o}{(K_o + S_o)} \cdot X_{ss}$	Anoxic sorption of Szf	(3.16)

The model in this case study was calibrated using the data provided in Plosz et al. 2010 [30]. The plant configuration for this study is shown in Figure 3.2. Since aerobic and anoxic biodegradation were included as removal mechanisms for SMX and its metabolite removal, aerobic and anoxic compartments were employed in the activated sludge process plant. For the sensitivity analysis of this case against SRT and HRT, only aerobic parent compound transformation, aerobic biodegradation, and aerobic sorption-desorption were considered (see Appendix D1 for the process matrix of this model) to simplify the data interpretation.

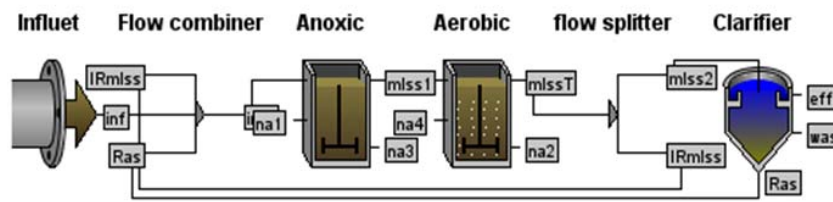


Figure 3.2 Plant configuration for the removal of SMX

The WWTP physical and operational parameters are shown in Table 3.4. These parameters were extracted from the work by Plosz et al. 2010 [30]. Calibration was conducted using the WWTP physical and operational parameters, presented in Table 3.4, and the experimental data provided for both conventional parameters and SMX and its metabolite.

Table 3.4 WWTP Physical and Operational Parameters

Influent flow rate	21390 m ³ /d
RAS flow rate	21400 m ³ /d
Wastage flow rate	302.1 m ³ /d
SRT	16 d
HRT	5.33 hr
Aeration tank volume	9500 m ³
Anoxic tank volume	9750 m ³
Aeration volume	19250 m ³
HRT*	10.8 hr
Secondary Flat bottom Clarifier dimensions	Surface: 458 m ² Water Depth: 6 m
DO concentration in Aeration Tank	3 mg/l
Temperature	20°C

* Anoxic zone omitted

3.4.5 Case study 2

This case study assessed the fate of nonylphenol ethoxylates (NPEOs) in an activated sludge process. A mechanism that has been reported to contribute to the removal of NPEO's is an abiotic oxidative cleavage process [19]. In this process, the NPEO's are converted to slowly biodegradable NPEOs, readily biodegradable NPEOs and non biodegradable NPEOs. In addition, through a hydrolysis process the slowly biodegradable portion of this compound is converted to the readily biodegradable form, and then this portion is biodegraded during the growth processes. This submodel was designed to predict the fate of NPEO's along with conventional compounds that was based on the Mantis model the relevant matrix is shown in appendix E. The process rates are described in Table 3.5.

Table 3.5 process matrix of NPEO

NPEO Components				Process rate	Process rate Description	
Sza	Szb	Szc	Szd			
$-(1-f_{INPEO})$	α	$1-\alpha$	f_{INPEO}	$K_{OCL} \cdot Sza$	Abiotic cleavage	(3.17)
	1	-1		$k_{hNPEO} \cdot \left[\frac{(Szc / xbh)}{K_{xNPEO} + (Szc / xbh)} \right] \cdot xbh$	Hydrolysis of NPEO	(3.18)
	-1			$K_{bioNPEO} \cdot Szb \cdot \frac{K_s}{(K_s + S_s)} \cdot \frac{S_o}{(K_{oh} + S_o)} \cdot xbh$	Growth on SS _{NPEO}	(3.19)

The structure of the expression for the hydrolysis rate of NPEO's is similar to that of entrapped organics in Mantis model. The biodegradation structure of the SS_{NPEO} is similar to that employed for the biodegradation of SMX and included a modifying term for readily biodegradable substrate $[(K_s)/(K_s+S_s)]$ as the uptake of Ss can reduce the biodegradation of SS_{NPEO} [19]. In this case study the model was calibrated using the experimental data provided in Karahan et al. 2010 [19]. The plant configuration for this study is shown in Figure 3.3. The WWTP physical and operational parameters are shown in Table 3.6. These parameters were also extracted from [19].

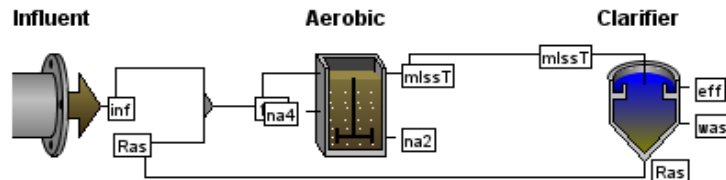


Figure 3.3 Plant configuration for the removal of NPEOs

Table 3.6 WWTP physical and operational parameters

Influent flow rate	1000 m ³ /d
RAS flow rate	1000 m ³ /d
Wastage flow rate	71.49 m ³ /d
SRT	15 d
HRT	24 hr
Aeration tank volume	2000 m ³
Secondary flat bottom clarifier dimensions	Surface: 200 m ² Water Depth: 4 m
DO concentration in aeration tank	2 mg/l
Temperature	20°C

The calibration process was conducted using the WWTP physical and operational parameters presented in Table 3.6, and experimental data provided for both conventional and NPEOs responses. Details on calibration and validation process are explained in sections 4.2.2.1 and 4.2.2.2, respectively. Appendix J presents the optimal values for stoichiometric and kinetic parameters of NPEO and conventional parameters.

3.4.6 Case study 3

Case Study 3 was developed to address the neutral and ionized compounds, Ibuprofen and Bisphenol-A. In this study, the biodegradation and sorption of this compound was considered. Since pH is an important parameter in the removal of ionized compounds, the biodegradation and sorption processes were modified to include a pH effect. Equation 3.20 describes the equilibrium reaction that was taken into account while equation 3.21 addresses the equation relating the extent of dissociation of an acid.



$$k_a = \frac{[H^+] + [A^-]}{[HA]} \quad (3.21)$$

Figure 3.4 presents an overall schematic of the general model for ionized compound fate and includes the dissociation of the acid:

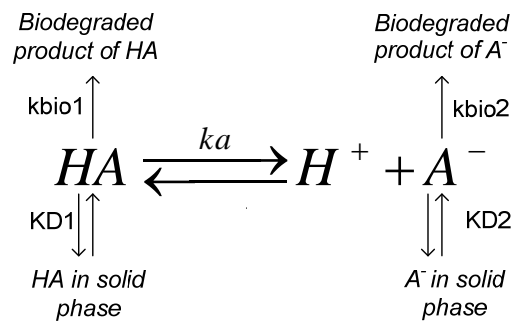


Figure 3.4: Schematic of general model for ionized compound fate model

In this model biodegradation and sorption of both the neutral, (HA) and ionized forms (A⁻) were considered. Combining equations 3.20, 3.21, 2.2, 2.3, 2.4, and 2.18, the process rates for these compounds were developed and the matrix was shown in Table 3.7.

Table 3.7 Process matrix of Ibuprofen

Ibuprofen Components				Process rate	Process rate Description
Szh	Szi	Xzb	Xzc		
-1				$K_{bio1} \cdot \frac{(Szh + Szi)}{(10^{(pH-pka)} + 1)} \cdot xbh$	Biodegradation of neutral form of compound (3.22)
	-1			$K_{bio2} \cdot \frac{(Szh + Szi)}{(10^{(pka-pH)} + 1)} \cdot xbh$	Biodegradation of ionized form of compound (3.23)
-1		1		$K_{1des} \cdot K_{D1} \cdot Szh \cdot X_{ss}$	Sorption of neutral form of compound (3.24)
1		-1		$K_{1des} \cdot Xzb$	Desorption of neutral form of compound (3.25)
	-1		1	$K_{2des} \cdot K_{D2} \cdot Szi \cdot X_{ss}$	Sorption of ionized form of compound (3.26)
	1		-1	$K_{2des} \cdot Xzc$	Desorption of ionized form of compound (3.27)

For modeling of neutral compounds, dissociation was not considered and hence the process rates were written according to equations 2.2, 2.3 and 2.18. Table 3.8 presents the matrix for Bisphenol-A.

Table 3.8 process matrix of Bisphenol-A

Bisphenol-A Components		Process rate	Process rate Description
Szj	Xzd		
-1		$K_{bio3} \cdot Szj \cdot \frac{S_o}{(K_{oh} + S_o)} \cdot xbh$	Biodegradation of neutral compound (3.28)
-1	1	$K_{3des} \cdot K_{d3} \cdot Szj \cdot X_{ss}$	Sorption of neutral compound (3.29)
1	-1	$K_{3des} \cdot Xzd$	Desorption of neutral compound (3.30)

This case study was calibrated using the experimental data provided in Zhao et al. 2007 [137] for the neutral compound and Collado et al. 2012 [146] for the ionized compound. The plant configuration for this study is shown in Figure 3.5. It should be noted that the plant configurations for the neutral and ionized compounds were similar with different wastewater characteristics, design and operational parameters.

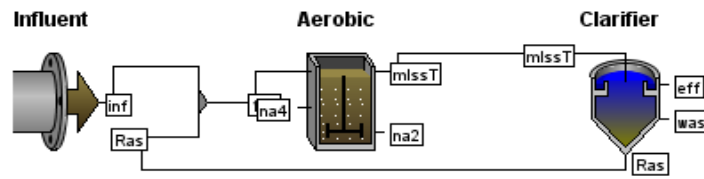


Figure 3.5 Plant configuration for the removal of Ibuprofen

The WWTP physical and operational parameters employed in the calibration for Ibuprofen and Bisphenol-A are shown in Tables 3.9 and 3.10. These parameters were extracted from [137, 146] respectively. The calibration was conducted using the WWTP physical and operational parameters, presented in Tables 3.9 and 3.10, and experimental data provided for conventional, Ibuprofen, and Bisphenol-A responses. Further details on calibration and validation processes are explained in sections 4.2.3.1 and 4.2.3.2, respectively and the results of calibration are provided in Appendix K, which presents the optimal values for the stoichiometric and kinetic parameters of Ibuprofen, Bisphenol-A, and conventional parameters.

Table 3.9 WWTP Physical and Operational Parameters for Case Study 3-Ibuprofen

Influent flow rate	3000 m ³ /d
RAS flow rate	1000 m ³ /d
Wastage flow rate	34.55 m ³ /d
SRT	15 d
HRT	12 hr
Aeration tank volume	2000 m ³
Secondary flat bottom clarifier dimensions	Surface: 200 m ² Water Depth: 4 m
DO concentration in aeration tank	2 mg/l
Kinetics	CNIPLIB library in GPS-X V.6.02
Temperature	20°C

Table 3.10 WWTP Physical and Operational Parameters for Case Study 3-Bisphenol-A

Influent flow rate	2800 m ³ /d
RAS flow rate	2000 m ³ /d
Wastage flow rate	21 m ³ /d
SRT	25 d
HRT	10 hr
Aeration tank volume	2000 m ³
Secondary flat bottom clarifier dimensions	Surface: 250 m ² Water Depth: 3.5 m
DO concentration in aeration tank	2 mg/l
Kinetics	CNIPLIB library in GPS-X V.6.02
Temperature	20°C

CHAPTER 4

SIMULATION RESULTS AND DISCUSSION

4.1 Introduction

In the previous chapter, the development of the fate model and its integration with the GPS-X software was explained. Three case studies that included different mechanisms for the removal of specific groups of compounds were introduced. At the end of the chapter, the plant configurations and parameters in each case study were explained. This chapter describes the model calibration in each case study, the implementation of the model in GPS-X in each case study through use of the model developer tool and the model validation with different data sets. A sensitivity analysis is presented at the end to investigate the effect of SRT, HRT and pH on the removal efficiencies.

4.2 Model calibration and validation

In this section, the model calibration in the three case studies is described and the optimal values for the model parameters are reported. The calibration step was carried out for both conventional and fate model parameters. At the end, the validation process of each case study is explained in detail.

4.2.1 Case study 1

This case study was created to investigate the removal of Sulfamethoxazole (SMX). Parent compound transformation, competitive inhibition and co-metabolism mechanisms were included in the structure of this submodel. In this case study, calibration, simulation, validation and sensitivity analysis were performed for SMX only.

4.2.1.1 Calibration and simulation

The calibration of the model was performed for both conventional and fate model parameters. Since the estimation of biomass production is one of the key parameters for addressing the fate of trace compound, matching of the biomass production in the steady state condition with the data set was employed for calibration. The experimental data presented in [30] was used for the calibration of this model. The data set for the SMX was presented from continuous effluent flow of both the anoxic and aerobic reactor (Figure 4.1) in soluble form. Since the full data set was not available, the conventional parameters including total COD, inert inorganic suspended solids, particulate inert organic material, total suspended solids in the waste water influent, plant configuration, and plant operational parameters, (SRT=16 days and HRT=5.33 hr) were set to those described by Plosz et al. 2010 [30].

For other ASM1 parameters that were not reported in the related literature, the default values for municipal wastewater treatment plants were employed. By adjusting the inert organic suspended solids, influent VSS and the ratio of inert particulate COD to biodegradable COD in the wastewater influent by trial and error within the GPS-X software, and running simulations on the submodel of this case study, the biomass concentration in the bioreactor at steady state was matched with the corresponding experimental data presented in the literature. The relative error for this calibration was 0.5%. As mentioned in section 2.3.2 active biomass is not measurable experimentally; thus, it is often assumed in fate models that the MLSS or MLVSS can represent the active biomass. However, in the new fate model that was developed in this research, the active heterotrophic biomass was used as the active fraction of the MLSS and was predicted by the conventional part of the model within GPS-X. Hence, the parameter values (kb , kd , etc) predicted in this research can be expected to be different from that reported in the literature. The values of the conventional parameters are presented in Appendix I.

After conventional parameter calibration, according to the plant layout and submodel matrix, which are presented in appendix D, a corresponding set of differential equations were transferred to MATLAB where the fate model was calibrated with experimental data reported for the trace compound (SMX). To this goal, for each parameter of interest in the structure of the model matrix (see Appendix D), the mean (μ) and standard deviation (σ) of the literature reported ranges were calculated. The mean and standard deviation were calculated over those reported in each reference, i.e., in most references, the reported values were in the form of uncertainty ranges ($\mu \pm \sigma$). Then lower and upper bounds for the calibration parameters were set to $\mu - \sigma$ and $\mu + \sigma$, respectively, see Table 4.1. For the anoxic bioreactor, as the work by [30] provided the only reported parameter values, the lower and upper bounds were set to 0.1 and 10 times the reported values [30]. For this case, the following objective function was considered:

$$\begin{aligned}
 SSE = & 0.25 \sum_{i=1}^n \left(\frac{Szf_{i,aerobic}^{sim} - Szf_{i,aerobic}^{ref}}{\max(Szf_{aerobic}^{ref})} \right)^2 + 0.25 \sum_{i=1}^n \left(\frac{Szg_{i,aerobic}^{sim} - Szg_{i,aerobic}^{ref}}{\max(Szg_{aerobic}^{ref})} \right)^2 + \\
 & 0.25 \sum_{i=1}^n \left(\frac{Szf_{i,anoxic}^{sim} - Szf_{i,anoxic}^{ref}}{\max(Szf_{anoxic}^{ref})} \right)^2 + 0.25 \sum_{i=1}^n \left(\frac{Szg_{i,anoxic}^{sim} - Szg_{i,anoxic}^{ref}}{\max(Szg_{anoxic}^{ref})} \right)^2
 \end{aligned} \tag{4.1}$$

where index i refers to the i^{th} data point, $Szf_{aerobic}^{sim}$ is the simulated value for Szf (effluent concentration of SMX), Szf_{anoxic}^{sim} , is the simulated value for Szf (effluent of anoxic reactor), $Szf_{aerobic}^{ref}$ and Szf_{anoxic}^{ref}

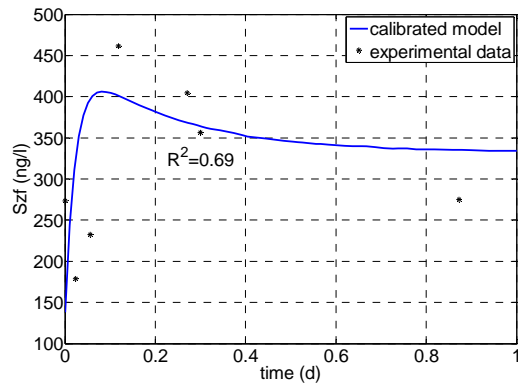
represent the experimental data for Szf in effluent of aeration and anoxic reactor, respectively from Plosz et al. 2010 [30], $Szg_{aerobic}^{sim}$ is the simulated Szg (the compound concentration biotransformed via the Szf in aerobic reactor effluent), Szg_{anoxic}^{sim} is the simulated Szg in effluent of anoxic reactor, and Szg_i^{ref} denotes the model results by [30]. Note that no experimental data was reported for Szg [30]. It should be added that the objective function is written in a non-dimensionalized form to provide relatively similar effects of the two terms on the SSE; otherwise, the four terms could have such different values the optimizer would mostly reduce only the larger terms. For more information regarding the calibration process and the involved optimization, see section 3.3.2.1.

A summary of the calibration results is presented in the following table:

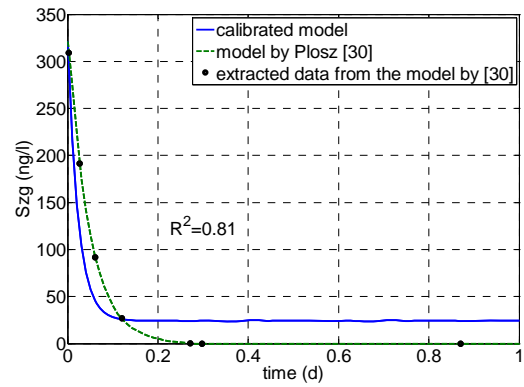
Table 4.1 Calibration results for case study 1

Parameter	Lower Bound	Upper Bound	Optimal Value \pm Standard Error
K_{1BioOx} ($m^3/gbiomass/d$)	6.937E-4	1.904E-3	1.529E-3 \pm 3.7E-4
K_{1BioAx} ($m^3/gbiomass/d$)	6.937E-4	1.904E-3	1.529E-3 \pm 3.7E-4
K_{1DecOx} ($m^3/gbiomass/d$)	6.8E-4	6.8E-2	3.312E-2 \pm 6.3E-3
K_{1DecAx} ($m^3/gbiomass/d$)	7.85E-4	7.85E-2	3.823E-2 \pm 5.8E-3
K_{1Dox} ($m^3/gbiomass$)	5.110E-5	3.893E-4	2.914E-4 \pm 3.4E-5
K_{1DAx} ($m^3/gbiomass$)	5.5E-5	5.5E-3	5.500E-4 \pm 4.1E-5
η_{bio}	1	3	2.886 \pm 0.46
η_{1Dec}	1	3	1.920 \pm 0.31

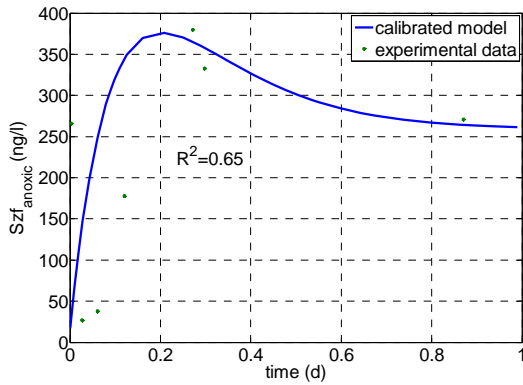
To examine the quality of model calibration for case 1, a comparison of the simulated Szf and Szg values against the corresponding target values as well as the R^2 values are presented in Figure 4.1. It should be pointed out that for Szg , the R^2 is calculated using the same points existing in Szf . To do so, the Szg values were extracted at the points that Szf was provided experimentally; these values are shown in solid circles. Therefore, there were the same number and distribution of data points in all 4 figures, and the R^2 values were calculated consistently.



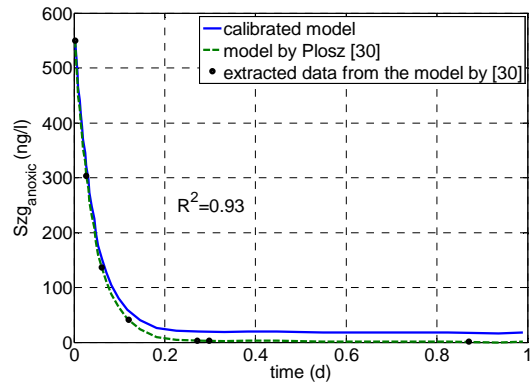
(a)



(b)



(c)



(d)

Figure 4.1 Simulated against the target concentrations in the calibration of case 1 model.

Figures 4.1 shows the quality of fit for the calibration process of case study one. Figures 4.1 (a and c) show the curves for SMX in the aerobic and anoxic conditions, respectively; whereas Figures 4.1 (b and d) show the curves for the metabolite under aerobic and anoxic conditions, respectively. As shown in Figures 4.1 (a and c), the model (solid line) followed the experimental data (solid circles) relatively well; the R^2 values were 0.69 for the aerobic condition and 0.65 for anoxic condition, respectively, which can be related to the sparsity of the experimental data. Additionally, the first data point (at time=0) had a significantly higher value compared to the second data point (at nearly 0.02 d), which is in contrast with the trend of the data set. The first data point could be considered as an outlier, but as Plosz et al. 2010 [30] had included that data point, it was considered in this thesis too, which resulted in the lower R^2 value.

Figure 4.1(b and d) show how the calibrated model could follow the target values of S_{zg} . As mentioned, the target values only for this compound were the output data from Plosz's model, since no experimental data was reported in the reference. The trends in the responses were similar in shape and the R^2 values were deemed to be reasonable.

Simulation outputs according to the calibrated results of Table 4.1 are reported in Table 4.2 for the soluble concentration of SMX in the effluent stream and the solid phase concentration of SMX in the wastage stream. Soluble COD in the effluent stream, heterotroph biomass production in aeration bioreactor, total suspended solid (*TSS*) production in bioreactor and total *TSS* production in wastage flow are also presented in Table 4.2. The solids retention time for this simulation was 16 days and the hydraulic retention time was 5.33 hours. The details of the plant configuration were presented in section 3.4.4, Table 3.7. These results were obtained by running simulation in steady state condition within the GPS-X software. From Table 4.2 it can be seen that the simulated effluent concentration for SMX is higher than that in the influent (0.00021 g/m^3). The biotransformation of this compound includes two phenomena: biodegradation and the other one transforming the metabolite (S_{zg}) to the parent compound. Hence the concentration of this compound would be reduced due to the biodegradation process, but would increase as a result of the conversion of the metabolite to the parent compound. The higher effluent concentration of SMX in comparison with the influent concentration, results in a removal efficiency that is negative, which is in agreement with results of Plosz et al. 2010 [30] and also [9, 151]. The simulation results showed the sorption of SMX as well; the particulate concentration of SMX in solid phase was estimated to be 0.000744 g/m^3 . The simulation results also showed the biodegradation of metabolite (S_{zg}), for which the removal efficiency was 98%. This metabolite was converted to SMX during the biotransformation process. In Table 4.2, the viable biomass prediction was addressed as well, since the fate model is ASM-based.

Table 4.2 Simulation results of case study 1, Considering aerobic and anoxic parent compound transformations

S_{zf_i} (g/m^3)	S_{zf} (g/m^3)	S_{zg_i} (g/m^3)	S_{zg} (g/m^3)	X_{za} in WAS (g/m^3)	fCOD (gCOD/m^3)	xbh (gCOD/m^3)	TSS in AR (g/m^3)
0.00021	0.0003314	0.000467	1.086E-5	0.000744	37.74	965.2	3116

4.2.1.2 Case study 1 validation

Following calibration, the fate model was validated with a different data than that used for calibration; therefore, in the validation phase, the experimental results of Suarez et al. 2010 [37] were used. To this goal, the wastewater characteristics and the plant operation conditions in the fate model were set to those presented in [37]. Those parameters are shown in Table 4.3. The fate model was run with these parameters at steady state condition. The removal efficiency of the SMX was predicted as -51%, which was somewhat different from that of reported by [37].

Table 4.3 Characteristics and the plant operating conditions used for validation of SMX removal in wastewater treatment

Parameter	Suarez et al. 2010 ^[37]
Influent concentration of SMX (g/m ³)	0.02
Removal efficiency (%)	22±5
SRT (days)	<20
HRT (hours)	24
Mixed liquor suspended solid (MLSS) in steady state condition (g/m ³)	1600
Total COD in influent (gCOD/m ³)	500
Temperature (°C)	20

The removal efficiency was reported based on the parent compound that led to negative removal efficiency. The metabolite compound, which was called daughter compound, during biotransformation process was converted to the SMX. The main reason of the difference in removal efficiencies between Suarez et al. 2010 [37] and the calibrated model could be because of the different ratio of the SMX and its metabolite, since in Suarez et al. 2010 [37] the concentration of metabolite was not reported. This ratio in the calibrated model was inserted from the wastewater characteristics provided by [30]. Temperature changes do not have influence on the removal of SMX [37]. Removal efficiencies reported in the literature varied in a wide range. For example, eliminations of 33±64, 0–84% and (-138)–60% can be found in [151, 150] and [9] respectively. The reason for this wide range removal efficiency is due to the fact that real wastewaters, which have a more complex matrix, were used in these works. Negative elimination has also been found in the literature because of presence of conjugated metabolites in the complex wastewater [30, 37, 151].

4.2.2 Case study 2

Case study 2 evaluated abiotic cleavage, hydrolysis and biodegradation mechanisms that are responsible for the removal of nonylphenol ethoxylates (NPEO's). The details of each mechanism were discussed in chapter 2.

4.2.2.1 Case study 2 calibration

The submodel for case study 2 was calibrated for both conventional and fate model parameters before running simulations. In the conventional parameter calibration effort, wastewater characteristics, the biomass production at steady state conditions, SRT, and HRT in the system were adjusted to the plant data that were used for the calibration. The batch experimental data presented by Karahan et al. 2010 [19] was used for the calibration of this model. For the other ASM1 parameters that were not reported in the related literature, the default value for municipal wastewater treatment plant was inserted into the GPS-X software. The SRT of 15 d and HRT of 24 hr were tuned with those of [19]. By adjusting the inert organic suspended solids, influent VSS and the ratio of inert particulate COD to biodegradable COD in wastewater influent by trial and error within the GPS-X software and running simulation on the submodel of this case study, the biomass concentration in the bioreactor at steady state was matched with the corresponding experimental data presented in that literature. This relative error for this calibration was 1.6% where the relative error (RE) for the calibration was calculated as $100 * (\text{experimental value} - \text{estimated value for } TSS \text{ (gXssL}^{-1}\text{)}) / \text{experimental value for } TSS$. In recent fate models, in the structure of trace compound biodegradation process, the active biomass is not measurable experimentally; thus, it is often assumed that the MLSS or MLVSS can represent the active biomass. However, in the new fate model, which was developed in this research, the active heterotrophic biomass was used as an active fraction of MLSS and was predicted by the conventional part of the model within the GPS-X. The aforementioned conventional parameters are presented in Appendix J.

After conventional parameter calibration, according to the plant layout and submodel matrix, which are presented in appendix E, the corresponding set of differential equations were transferred to MATLAB where the fate model was calibrated with experimental data reported for the trace compound (NPEO). The calibration for case study 2 is detailed here according to data presented for total COD and NPEO concentration in bulk liquid. The mean μ and standard deviation σ of the literature ([19, 70, 139,140, 141,142, 143]) for the parameters of interest were calculated. It should be noted that the values in most references of the literature were reported as uncertainty intervals ($\mu \pm \sigma$), and there was no deterministic range for each parameter reported in the literature. Hence, a total mean

and standard deviation over those reported means and standard deviations was calculated. Then lower and upper bounds of each parameter for the calibration were set to $\mu-\sigma$ and $\mu+\sigma$, respectively, see Table 4.4. For this case, the following objective function was considered:

$$SSE = 0.5 \sum_{i=1}^n \left(\frac{Sza_i^{sim} - Sza_i^{exp}}{\max(Sza^{exp})} \right)^2 + 0.5 \sum_{i=1}^n \left(\frac{COD_i^{sim} - COD_i^{exp}}{\max(COD^{exp})} \right)^2 \quad (4.3)$$

where i is the data point index, Sza is the effluent concentration of NPEO in bulk liquid, the superscripts “*sim*” and “*exp*” represent simulation (model) and experimental data (from Karahan et al. 2010 [19]), respectively. Note that the objective function is written in a non-dimensionalized form to provide relatively similar effects of the two terms on the SSE ; otherwise, the two terms could have such different values that the optimizer would reduce only the larger term. A summary of the calibration results is presented in the following table:

Table 4.4 Calibration results for case study 2

Parameter	Lower Bound	Upper Bound	Optimal Value ± Standard Error
K_{OCL} (1/d)	0	-	250±13
K_{hNPEO} (1/d)	0	-	1.45±0.09
$K_{bioNPEO}$ (m3/gbiomass/d)	0.122	0.312	0.237±0.072

To investigate the quality of this calibration, a comparison of simulated and corresponding target values as well as the R^2 values are presented in Figure 4.2:

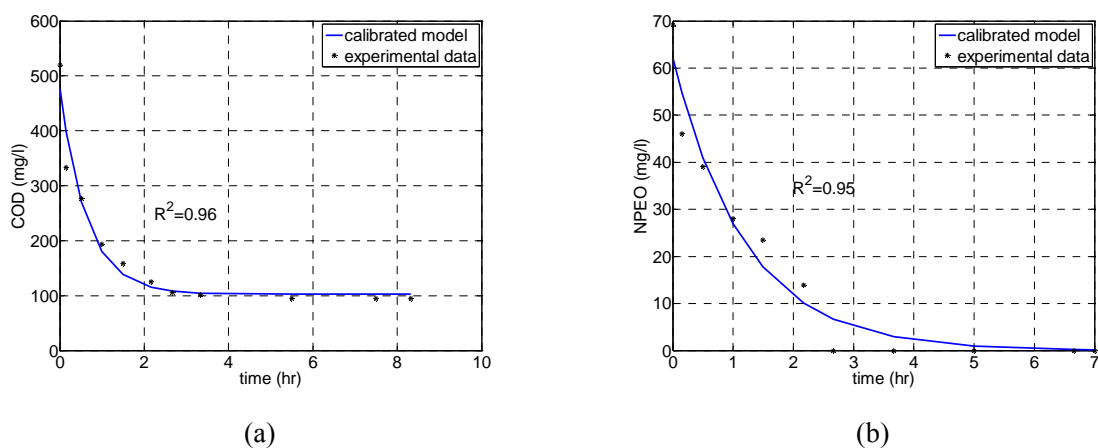


Figure 4.2 Simulated against the target concentrations in the calibration of case 2 model.

As shown in Figure 4.2(a), model (solid line) has followed the experimental data (solid circles) quite well; the R^2 value was 0.96, which indicates that the model was calibrated accurately. Figure 4.1(b) shows how the calibrated model could follow the target values of NPEO. The trends look quite the same and the R^2 value was 0.95. The high quality of the fit in the calibration was attributed to the accurate estimation of viable biomass production in the activated sludge process in the case 2 model.

During the abiotic cleavage process, NPEO's in the bulk liquid (S_{za}) are converted to readily biodegradable substrate (S_{zb}), slowly biodegradable substrate (S_{zc}), and non biodegradable substrate. During the hydrolysis process, slowly biodegradable substrate converts to readily biodegradable substrate, and then readily biodegradable substrate is biodegraded. Hence, these were the processes that were modeled in this case study. The simulated effluent concentration of S_{za} , S_{zb} , S_{zc} and S_{zd} are presented in Table 4.5. The details of plant configuration parameters were presented in section 3.4.5, Table 3.8. These results were obtained by running a simulation at steady state condition within the GPS-X software. The removal efficiency based on NPEO in the bulk liquid (S_{za}) was 99.7%, which was in good agreement with data provided by [19]. The estimation of total suspended solid concentration in the aeration basin was in a typical range and equal to the concentration in batch experiment by [19] in steady state condition. In Table 4.5, the viable biomass prediction was addressed as well, since the fate model is ASM-based.

Table 4.5 Simulation results of case study 2

S_{za_i} (g/m ³)	S_{za} (g/m ³)	S_{zb} (g/m ³)	S_{zc} (g/m ³)	S_{zd} (g/m ³)	SCOD (gCOD/m ³)	xbh (gCOD/m ³)	TSS in AR (g/m ³)	TSS in WAS (g/m ³)
114	0.300	0.570	0.997	35.910	26.530	760.70	1762	3286

4.2.2.2 Case study 2 validation

As mentioned previously, the fate model parameters for NPEOs were calibrated using data by Karahan et al. 2010 [19]. Following calibration, the fate model simulation results were validated with data reported by Zhang et al. 2007 [70]. To this goal, the wastewater characteristics and the plant operation conditions of the fate model were set to those presented in [70]. The value of total COD influent was considered as 232 gCOD/m^3 and the key parameters are shown in Table 4.6. The fate model was run with these parameters at steady state condition. The removal efficiency of the NPEO was predicted as 98%. Since the SRT was not reported by [70], that value was set to be 15 days. COD removal efficiency was estimated as 84%.

Table 4.6 Characteristics and the plant operation condition for prediction of NPEO removal in Wastewater Treatment

Parameter	Zhang et al. 2007 [70]
Removal efficiency (%)	>92
HRT (hours)	15.8
Mixed liquor suspended solid (MLSS) in steady state condition (g/m^3)	1500
Total COD in influent (gCOD/m^3)	232 ± 15
COD Removal efficiency (%)	82.3%

According to Table 4.6, the estimated value was in good agreement with the results reported by [70], even though the removal efficiency predicted by [70] was 92%, the calibrated fate model higher estimation removal efficiency could be because of higher SRT than that of [70].

4.2.3 Case study 3

This case study was created to investigate the removal of a group of compounds that are present in the water phase in neutral and ionized forms. Biodegradation in the aeration reactor and sorption were the major processes included in the structure of this submodel. In this case study, calibration, simulation and validation processes and sensitivity analysis against SRT, HRT were done for Bisphenol-A, which is a neutral compound, and Ibuprofen, which is an ionized compound. For the ionized compound, the pH was also considered as a sensitivity analysis parameter.

4.2.3.1 Case study 3 calibration and simulation

Similar to the previous case studies, the calibration of the model was performed for both conventional and fate parameters. The experiment results presented by Zhao et al. 2007 [137] was used for the calibration of the neutral compound (Bisphenol-A) parameters, and the experimental results of Collado et al. 2012 [146] were used for calibration of the ionized compound (Ibuprofen) parameters. The biomass production in the aeration basin in steady state condition (MLSS in steady state) was kept the same as those in the mentioned references, respectively for each case. In order to achieve this, the wastewater characteristics in terms of inert inorganic suspended solids, particulate inert organic material and total suspended solid in the waste water influent and also operational parameters, such as SRT and HRT, were tuned with corresponding reported values. Since only total COD values were available for the influent, the default values for the wastewater characteristics and ASM1 model parameters within the typical range were used for the calibration. By adjusting the inert organic suspended solids, influent VSS and the ratio of inert particulate COD to biodegradable COD in wastewater influent by trial and error within the GPS-X software and running simulation on the submodel of this case study, the biomass concentration in the bioreactor at steady state was matched with the corresponding experimental data presented in that literature. This relative error for this calibration for the neutral and ionized compounds were 2.3 and 1.8% respectively where $R.E. = 100 * (\text{estimated value} - \text{experimental value for TSS (gXssL}^{-1}\text{)}) / \text{experimental value for TSS}$. As mentioned in section 2.3.2, in recent fate models, in the structure of trace compound biodegradation process, the active biomass is not measurable experimentally; thus, it is often assumed that the MLSS or MLVSS can represent the active biomass. However, in the new fate model that was developed in this research, the active heterotrophic biomass was used as the active fraction of MLSS and was predicted by the conventional part of the model within the GPS-X. Hence, it was expected that the parameter values (kb , kd , etc) predicted in this research would be different from that of reported in the literature. The aforementioned conventional parameters were presented in Appendix K.

After conventional parameter calibration, according to the plant layout and submodel matrix, which was presented in appendix F, the corresponding set of differential equations were transferred to MATLAB where the fate model was calibrated with experimental data reported for the trace compounds Bisphenol-A and Ibuprofen. To this goal, for each parameter of interest (see Appendix F), the mean μ and standard deviation σ of the literature reported range were calculated. It should be pointed out that the values in most references of the literature were reported as uncertainty intervals ($\mu \pm \sigma$), and there was no deterministic value and therefore range for each parameter reported in the literature. Hence, a total mean and standard deviation over the reported means and standard deviations was calculated. Then lower and upper bounds for the calibration were set to $\mu - \sigma$ and $\mu + \sigma$, respectively, see Table 4.7 and 4.8. For this case, the following objective functions were considered:

$$SSE = \sum_{i=1}^n \left(\frac{S_{zj}^{sim} - S_{zj}^{exp}}{\max(S_{zj}^{exp})} \right)^2 \quad (4.6)$$

$$SSE = \sum_{i=1}^n \left(\frac{S_{zh}^{sim} - S_{zh}^{exp}}{\max(S_{zh}^{exp})} \right)^2 \quad (4.7)$$

where index i refers to the i^{th} observation point, S_{zj}^{sim} is the simulated value for S_{zj} (effluent concentration of Bisphenol-A), S_{zj}^{exp} represents the experimental data for S_{zj} from Zhao et al. 2007 [137], S_{zh}^{sim} is the simulated S_{zh} (effluent concentration of Ibuprofen), and S_{zh}^{exp} denotes the model results by Collado et al. 2012 [146]. For more information regarding the calibration process and the involved optimization, see section 3.3.2.1.

A summary of the calibration results is presented in the following table:

Table 4.7 Calibration results for case study 3-ionized compound

Parameter	Lower Bound	Upper Bound	Optimal Value \pm Standard Error
K_{D1} ($\text{m}^3/\text{gbiomass}$)	1.59E-5	7.53E-4	3.23E-4 \pm 6.02E-5
K_{bio1} ($\text{m}^3/\text{gbiomass/d}$)	0.0681	0.2877	0.1943 \pm 0.10
K_{D2} ($\text{m}^3/\text{gbiomass}$)	1.32E-6	6.26E-5	1.96E-5 \pm 5.72E-6

Table 4.8 Calibration results for case study 3-Neutral compound

Parameter	Lower Bound	Upper Bound	Optimal Value \pm Standard Error
K_{d3} ($\text{m}^3/\text{gbiomass}$)	5.747E-5	7.186E-4	4.935E-4 \pm 5.3E-5
K_{bio3} ($\text{m}^3/\text{gbiomass/d}$)	0.0047	0.0697	0.0502 \pm 7.9E-3

To examine the quality of model calibration for this case, a comparison of the simulated S_{zj} and S_{zh} values against the corresponding target values as well as the R^2 values are presented in Figures 4.3:

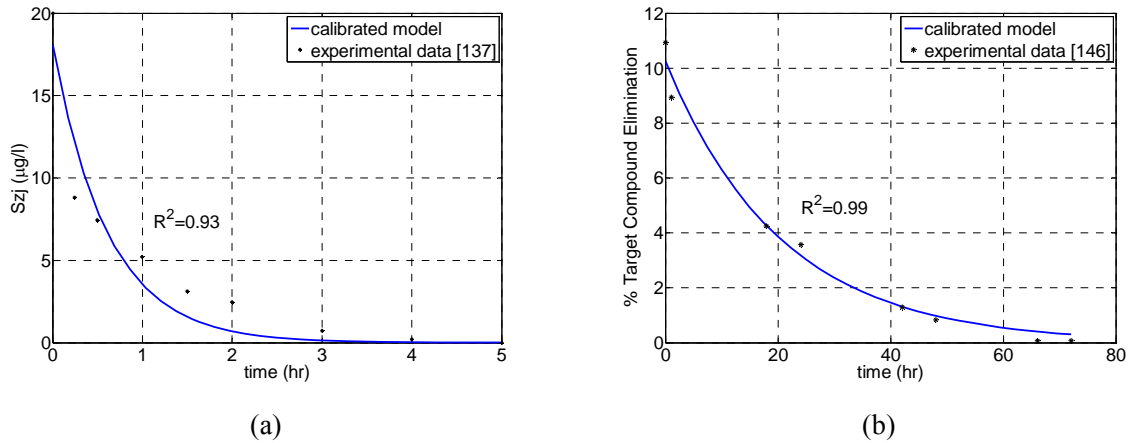


Figure 4.3 Results of Case 3 calibration. (a) Bisphenol-A, (b) Ibuprofen

As shown in Figure 4.3(a), model (solid line) followed the experimental data (solid circles) fairly well; the R^2 value is 0.93. Figure 4.3(b) shows how the calibrated model could follow the target compound elimination values. The trends look similar and the R^2 value was very good (0.99).

After model calibration, the soluble and solid phase concentrations of Bisphenol-A and Ibuprofen were simulated in the effluent and wastage flow, at steady state for the plant reported in section 3.4.6. The soluble COD in the effluent stream, heterotroph biomass production in the aeration bioreactor and total suspended solid (*TSS*) production in the bioreactor and the wastage stream were also simulated. These results are shown in Table 4.9 and 4.10. The solids retention time for this simulation was 15 days and hydraulic retention time was 12 hours. More details of the plant configuration are presented in section 3.4.6, Table 3.6. The removal efficiencies predicted by the fate model for the neutral and ionized compounds were 95.5% and 99.5% with were in good agreement with the works by [137] for the Bisphenol-A and [146] for the Ibuprofen.

Table 4.9 Simulation results of case study 3 (Neutral compound)

Szj_i (g/m ³)	Szj (g/m ³)	Xzd in WAS (g/m ³)	SCOD (gCOD/m ³)	xbh (gCOD/m ³)	TSS in AR (g/m ³)	TSS (g/m ³)
0.02	9 E(-4)	0.003	23.01	1137	3449	13300

Table 4.10 continued: Simulation results of case study 3 (Ionized compound)

Szh_i (g/m ³)	Szi_i (g/m ³)	Szh (g/m ³)	Szi (g/m ³)	Xzb in WAS (g/m ³)	Xzc in WAS (g/m ³)	SCOD (gCOD/m ³)	xbh (gCOD/m ³)	TSS in AR (g/m ³)	TSS (g/m ³)
0.024	4.37	1.2E(-4)	0.022	8.58E(-6)	1.3E(-4)	21	1137	3453	13320

4.2.3.2 Case study 3 validation

The data reported by Athanasios et al. 2010 [138] for bisphenol-A in a batch experiment was employed for validation in this case. The wastewater characteristics and operational plant parameters that were used for validation are shown in Table 4.11 and 4.12. The removal efficiency predicted by the fate model was 97.5%, which was in the range reported by [138].

Table 4.11 Characteristics and the plant operation condition for prediction of Bisphenol-A removal in Wastewater Treatment

Parameter	Athanasios et al. 2010 [138]
Influent concentration of Bisphenol-A (g/m ³)	0.0019
Removal efficiency (%)	93.8±5.9
SRT (d)	20
HRT (hr)	10
Mixed liquor suspended solid (MLSS) in steady state condition (g/m ³)	3000
Total COD in influent (gCOD/m ³)	358 ± 46
Temperature (°C)	22.0 ± 1.0

Table 4.12 Characteristics and the plant operation condition for prediction of Ibuprofen removal in Wastewater Treatment

Parameter	Smook et al. 2008 [145]
Influent concentration of Ibuprofen (g/m ³)	0.009
Removal efficiency (%)	>95
SRT (d)	9.5
HRT (hr)	14.2
Mixed liquor suspended solid (MLSS) in steady state condition (g/m ³)	2330
Temperature (°C)	12-21

Table 4.11 presents experimental conditions that were reported by Smook et al. 2008 [145] and which were used for validation of the Ibuprofen model. Using these values as input, the predicted removal efficiency for Ibuprofen was 96.3% and this was in good agreement with that of [145].

4.3 Sensitivity analysis of the fate model

In wastewater treatment, certain design and operational parameters that affect the fate of micro-constituents can be controlled, while other parameters may be determined by the facility design and/or geographic area. The crucial controllable operational parameter for relatively non-volatile compounds such as XOCs is the solid retention time (SRT), which has been identified in the literature as an important factor. Hydraulic retention time (HRT), which is fixed by the process unit design volume and influent flow rate, is an example of relatively non-controllable parameters. pH is another factor that mainly influences the removal of ionized compounds. The importance of the three aforementioned factors in removal of XOCs was investigated via a sensitivity analysis in the GPS-X software.

Other parameters in the proposed model, such as biodegradation and sorption rate coefficients (kb , kd) have been reported in the literature to span a range of values. Although in chapter 3, values for these parameters were computed through a calibration process, to study the robustness of the simulation results, a sensitivity analysis was performed in this section. To this goal, different parameter values were collected from the literature, the mean and standard deviation of these were calculated, and separate simulations using $\mu+\sigma$ (upper bound), and $\mu-\sigma$ (lower bound) and the calibrated parameter value for these parameters were run. The results of the various cases were plotted for analysis purposes. For case study 1 the anoxic compartment was excluded to simplify the sensitivity analysis interpretation. The modified matrix of this model is presented in Appendix D1.

4.3.1 Effect of solid retention time

SRT has been identified earlier in the literature as an operational parameter that can be used to minimize the effluent concentrations of XOCs [5, 9, 37, 112]. The effect of solid retention time on XOC fate over a range of approximately 5 to 20 days at 20°C was investigated in each case study. The fate model was the ASM based model, so it addresses the fate of conventional compounds and xenobiotic organic compounds simultaneously. To explain the effect of SRT on the fate of xenobiotic organic compounds, the effect of SRT on heterotrophic biomass concentration and total suspended solid concentration in the aeration basin were plotted for each case study.

4.3.1.1 Case study 1

Figure 4.4 presents some of the predicted conventional responses versus SRT for the sensitivity study. The HRT in this sensitivity analysis was set to 10.8hr. The concentrations of active heterotrophic biomass (xbh) (Figure 4.4a) and total suspended solids (TSS) in the aeration basin (Figures 4.4b)

increased with increasing SRT. Since x_{bh} and TSS in the aeration basin are important parameters in the biodegradation and sorption of SMX, the effect of SRT on the fate of this compound could be explained by the variation of x_{bh} and TSS concentration with respect to SRT.

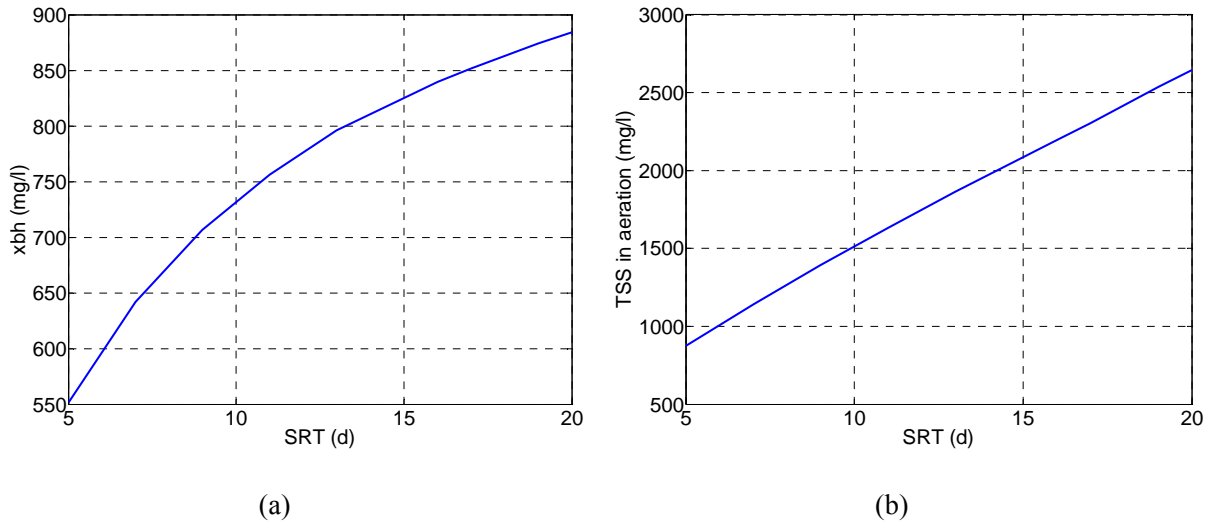


Figure 4.4 (a) Active heterotrophic biomass (x_{bh}), (b) Total suspended solid (TSS) in aeration, HRT=10.8hr

The influent concentration of the soluble (S_{zf}) and particulate (X_{za}) forms of SMX were set at 210 ng/l and 0 ng/l respectively, and the influent concentration of the daughter compound (S_{zg}) was set at 467 ng/l. Figure 4.5 presents the influence of SRT on the concentration of the soluble form of SMX (S_{zf}) over a range of values of k_d and k_b . Figure 4.6 presents the corresponding solid phase concentration of SMX (X_{za}) in the waste stream while Figure 4.7 shows the effluent concentration and rate of biodegradation of S_{zg} . From Figure 4.5 it can be see that there was a significant reduction in the effluent concentration of S_{zf} (about 34% increase in removal efficiency of S_{zf} between SRT=5 and SRT= 20 days) and S_{zg} (about 15% increase in removal efficiency between SRT=5 and SRT= 20 days). During the biotransformation process, there was an interaction between metabolite compounds (S_{zg}) and the parent compound (S_{zf}). As a result of the biotransformation of S_{zg} , these compounds were converted to the parent compounds and also the parent compound was biodegraded itself. The net result of these biotransformation processes was the production of the parent compound. As can be seen in Figure 4.5 at SRT= 16 days and k_b and k_d equal to the optimal values, with influent concentration of 210 ng/l, the effluent concentration of S_{zf} was approximately 358 ng/l, so the removal efficiency of S_{zf} was negative (See Table 4.9). The increase in concentration of active biomass (x_{bh}) due to increase of SRT (Figure 4.4a) resulted in increases in the biodegradation rate of

S_zf (Figure 4.8) and S_zg (Figure 4.7b) (about 27% increase in biodegradation of S_zf and 3% increase in biodegradation of S_zg).

Figure 4.9 presents the sorption rate for SMX and represents the net effect of the sorption and desorption rates. The positive value shows that the rate of sorption was greater than the rate of desorption. The net sorption rate of SMX increased nearly 32% (Figure 4.9) over the range of SRTs examined. With the increase of MLSS concentration, the amount of sorbed SMX to the sludge increases. This is because an increase of suspended solids in the system increases the number of reactive sites available to sorb SMX from solution. Following that the amount of SMX sorbed to the sludge was increased. Therefore, the increase of solid sludge in the solution enhanced the total sorption of SMX (X_{za}) (growth about 88%) by sludge and benefited the removal of SMX from water phase (Figures 4.6a and b) [137]. However the wastage rate of SMX decreased with increasing SRT, because for regulating SRT wastage flow rate was increased and this term was dominant in wastage flow of SMX (See Table 4.11)

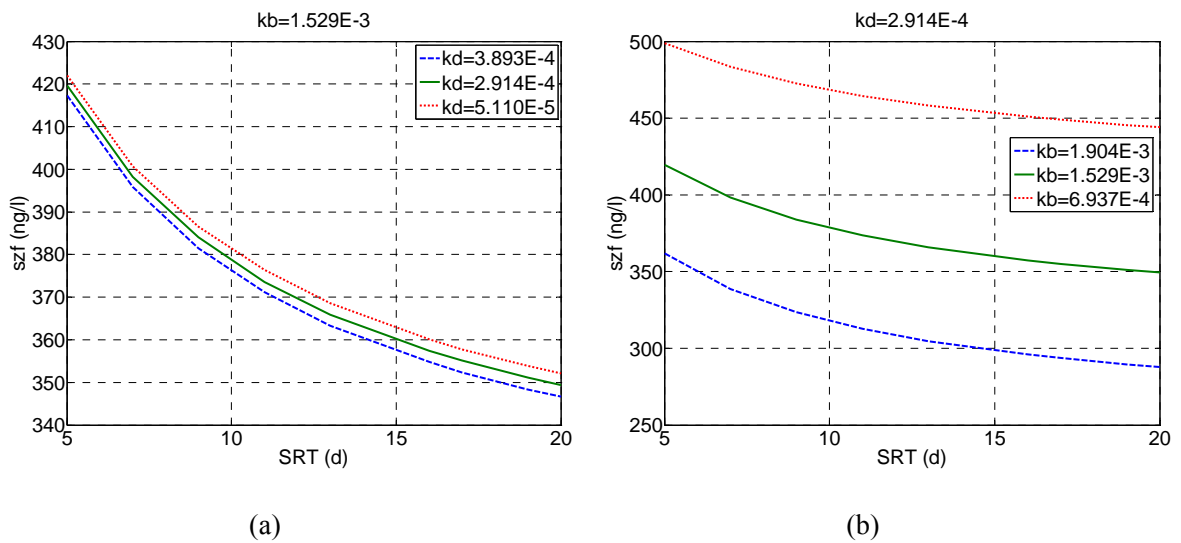
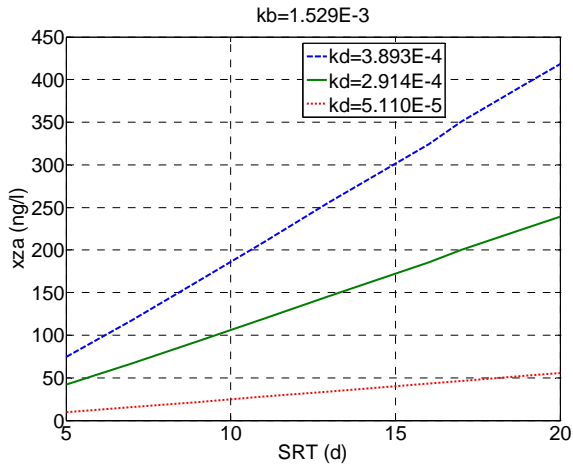
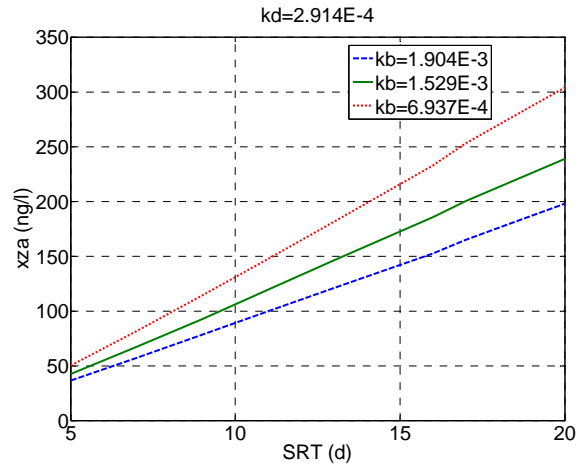


Figure 4.5 (a) Soluble SMX conc. in the effluent (S_zf) with respect to k_d in constant k_b (b) Soluble SMX in effluent (S_zf) with respect to k_b in constant k_d , Influent concentration of $S_zf= 210$ ng/l, HRT=10.8hr

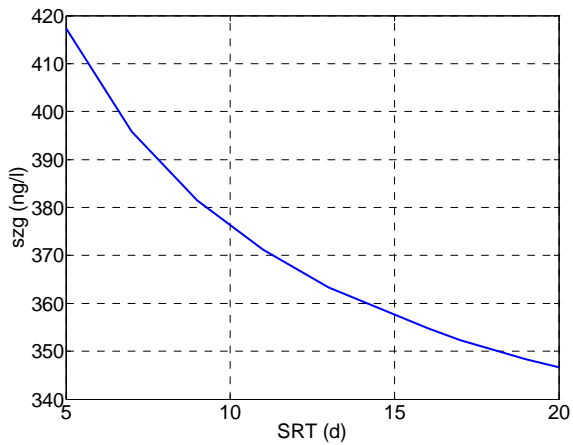


(a)

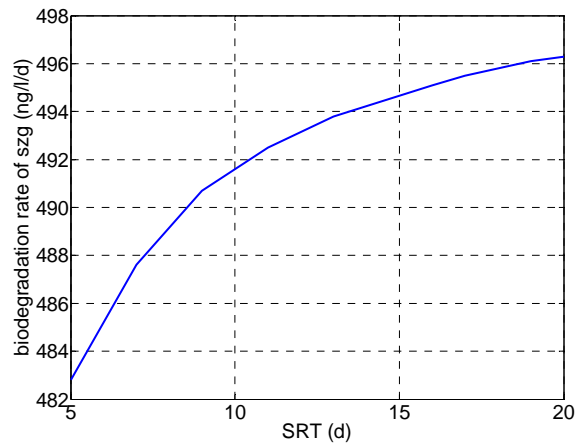


(b)

Figure 4.6 (a) Particulate SMX conc. in wastage flow (X_{za}) with respect to k_d in constant k_b (b) Particulate SMX conc. in wastage flow (X_{za}) with respect to k_b in constant k_d , Influent concentration of $X_{za}=0$, HRT=10.8hr

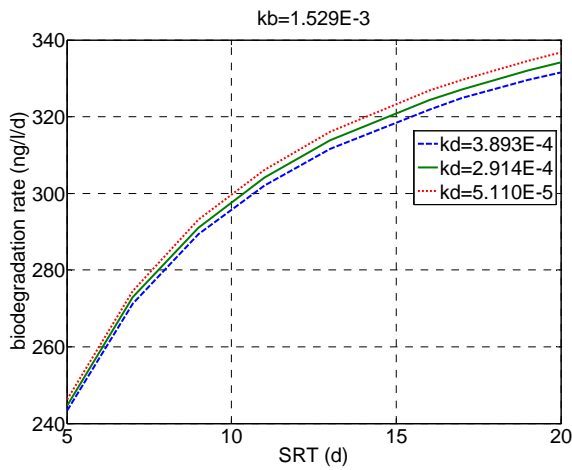


(a)

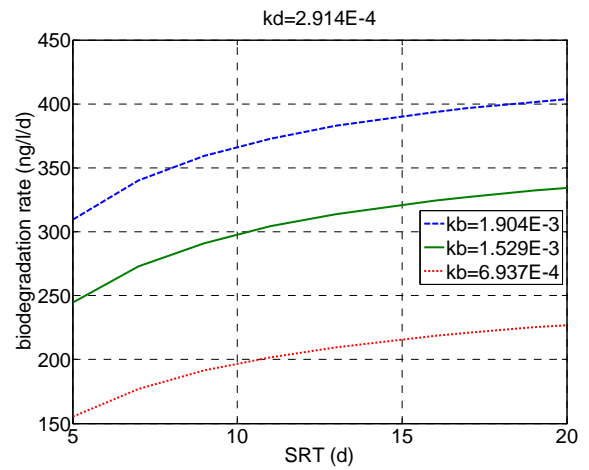


(b)

Figure 4.7 (a) S_{zg} conc. (b) and biodegradation rate for S_{zg} , Influent concentration of $S_{zg}=467$ ng/l, HRT=10.8hr

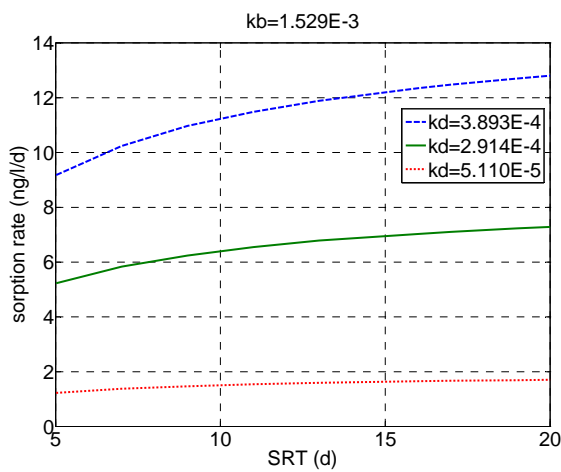


(a)

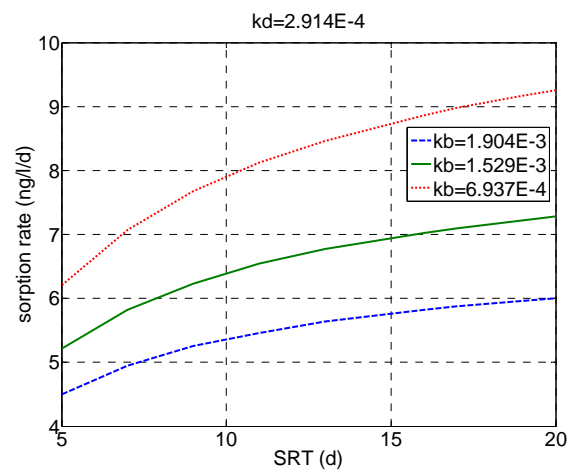


(b)

Figure 4.8 (a) Biodegradation rate for SMX with respect to k_d in constant k_b and (b) Biodegradation rate for SMX with respect to k_b in constant k_d , HRT=10.8hr



(a)



(b)

Figure 4.9 (a) Net sorption rate for SMX with respect to k_d in constant k_b and (b) Net sorption rate for SMX with respect to k_b in constant k_d versus SRT, HRT=10.8hr

To investigate the effect of biodegradation and solid liquid partitioning rate parameters on the removal of SMX, two different sets of plots (Figures 4.5-4.9) have been presented. The first set (Figures 4.5a-4.9a) shows the responses with three different solid liquid partitioning coefficient values ($kd = \mu + \sigma$, calibrated value and $\mu - \sigma$) at a fixed biodegradation rate coefficient (set to the calibrated value, $kb = 1.529E-3$). The second set demonstrates the effects of varying the biodegradation rate coefficient ($kb = \mu + \sigma$, calibrated value and $\mu - \sigma$) at a fixed solid liquid partitioning coefficient (set to the calibrated value, $kd = 2.914E-4$). The purpose of presenting these two sets of plots was to see the influence of these parameters on removal of XOCs.

Table 4.13 shows the percent of SMX removed, biotransformed and wasted at constant kb , SRT= 16 days, and HRT=10.8 hr. Increasing the value of kd resulted in a decrease of SMX in the soluble phase and an increase in the concentration of particulate SMX (X_{za}). Therefore, there was more removal in the liquid and solid phases (Figure 4.5a and Figure 4.6a). Furthermore, at constant kb , the higher kd has a higher net sorption rate, (Figure 4.9a) but a lower biodegradation rate, although, as can be seen in Figure 4.8, there was not a significant reduction of the biodegradation rate with higher kd values (Figure 4.8a). The concentration of particulate SMX (X_{za}) contributed to the wasted mass. Since X_{za} increases in the wastage flow by the sorption process the wastage percentage was positive, but the removal and biotransformed percentage due to increasing soluble SMX in effluent were negative.

Table 4.13 Quantified effects of kd on percentage of removed, biotransformed and wasted SMX

Rate Parameter		%removed*	%biotransformed*	%wasted
$Kb=1.529E-3$	$Kd1=3.893E-4$	-68.95	-78.35	9.40
	$Kd2=2.914E-4$	-70.19	-77.71	7.52
	$Kd3=5.110E-5$	-71.47	-77.06	5.59

* It should be noted that negative %removed and %biotransformed was because of biotransformation of metabolite to the SMX

Table 4.14 presents the percentage of SMX removed, biotransformed and wasted at constant kd with SRT= 16 days, HRT=10.8 hr. With kd constant, at the higher values of kb , the biodegradation rate increases (Figure 4.8b) and effluent concentration becomes lower (Figure 4.5b). Therefore, there is more removal in liquid phase; however, in this case, the sorption rate decreases (Figure 4.9b) and the particulate concentration in solid phase is lower (Figure 4.6b).

Table 4.14 Quantified effects of kb on percentage of removed, biotransformed and wasted SMX

Rate Parameter		%removed	%biotransformed	%wasted
$Kd=2.914E-4$	$Kb1=1.904E-3$	-41	-47.21	6.21
	$Kb2=1.529E-3$	-70.19	-77.71	7.52
	$Kb3=6.937E-4$	-114.76	-124.23	9.47

* It should be noted that negative %removed and %biotransformed was because of biotransformation of metabolite to the SMX

Generally, at higher SRTs, there was higher removal and biotransformation of SMX and a lower wasted percentage of SMX (Table 4.14). The wastage of SMX decreased with increasing SRT, because the wastage flow rate regulated for SRT control and this term was dominant in wastage of SMX (See Table 4.15). The negative removal efficiency and biotransformation were due to the conversion of the conjugate form to the parent compound (SMX) that compensated for the biodegradation of SMX. At higher SRT, more of SMX was biodegraded and at lower SRT, the conversion of the conjugated compound to parent compound dominated (Table 4.15).

Table 4.15 Variation of removed, biotransformed and wasted percentage of SMX at constant kb and kd , $kb=1.529E-3$, $kd=2.914E-4$, versus SRT, HRT=10.8hr

SRT (d)	%removed	%biotransformed	%wasted
5	-99.86	-121.86	22.00
9	-82.86	-94.89	12.03
13	-74.24	-83.03	8.79
16	-70.19	-77.71	7.52
20	-66.38	-72.86	6.48

* It should be noted that negative %removed and %biotransformed was because of biotransformation of metabolite to the SMX

Important results that can be obtained from sensitivity analysis in this section are as follows:

- Increases in SRT can enhance removal of SMX and its metabolite (daughter compound), since at higher SRT, there is higher removal efficiency and lower wasted of SMX and also lower effluent concentration of metabolite.
- Due to conversion of metabolite to the parent compound, net biotransformation of parent compound causes producing of this compound. Therefore, the removal efficiency and also biotransformation rate of SMX were negative.
- At SRT higher than 16 days, the removal efficiency does not change significantly, so SRT=16 days can be reported as the optimal SRT for this case.
- In the region of low SRT, the descending rate of effluent concentration of SMX is higher than that of higher region.
- Results of Table 4.13 and 4.14 show the removal efficiency is more sensitive to biodegradation rate than sorption rate.

4.3.1.2 Case study 2

Case study 2 addressed the sensitivity of NPEO responses to SRT. The effect of SRT on fCOD in effluent, and viable biomass, xbh in aeration basin, and TSS in aeration basin are presented here. Similar to the other case studies, the model employed in this case study is ASM-based. Hence, it takes advantage of xbh prediction in ASM-based model to address biodegradation and hydrolysis processes. The concentration of soluble COD (fCOD) in Figure 4.10a decreased by increasing SRT. The concentrations of active heterotrophic biomass (xbh) in Figures 4.10b and total suspended solid (TSS) in aeration in Figures 4.10c increased with increasing SRT.

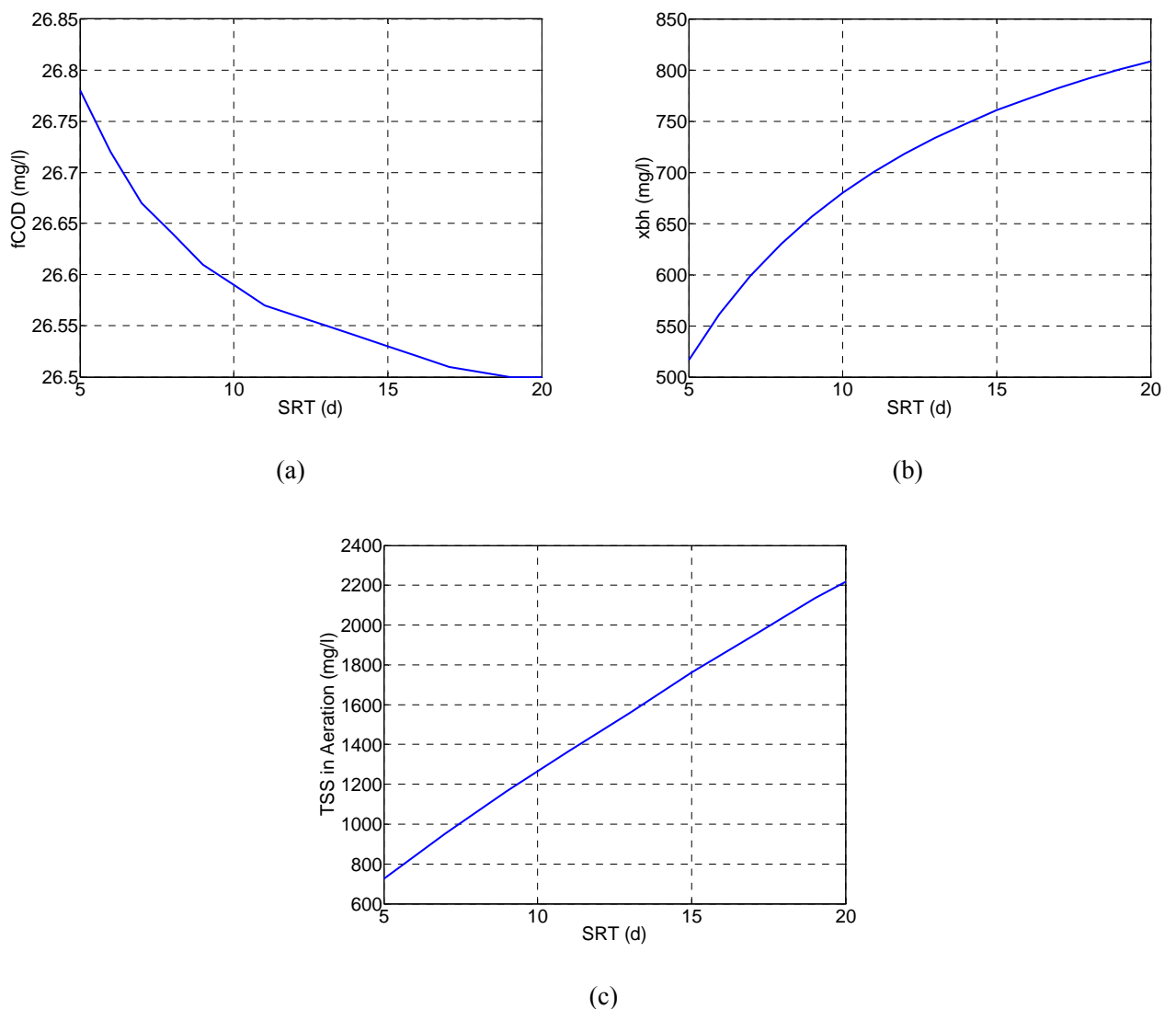


Figure 4.10. (a) Filtered COD (soluble COD), (b) Active heterotrophic biomass (xbh), (c) Total suspended solid (TSS) in aeration

This case study addressed the degradation of NPEO that involves multiple transformations including initial conversion of NPEO (S_{za}) to a readily biodegradable substrate (S_{zb}), a slowly biodegradable substrate (S_{zc}) and a non biodegradable substrate (S_{zd}) as a result of abiotic cleavage process. In addition, the slowly biodegradable substrate (S_{zc}) was converted to readily biodegradable substrate (S_{zb}) through a hydrolysis process. Since the cometabolism effect was involved in the biodegradation process of NPEO, the integration of cometabolism in models requires that both macropollutants (S_s) and micropollutant (NPEO) fate be modelled simultaneously.

Figure 4.11 depicts the effect of SRT on the effluent concentrations of S_{za} , S_{zb} and S_{zc} . The influent concentration of NPEO in the bulk liquid was 114 mg/l. HRT was set at 24 hours in this study. The concentration of NPEO in the bulk liquid (S_{za}) did not change with increasing SRT, because the abiotic cleavage process rate was not a function of biomass production in the reactor. The concentration of S_{zb} decreased with increasing SRT (Figure 4.11a), because of the increasing viable biomass concentration that increased the biodegradation rate of NPEO (Figure 4.11d). The concentration of S_{zc} decreased with SRT, as the hydrolysis process rate is also a function of viable biomass. By increasing the SRT, more S_{zc} is converted to S_{zb} , and this leads to reduction in concentration of S_{zc} over the range of SRT between 5 and 20 days.

Figure 4.11 also presents the final effluent concentrations and rate of biodegradation of NPEO that were predicted over a range of biodegradation rate coefficients that have been reported in the literature (kb). The upper and lower kb values are the $\mu \pm \sigma$, which μ is the mean of experimental data range on biodegradation rate parameter and σ is the standard deviation of experimental data. The intermediate curve (solid line) shows results with the previously calibrated value of kb . From this figure, it can be seen that, with increasing kb value, the reduction in S_{zb} , which was the biodegradable portion of NPEO, was about 60.83%. However, the reduction in S_{zb} over the range of SRT=5-20 days, with constant kb varied by 37.5%. This result shows that the fate of NPEO was more sensitive to the biodegradation rate constant than SRT. Due to different biodegradation rates that were reported in the literature, the different removal efficiency can be expected in practice due to the sensitivity of the model to the biodegradation rate constant.

Generally, at higher SRT, there was higher removal and more biodegradation; therefore, higher SRT provides a good operational condition for removal of NPEO. For SRT values higher than 15 days, the removal efficiency did not change significantly, i.e. SRT=15 days can be reported as optimum SRT for this case. At low SRT, the change in effluent concentration of NPEO with SRT was higher than

that at high SRT. As per different kb , at lower SRT, the difference between biodegradation rates is more significant than that at higher SRT. These results also can be seen in Figures 4.11 b.

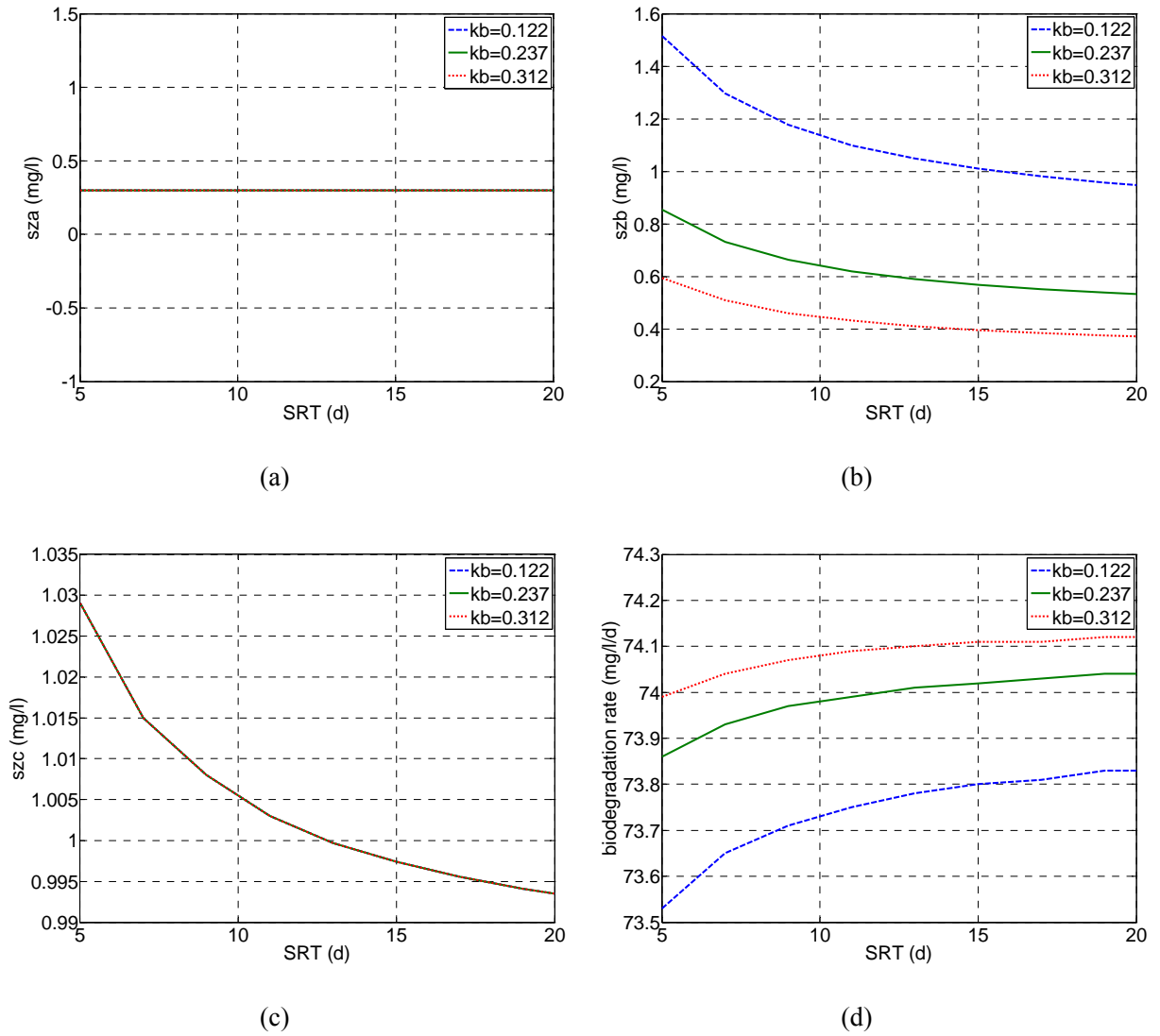


Figure 4.11. (a) CNPEO (Sz_a) (NPEO in the bulk liquid CNPEO), (b) SS,NPEO (Sz_b) (readily biodegradable substrate portion of NPEO), (c) SH,NPEO (Sz_c) (slowly biodegradable portion of NPEO) and (d) Biodegradation of NPEO with respect to different kb

4.3.1.3 Case study 3

In this section, the effect of SRT on the fate of the ionized compound Ibuprofen was investigated over a range of SRTs between 5 and 20 days. Biodegradation and sorption were the main mechanisms for the removal of this compound. Since pH is a crucial parameter for biodegradation of this compound, the effect of this parameter was investigated in section 4.3.3.

Similar to case studies 1 and 2, the responses of the conventional compounds, xbh and TSS versus SRT are also provided in this section, since the fate model addresses the fate of conventional and trace compounds simultaneously. Since xbh and TSS in aeration basin are important parameters in the biodegradation and sorption of Ibuprofen, the effect of SRT on the fate of this compound could be examined by looking at the xbh and TSS concentrations versus SRT. The concentrations of active heterotrophic biomass (xbh) in Figures 4.12a and total suspended solid (TSS) in aeration in Figures 4.12b were predicted to increase with increasing SRT.

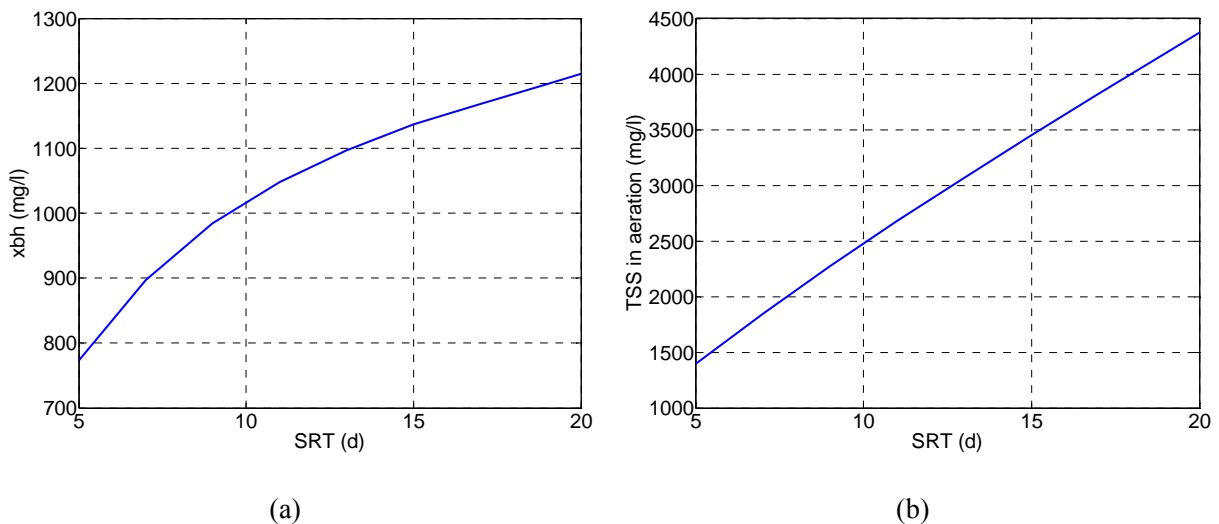


Figure 4.12 (a) Active heterotrophic biomass (xbh), (b) Total suspended solid (TSS) in aeration, HRT=12hr

Figure 4.13 shows the effect of SRT on the effluent concentrations of soluble ibuprofen in both the neutral and ionized forms. Figure 4.14 presents the corresponding solid phase concentrations. The influent concentrations of the neutral and ionized forms of Ibuprofen in the influent were $S_{zh}=24000$ ng/l and $S_{zi}= 4.3673E6$ ng/l. Since the availability of viable biomass increased with increasing SRT (Figure 4.12a), the concentration of total suspended solid (TSS) in aeration increased (4.12b), and as a result, the biodegradation rate of Ibuprofen also increased (Figure 4.15), which lead to a reduction in the concentration of the soluble compound in the effluent (Figure 4.13). The concentration of the

soluble compound in this case was the summation of the neutral and ionized forms of Ibuprofen. The concentration of the particulate compound (summation of neutral and ionized form of Ibuprofen) increased because of the increase of available solids (*TSS* in aeration) at higher SRT and higher sorption rate (Figure 4.14). Similar to case study 1, Figure 4.16 presents the net sorption rate for Ibuprofen in the neutral and ionized form, since the definition of sorption rate was in terms of sorption and desorption rates.

The concentrations of soluble and particulate Ibuprofen, and its biodegradation and sorption rates compound were predicted for three different biodegradation and sorption rate coefficients. The values consisted of the smallest value in the literature, the calibrated value, and the largest value in the literature. The purpose of presenting these two different series of plots (series 1: *kb* constant are equal to the calibrated value, series 2: *kd* constant and set to the calibrated value) was to see the influence of the parameters on the removal of Ibuprofen.

At constant *kb*, increasing the *kd* value caused the effluent concentration of the ionized compound in the soluble phase (*Szh* and *Szi*) to decrease, and the concentrations of the particulate species (*Xzb* and *Xzc*) to increase; therefore, there is a higher removal in the liquid and solid phases (Figure 4.13a and c, Figures 4.14a and c). Also at constant *kb*, the higher *kd* has a higher sorption rate (Figure 4.16a and c) but a lower biodegradation rate, because at a higher *kd*, the soluble phase concentration is lower that leads to reduction in biodegradation rate (Figure 4.15a and c). Details are presented in Table 4.16.

Table 4.16 Variation of removed, biotransformed and wasted percentage of Ibuprofen at constant *kb* with respect to *kd*, SRT= 15 days, HRT=12 hr

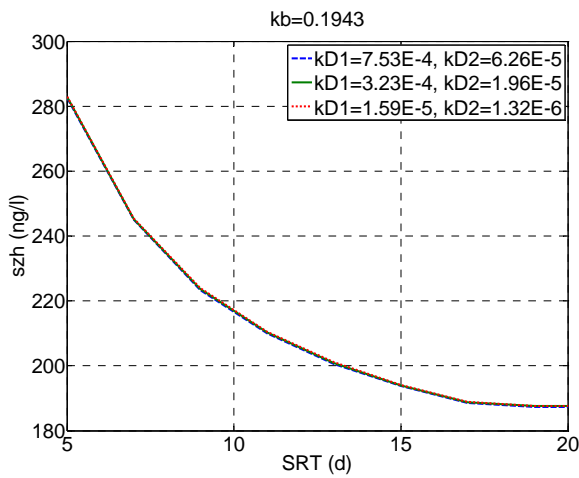
	Rate Parameter	%removed	%biotransformed	%wasted
Kb= 0.1943	Kd11=7.53E-4, Kd21=6.26E-5	99.23	98.79	0.44
	Kd12=3.24E-4, Kd22=1.96E-5	99.19	99.02	0.17
	Kd13=1.59E-5, Kd23=1.32E-6	99.07	99.01	0.06

When the value of *kd* was held constant *kb* was increased the biodegradation rate increased (Figures 4.15b, d), the effluent concentration was lower (Figures 4.13b, d), and there was an improved removal in the liquid phase. However the sorption rate decreased (Figure 4.16b and d) and the particulate concentration in the solid phase was lower, (Figure 4.14b, d). Table 4.17 presents details of these responses.

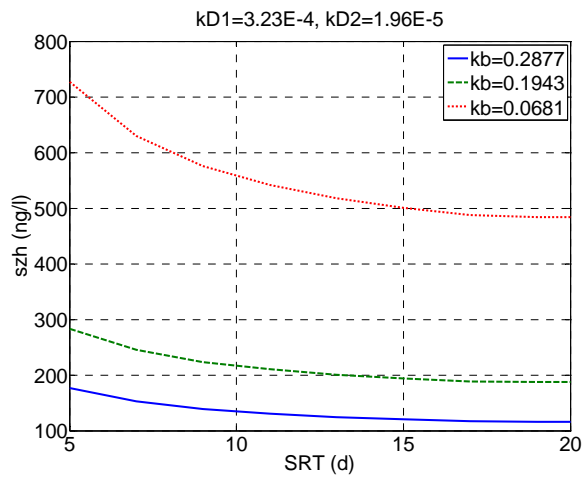
Table 4.17 Variation of removed, biotransformed and wasted percentage of Ibuprofen at constant kd with respect to kb , SRT= 15 days, HRT=12 hr

Rate Parameter		%removed	%biotransformed	%wasted
$Kd1=3.24E-4$, $Kd2=1.96E-5$	$Kb1=0.2877$	99.50	99.41	0.09
	$Kb2=0.1943$	99.19	99.02	0.17
	$Kb3=0.0681$	97.92	97.69	0.23

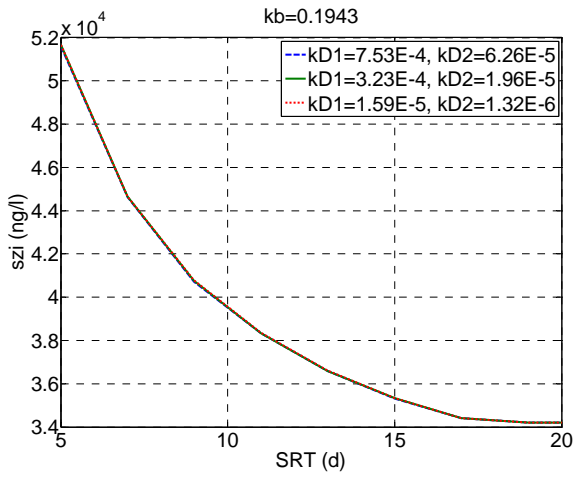
From Figure 4.13, it can be seen that, with increasing kb value at kd constant, the reduction in S_{zh} and S_{zi} , was about 75.96% and 75.93% respectively and the reduction of S_{zh} and S_{zi} with increasing kd at kb constant was just 0.154% and 0.085% respectively. However, the reduction in S_{zh} and S_{zi} over the range of SRT=5-20 days, with constant kb and kd was 33.6% and 33.8% respectively. This result shows that the fate of Ibuprofen was more sensitive to the biodegradation rate and SRT than the sorption rate constant. Due to different biodegradation and sorption rates that were reported in the literature, the different removal efficiency can be expected in practice due to the sensitivity of the model to the biodegradation rate constant.



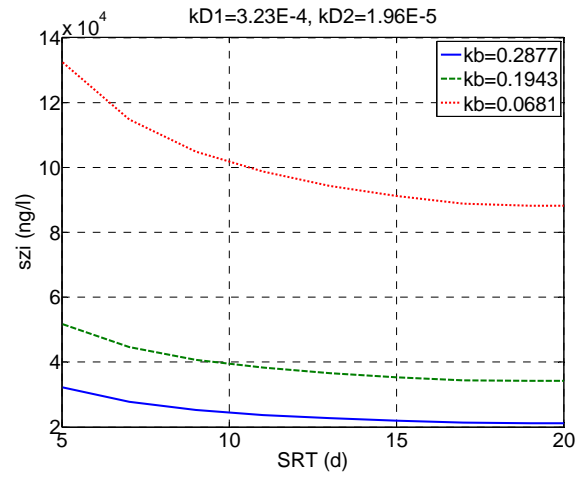
(a)



(b)

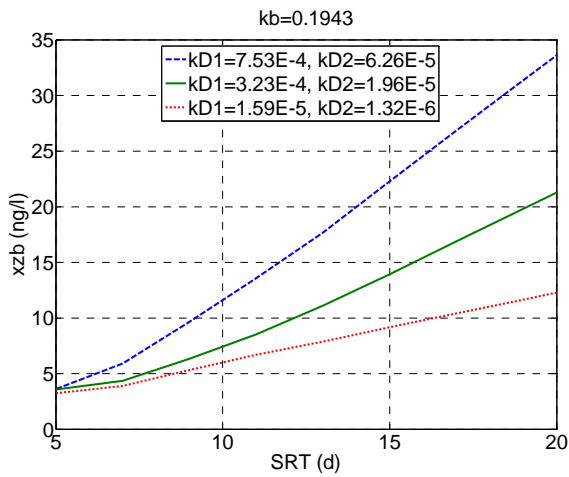


(c)

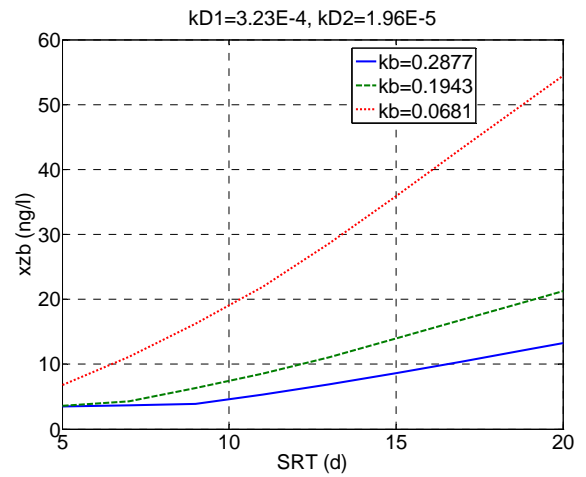


(d)

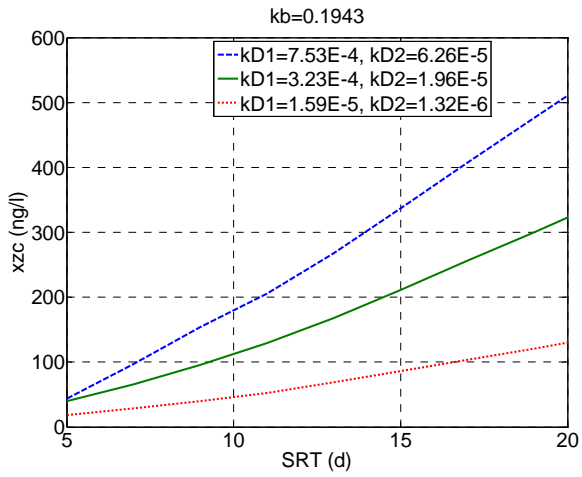
Figure 4.13. (a) Soluble Ibuprofen (neutral form) in effluent (Szh) with respect to kd in constant kb , (b) Soluble Ibuprofen (neutral form) in effluent (Szh) with respect to kb in constant kd , (c) Soluble Ibuprofen (ionized form) in effluent (Szi) with respect to kd in constant kb , and (d) Soluble Ibuprofen (ionized form) in effluent (Szi) with respect to kb in constant kd , Influent conc. of $Szh=24000$ ng/l, $Szi=4.3673E6$ ng/l, HRT=12hr



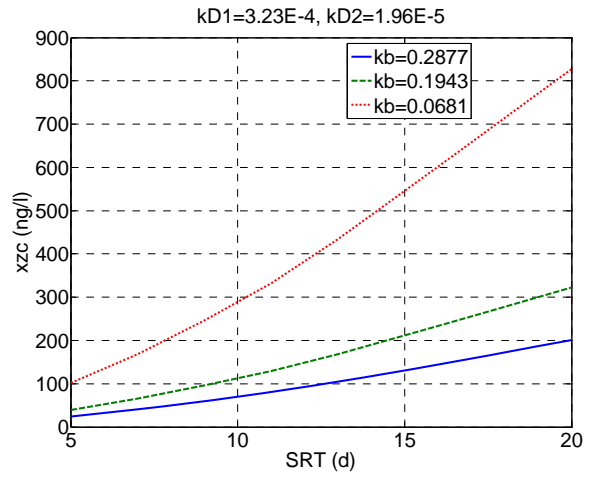
(a)



(b)

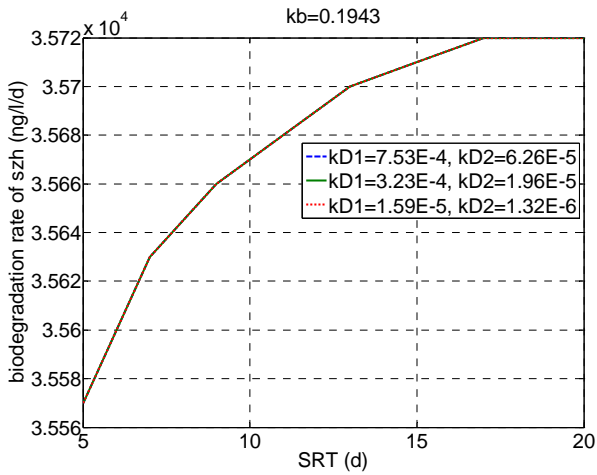


(c)

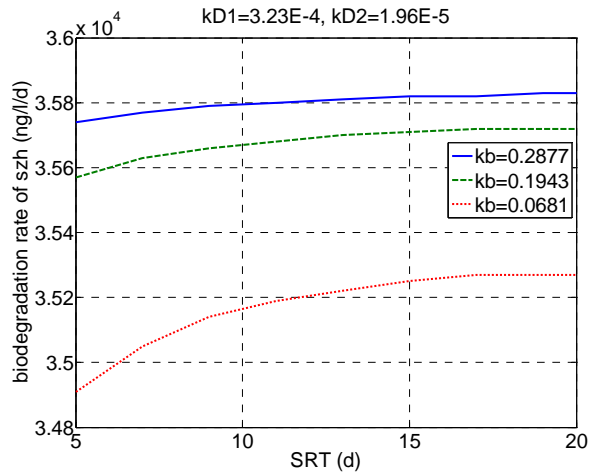


(d)

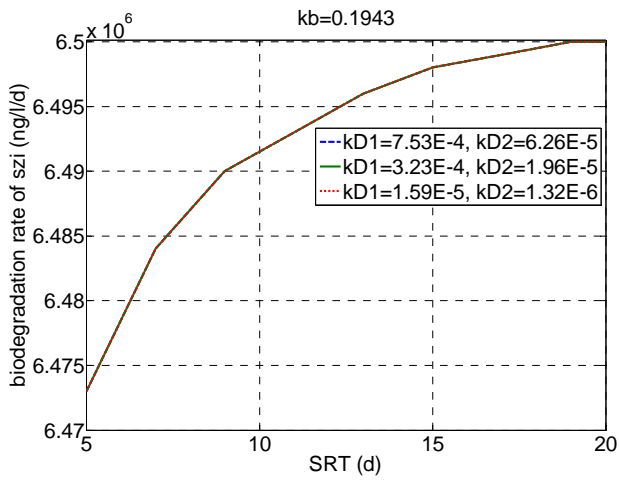
Figure 4.14. (a) Particulate Ibuprofen (neutral form) in effluent (X_{zb}) with respect to kd in constant kb , (b) Particulate Ibuprofen (neutral form) in effluent (X_{zb}) with respect to kb in constant kd , (c) Particulate Ibuprofen (ionized form) in effluent (X_{zc}) with respect to kd in constant kb , and (d) Particulate Ibuprofen (ionized form) in effluent (X_{zc}) with respect to kb in constant kd , Influent conc. of $X_{zc}=X_{zd}=0$, HRT=12hr



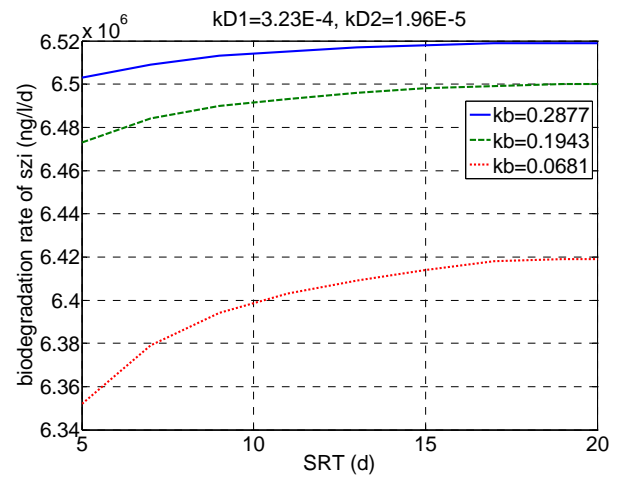
(a)



(b)

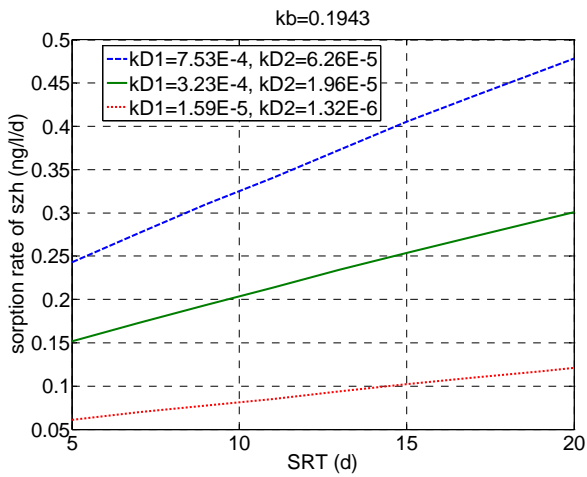


(c)

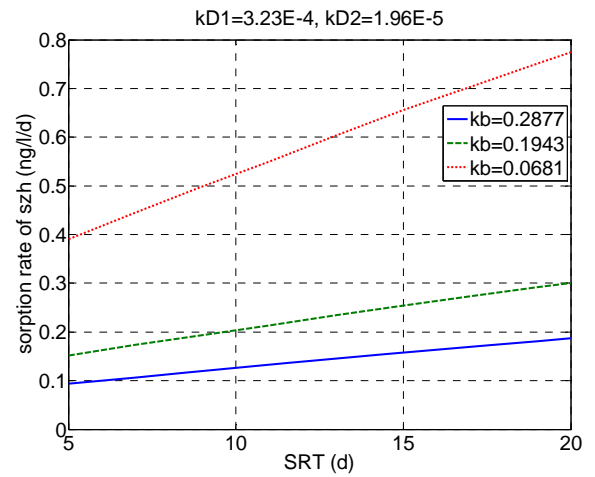


(d)

Figure 4.15. (a) Biodegradation rate for Ibuprofen (neutral form) with respect to kd in constant kb , (b) Biodegradation rate for Ibuprofen (neutral form) with respect to kb in constant kd , (c) Biodegradation rate for Ibuprofen (ionized form) with respect to kd in constant kb , and (d) Biodegradation rate for Ibuprofen (ionized form) with respect to kb in constant kd , HRT=12hr



(a)



(b)

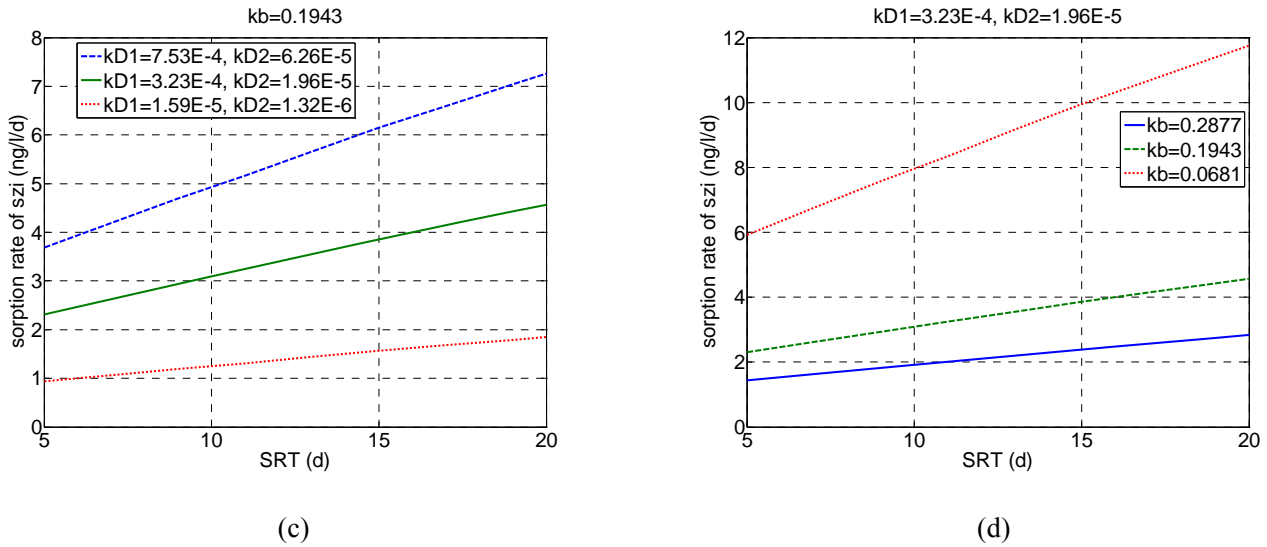


Figure 4.16. (a) Net sorption rate for Ibuprofen (neutral form) with respect to kd in constant kb , (b) Net sorption rate for Ibuprofen (neutral form) with respect to kb in constant kd , (c) Net sorption rate for Ibuprofen (ionized form) with respect to kd in constant kb , and (d) Net sorption rate for Ibuprofen (ionized form) with respect to kb in constant kd , HRT=12hr

Generally, at higher SRT, there was higher removal, biotransformation of Ibuprofen and a lower wasted percentage of this compound (Table 4.18).

Table 4.18 Variation of removed, biotransformed and wasted percentage of Ibuprofen at constant kb and kd , $kb=0.1943$, $kd1=3.24E-4$, $kd2=1.96E-5$, versus SRT, HRT=12

SRT (d)	%removed	%biotransformed	%wasted
5	98.82	98.65	0.17
9	99.07	99.05	0.018
13	99.16	99.15	0.011
17	99.21	99.202	0.008
20	99.22	99.213	0.007

Important conclusions that can be obtained from SRT sensitivity analysis in this section are as follows:

- Higher SRT provides a good operational condition for removal of Ibuprofen, since at higher SRT, there is higher removal efficiency and lower wasted of Ibuprofen.
- At SRT higher than 13 days, the removal efficiency does not change significantly, so SRT=13 days can be reported as the optimal SRT for this case.
- In the region of low SRT the decreasing rate of effluent concentration of SMX is higher than that higher SRT region.
- Results of Table 4.16 and 4.17 show the removal efficiency is more sensitive to biodegradation rate than sorption rate.

4.3.2 Effect of hydraulic retention time

The hydraulic retention time (HRT) of the aerobic reactor typically cannot be varied as an operational parameter. However it represents the time in the reactor during which the biomass can contact and utilize the XOCs as a secondary substrate. Hence, in this section, the effect of varying the aerobic reactor HRT was examined in each case study.

4.2.2.1 Case study 1

The effect of aeration hydraulic retention time on removal of SMX in Case study 1 was evaluated. For regulating HRT, the volume of aeration basin was changed and the range of HRT was between 5 and 24 hours. The concentrations of TSS and viable biomass in the aeration reactor decreased at higher HRT because of higher aeration volume (Figure 4.17).

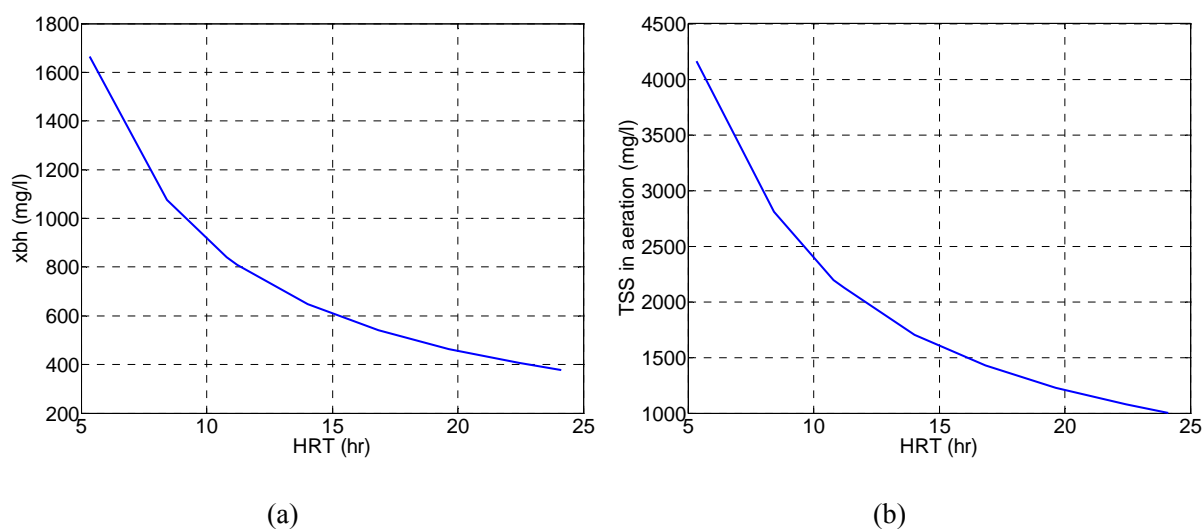


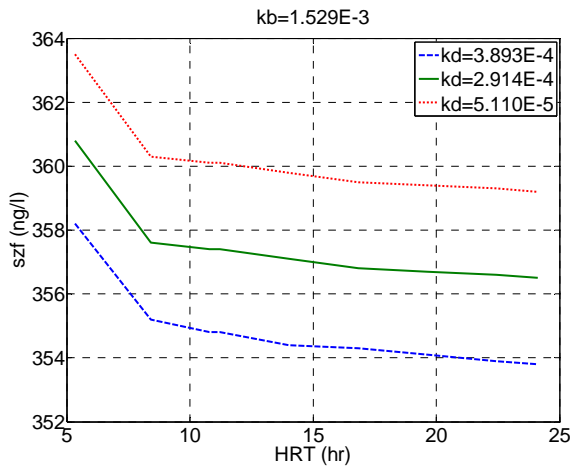
Figure 4.17. (a) Active heterotrophic biomass (x_{bh}), (b) Total suspended solid (TSS) in aeration, SRT=16d

In this analysis the influent concentrations of S_{zf} and S_{zg} were set at 210 and 467 ng/l respectively. The rate biodegradation of S_{zf} was found to decrease with increasing HRT (Figure 4.21) due to reduction in viable biomass (x_{bh}), (Figure 4.17a). However, the concentration of the soluble parent compound decreased, because the higher volume compensated for the lower biodegradation rate (Figure 4.18). The concentration of compound biotransformed via the parent compound (S_{zg}) decreased by increasing HRT (Figure 4.19a), although the biodegradation rate of this compound decreased. In this case, the higher volume compensated for the effect of the lower biodegradation

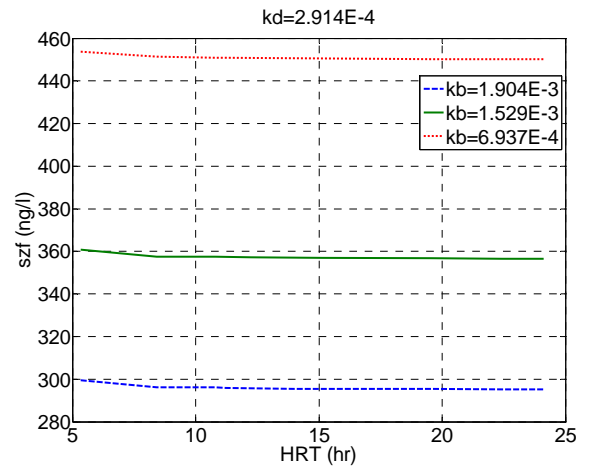
rate, (Figure 4.19b). The concentration of particulate SMX (X_{za}) in the wastage flow decreased at the higher HRT, (Figure 4.20) because of reduction in the TSS concentration in the aeration basin (Figure 4.17b), higher aeration volume and lower net sorption rate (Figure 4.22).

Figures 4.18-4.22 presents the responses for different biodegradation and sorption rate coefficients. These plots are similar in format to the plots presented in section 4.3.1.1. For example, with kd constant and a higher kb value, there was a lower effluent concentration in the liquid phase (Figure 4.18b) and a lower particulate compound concentration in the wastage flow (Figure 4.20b). At constant kb and higher kd values, there was a lower effluent concentration in liquid phase (Figure 4.18a) and higher particulate compound concentration in the wastage flow (Figure 4.20a). Higher kd values provided lower biodegradation rates, (Figure 4.21a) and higher net sorption rates (Figure 4.22a). On the other hand, higher kb values gave higher biodegradation rates (Figure 4.21b) and lower net sorption rates (Figure 4.22b). From these figures, it can be seen that, with increasing kb values at and kb constant, the reduction in Szf , was about 34% and the reduction of Szf with increasing kd at kb constant was just 1.47%. However, the reduction in Szf over the range of HRT= from 5 to 24 days, with constant kb and kd was 1.2%. This result shows that the fate of SMX was more sensitive to the biodegradation rate and sorption rate constants than HRT. Due to different biodegradation rates that were reported in the literature, the different removal efficiency can be expected in practice due to the sensitivity of the model to the biodegradation rate constant.

In Figure 4.18a and b, there was a sharp break in the curve around HRT= 8.5 days. That was due to the effects of two different phenomena, biodegradation of SMX and transformation of the conjugate to SMX, which are responsible for transformation of this compound. At HRT lower than 8.5, more conjugate compound is transformed to SMX, and for HRT higher than 8.5, there is lower amount of conjugate to be transformed. Therefore, the variations in concentration of SMX at HRT lower than 8.5 is more significant than that at higher SRT.

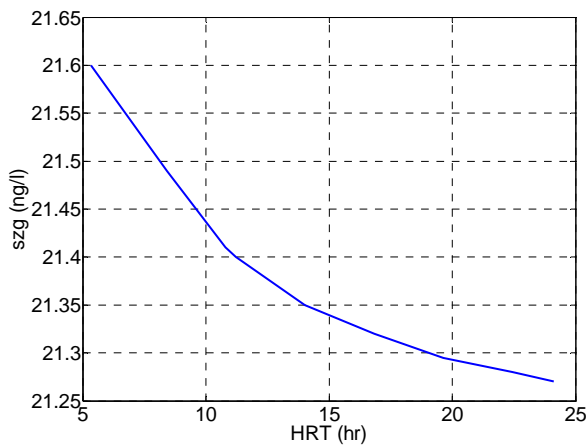


(a)

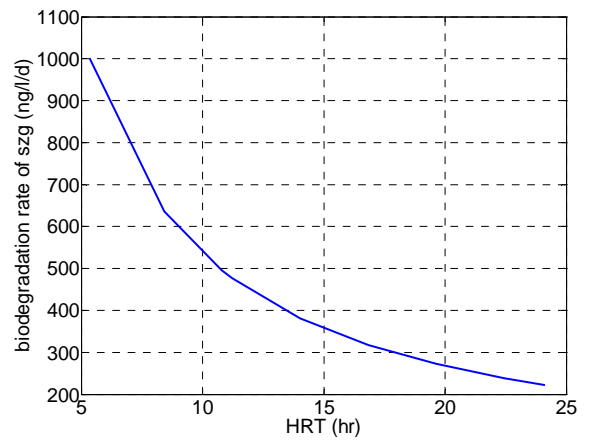


(b)

Figure 4.18. (a) Soluble SMX in effluent (S_{zf}) with respect to k_d in constant k_b and (b) Soluble SMX in effluent (S_{zf}) with respect to k_b in constant k_d , Influent concentration of $S_{zf} = 210$ ng/l, SRT=16d

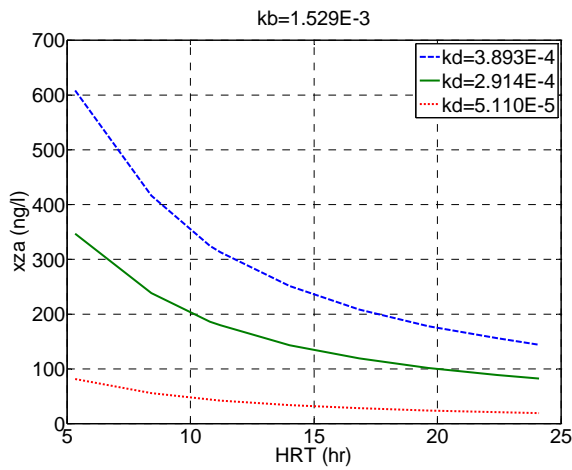


(a)

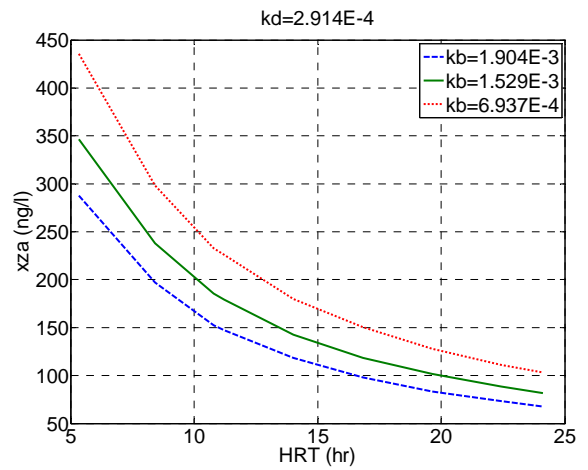


(b)

Figure 4.19. (a) S_{zg} and (b) Biodegradation rate for S_{zg} , SRT=16d

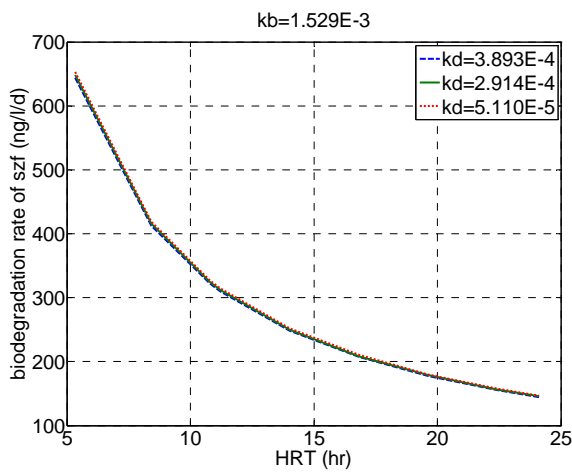


(a)

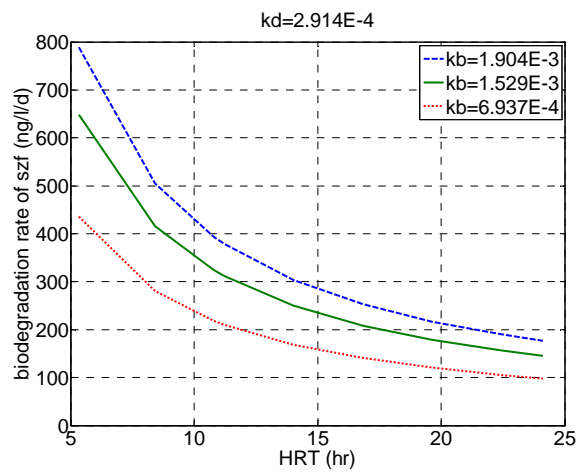


(b)

Figure 4.20. (a) Particulate SMX in wastage flow (X_{za}) with respect to k_d in constant k_b and Particulate SMX in wastage flow (X_{za}) with respect to k_b in constant k_d , Influent conc. of $X_{za}=0$, $SRT=16d$



(a)



(b)

Figure 4.21. (a) Biodegradation rate for SMX with respect to k_d in constant k_b and (b) Biodegradation rate for SMX with respect to k_b in constant k_d , $SRT=16d$

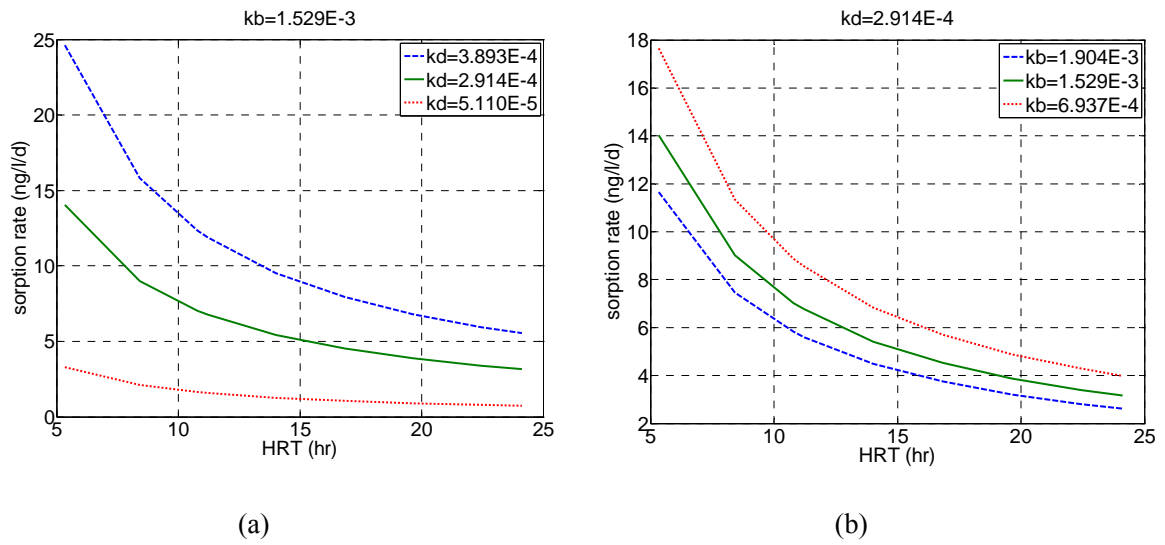


Figure 4.22. (a) Net sorption rate for SMX with respect to k_d in constant k_b and (b) Net sorption rate for SMX with respect to k_b in constant k_d , SRT=16d

The following conclusions were arrived at from the HRT sensitivity analysis:

- Higher HRT provides a reasonable operational condition for removal of SMX
- At HRT higher than 14 hours, the removal efficiency does not change significantly; therefore, HRT=10-14 hr according to also wasted percentage can be reported as the optimal HRT for this case.
- In the region of low HRT the decreasing rate of effluent concentration of SMX is higher than that of higher HRT region.

4.2.2.2 Case study 2

The effect of HRT on removal of NPEO component was studied. For regulating HRT, the aeration volume was changed and the range of HRT was between 7 and 24 hours. Figure 4.23 depicts the effect of HRT on fCOD in the effluent, viable biomass, x_{bh} in the aeration basin and also TSS in the aeration basin. Similar to case study 1, response of viable biomass (x_{bh}) versus HRT (Figure 4.23b) was used for the interpretation of other responses that described the effect of HRT on removal of NPEO. From Figure 4.23a it can be seen that the concentration of soluble COD (fCOD) decreased slightly with increasing HRT. The concentrations of active heterotrophic biomass (x_{bh}) in Figures 4.23b and total suspended solid (TSS) in aeration in Figures 4.23c decreased with increasing HRT because of the increase in the volume of aeration basin.

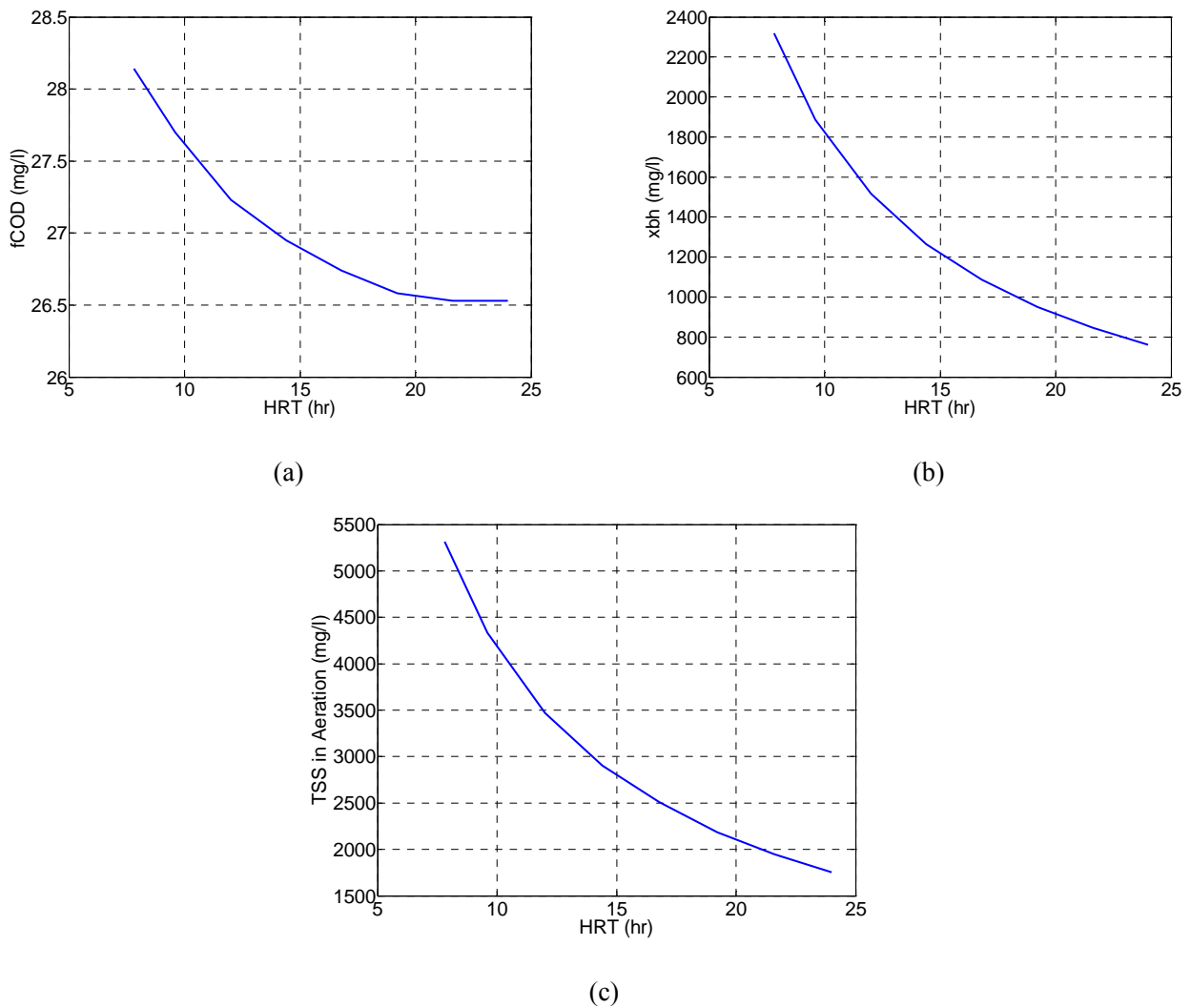
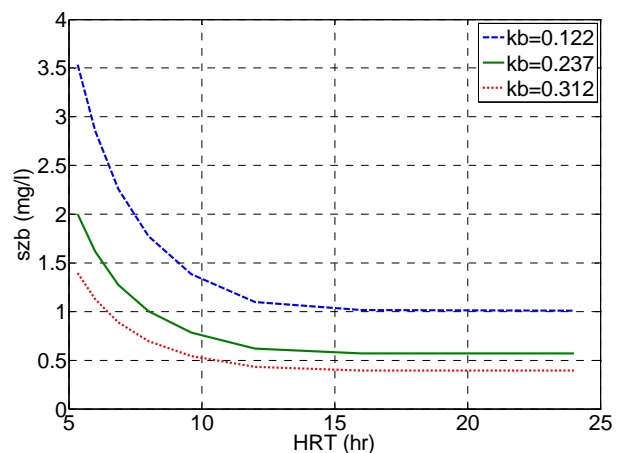
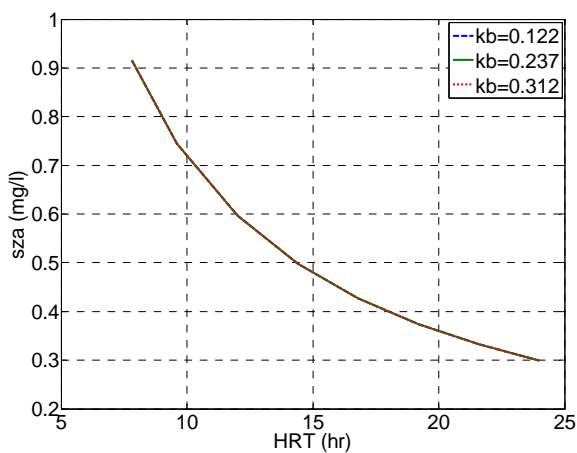


Figure 4.23. (a) Filtered COD (soluble COD), (b) Active heterotrophic biomass (x_{bh}), (c) Total suspended solid (TSS) in aeration, SRT=15d

Figures 4.24a, b and c depict the effect of HRT on the effluent concentrations of S_{za} , S_{zb} and S_{zc} , respectively. The concentration of NPEO in the bulk liquid decreased with increasing HRT (Figure 4.24a) while the concentration of S_{zb} decreased with increasing HRT (Figure 4.24b). The viable biomass is reduced with increasing HRT and this leads to a reduction in biodegradation and hydrolysis rates. However the higher volume compensated for these phenomena and as a result, the concentration of S_{zb} and S_{zc} decreases with increasing HRT.

Figures 4.24b and d also presented the responses for different biodegradation rate parameters kb , the upper and lower kb are the $\mu \pm \sigma$, where μ is the mean of experimental data range on biodegradation rate parameter and σ is the standard deviation of experimental data reported in the literature. The intermediate (solid) line presents results with the calibrated value for kb . Since different kb values affect only the biodegradation and hydrolysis rates, the concentration of S_{zb} changed with different kb . At higher kb , there was a lower concentration of S_{zb} in effluent. As there was not a large range of biodegradation rates of S_{zb} , the impact of different kb values for this species could not be discerned. From this figure, it can be seen that, with increasing kb value, the reduction in S_{zb} , which was the biodegradable portion of NPEO and at constant HRT and SRT was about 60.8%. However, the reduction in S_{zb} over the range of HRT=5-24 days, with constant kb was 70%. This result shows that the fate of NPEO was sensitive to both the biodegradation rate constant and HRT.

Generally, at higher HRT, there was higher removal and at HRT higher than 15 hours, the removal efficiency did not change significantly so HRT=15 days can be reported as optimum HRT for this case. At low HRT, the response of effluent concentration of NPEO to changes in kb was higher than that of the higher region.



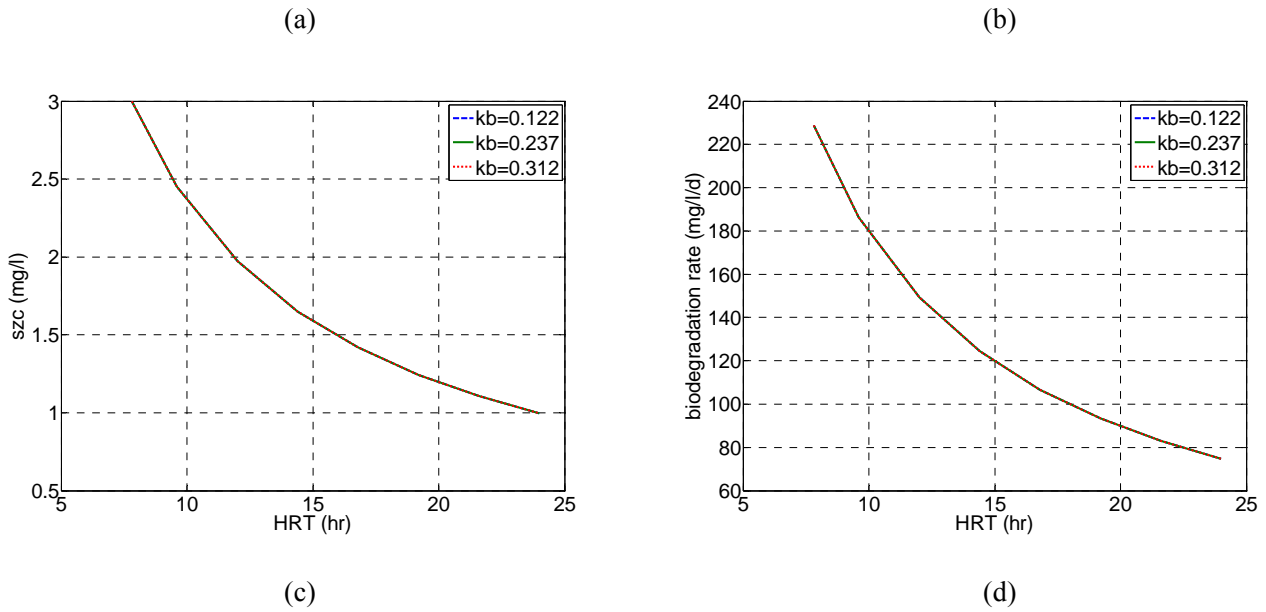


Figure 4.24 (a) CNPEO (S_{za}) (NPEO in the bulk liquid CNPEO), (b) SS,NPEO (S_{zb}) (readily biodegradable substrate portion of NPEO), (c) SH,NPEO (S_{zc}) (slowly biodegradable portion of NPEO) and (d) Biodegradation rate of NPEO with respect to different k_b , Influent conc. of S_{za} = 114mg/l, SRT=15d

4.3.2.3 Case study 3

In this section, the effects of Hydraulic Retention Time (HRT) on removal of an ionized compound (Ibuprofen) were investigated. For regulating HRT, the aeration volume was changed and the range of HRT was between 5 and 19 hours. The concentrations of TSS and viable biomass in the aeration reactor decreased at higher HRT and constant SRT because of the higher aeration volume (Figure 4.25).

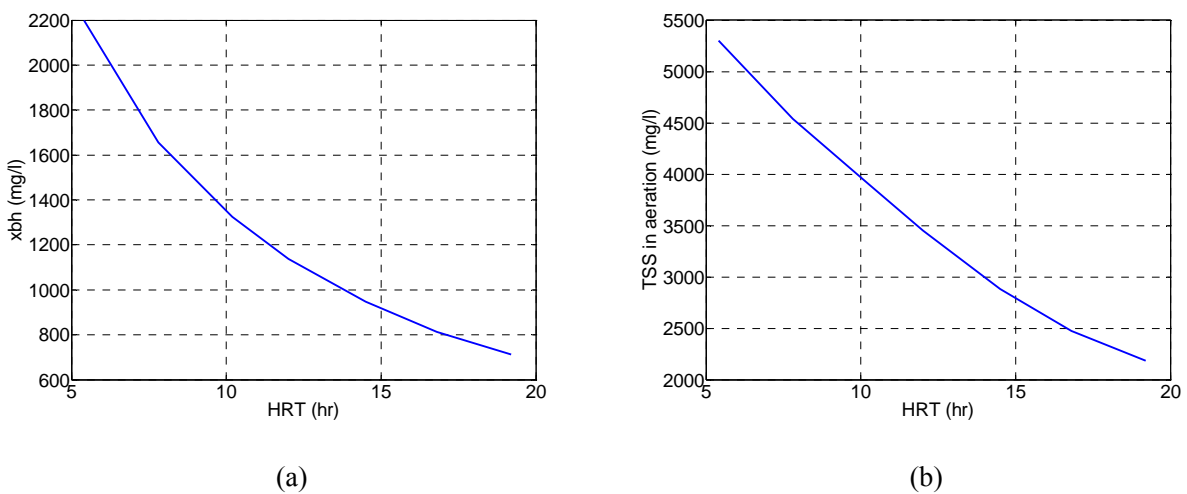
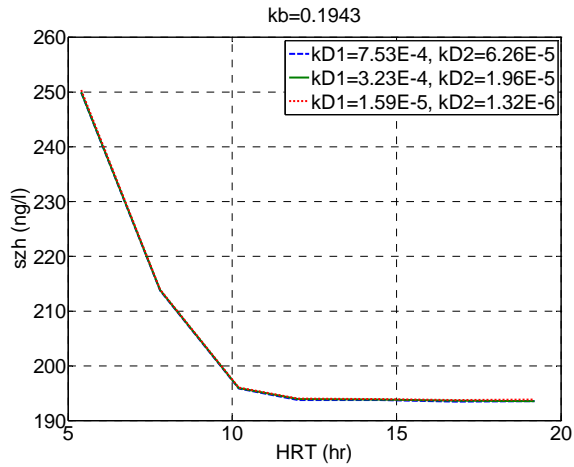


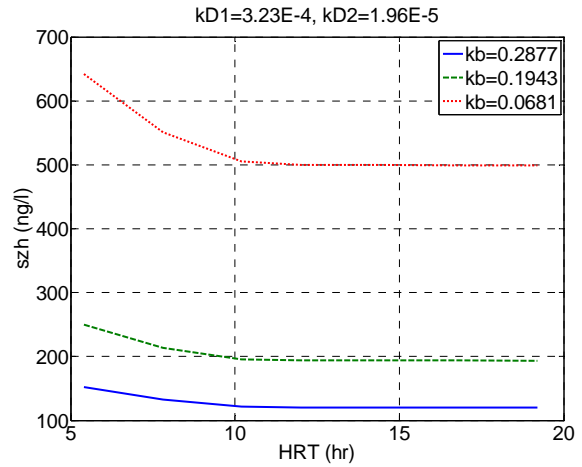
Figure 4.25. (a) Active heterotrophic biomass (x_{bh}), (b) Total suspended solid (TSS) in aeration, SRT=15d

The biodegradation rates for S_{zh} and S_{zi} were predicted to decrease with an increase in HRT (Figure 4.28) due to the reduction in viable biomass x_{bh} (Figure 4.25a). However, the concentrations of the soluble compounds (S_{zh} and S_{zi}) decreased, because the higher volume compensated for the lower biodegradation rate (Figure 4.26). The concentration of particulate Ibuprofen (X_{zb} and X_{zc}) in the wastage flow, decreased at higher HRT (Figure 4.27), because of the reduction in TSS concentration in aeration basin (Figure 4.25b), the higher aeration volume and lower net sorption rate (Figure 4.29).

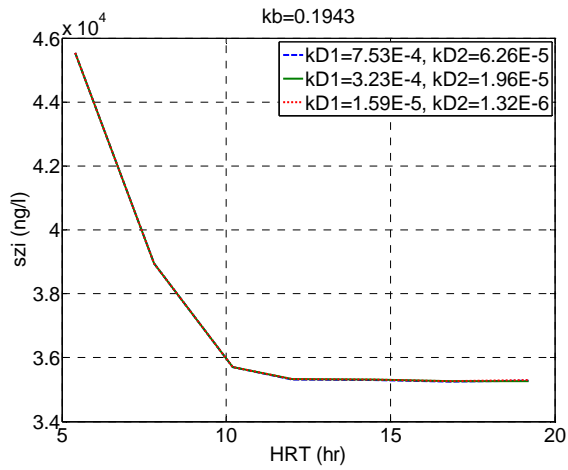
Figures 4.26-4.29 present the effect of different biodegradation and sorption rates on ibuprofen fate over a range of HRTs. The plots have similar formats to those of the SRT plots in section 4.3.1.3. For example, with constant kb , higher kd values result in lower effluent concentrations in the liquid phase (Figure 4.26a and c) and higher particulate compound concentrations in the wastage flow (Figure 4.27a and c). With kd constant and higher kb values there were lower effluent concentrations in the liquid phase (Figure 4.26 b and d) and lower particulate compound concentrations in the wastage flow (Figure 4.27b and d). Higher kd values provide lower biodegradation rates (Figure 4.28a and c) and higher net sorption rates (Figure 4.29a and c). On the other hand, higher kb values gives higher biodegradation rate (Figure 4.28b and d) and lower net sorption rates (Figure 4.29b and d). From this figure, it can be seen that, with increasing kb values and kd constant, the reduction in S_{zh} and S_{zi} , were about 75.96% and 75.93% respectively and the reduction of S_{zh} and S_{zi} with increasing kd at kb constant was just 0.154% and 0.085% respectively. However, the reduction in S_{zh} and S_{zi} over the range of HRT=5-19 days, with constant kb and kd was 22.6% and 29% respectively. This result shows that the fate of ibuprofen was more sensitive to the biodegradation rate and HRT than the sorption rate constant. Due to different biodegradation and sorption rates that were reported in the literature, the different removal efficiency can be expected in practice due to the sensitivity of the model to the biodegradation rate constant.



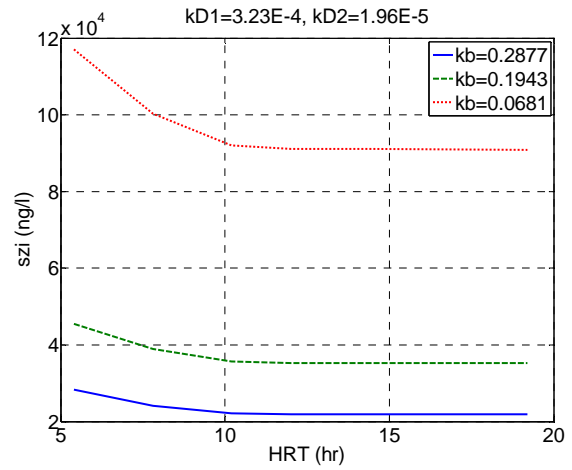
(a)



(b)

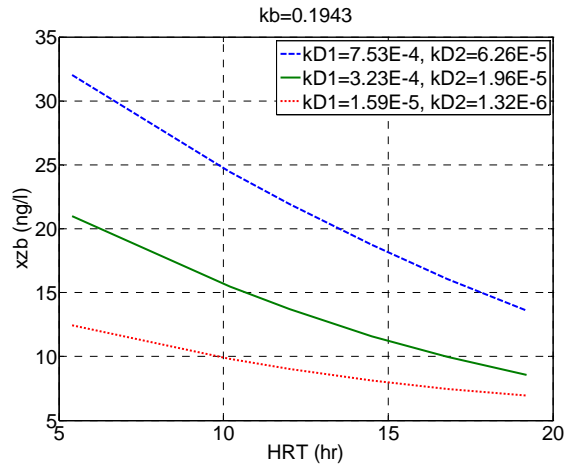


(c)

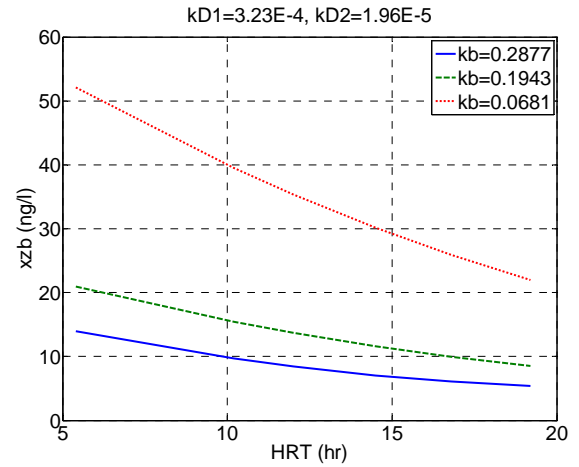


(d)

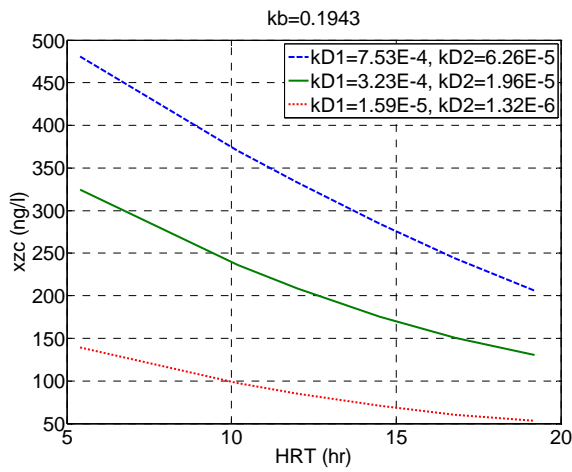
Figure 4.26 (a) Soluble Ibuprofen (neutral form) in effluent (S_{zh}) with respect to kd in constant kb , (b) Soluble Ibuprofen (neutral form) in effluent (S_{zh}) with respect to kb in constant kd , (c) Soluble Ibuprofen (ionized form) in effluent (S_{zi}) with respect to kd in constant kb , and (d) Soluble Ibuprofen (ionized form) in effluent (S_{zi}) with respect to kb in constant kd , Influent conc. of S_{zh} = 24000ng/l, S_{zi} = 4.3673E6ng/l, SRT=15d



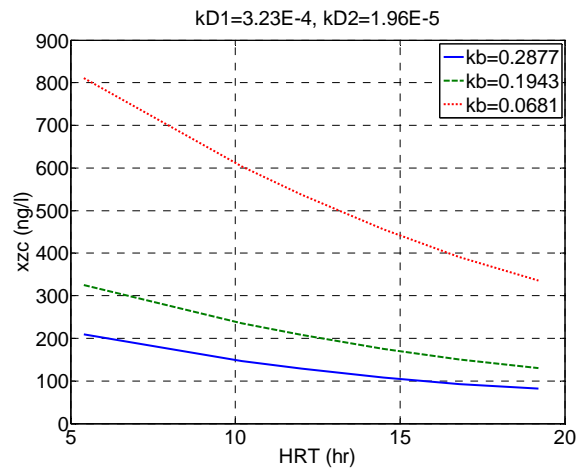
(a)



(b)

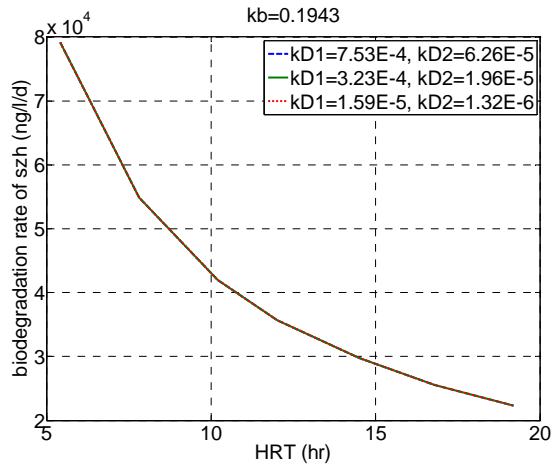


(c)

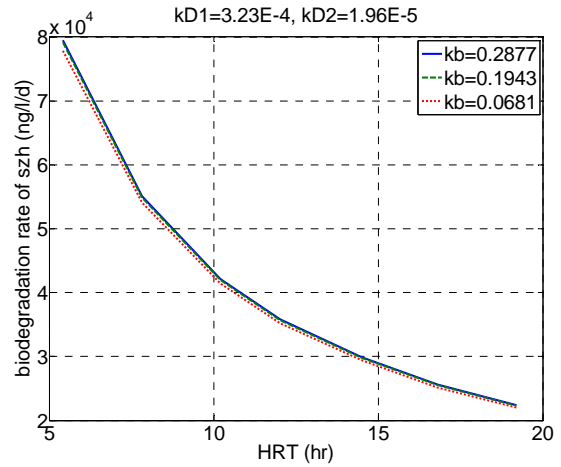


(d)

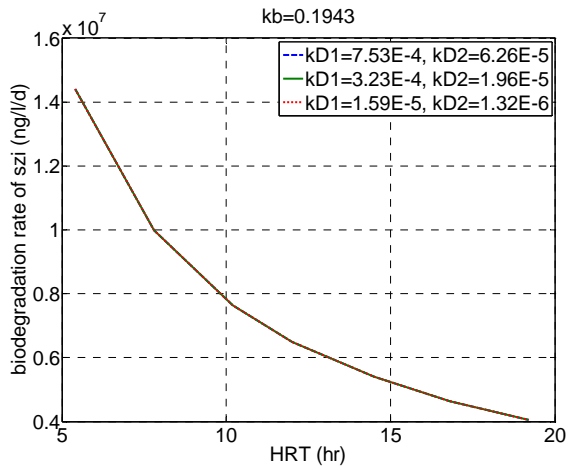
Figure 4.27 (a) Particulate Ibuprofen (neutral form) in effluent (X_{zb}) with respect to kd in constant kb , (b) Particulate Ibuprofen (neutral form) in effluent (X_{zb}) with respect to kb in constant kd , (c) Particulate Ibuprofen (ionized form) in effluent (X_{zc}) with respect to kd in constant kb , and (d) Particulate Ibuprofen (ionized form) in effluent (X_{zc}) with respect to kb in constant kd , Influent conc. of $X_{zb}=X_{zc}=0$, $SRT=15d$



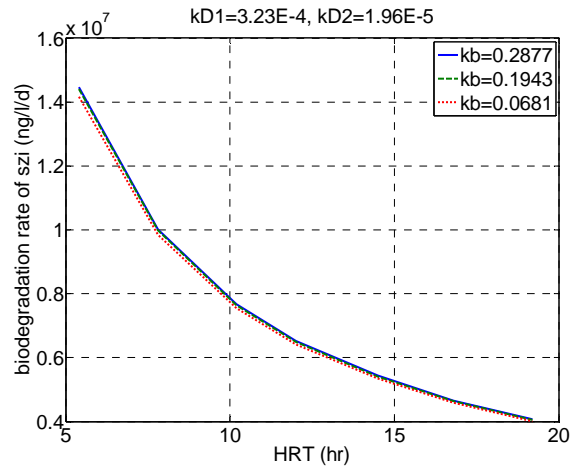
(a)



(b)

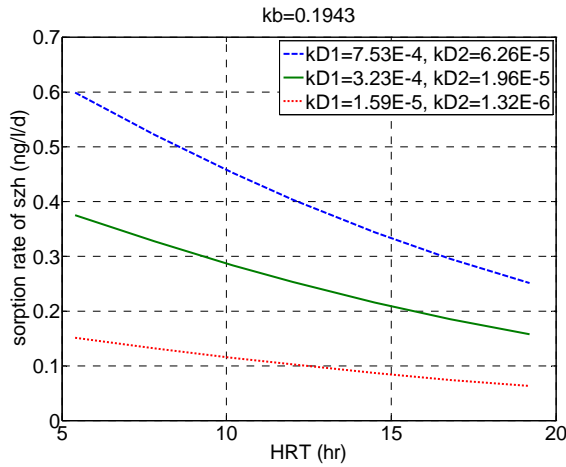


(c)

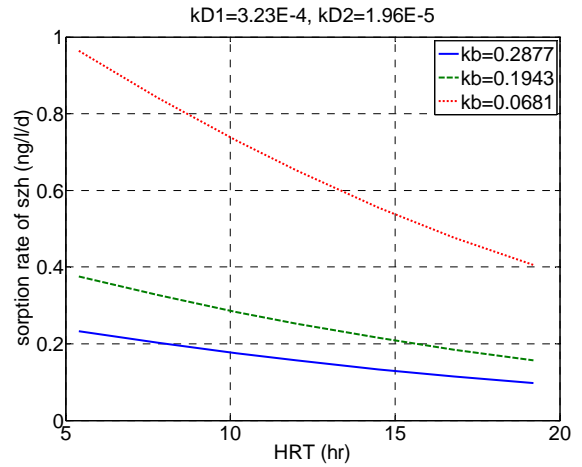


(d)

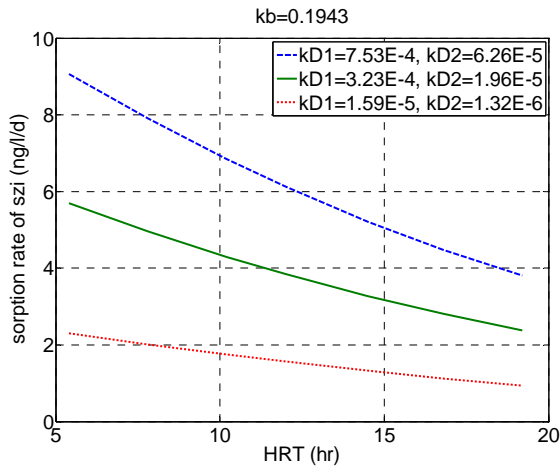
Figure 4.28 (a) Biodegradation rate for Ibuprofen (neutral form) with respect to kd in constant kb , (b) Biodegradation rate for Ibuprofen (neutral form) with respect to kb in constant kd , (c) Biodegradation rate for Ibuprofen (ionized form) with respect to kd in constant kb , and (d) Biodegradation rate for Ibuprofen (ionized form) with respect to kb in constant kd , SRT=15d



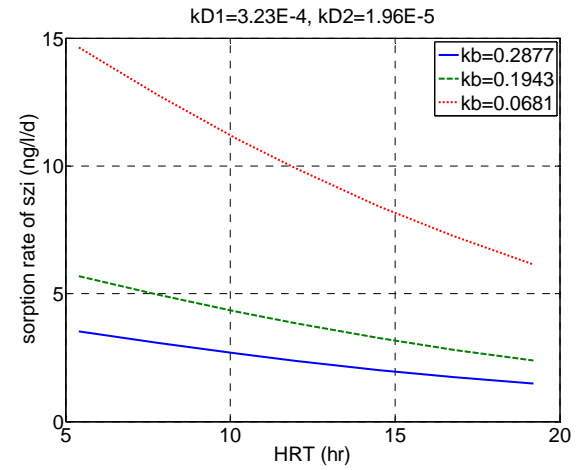
(a)



(b)



(c)



(d)

Figure 4.29. (a) Net sorption rate for Ibuprofen (neutral form) with respect to kd in constant kb , (b) Net sorption rate for Ibuprofen (neutral form) with respect to kb in constant kd , (c) Net sorption rate for Ibuprofen (ionized form) with respect to kd in constant kb , and (d) Net sorption rate for Ibuprofen (ionized form) with respect to kb in constant kd , $SRT=15d$

Important results that can be obtained from HRT sensitivity analysis in this section are as follows:

- Higher HRT provides a good operational condition for removal of Ibuprofen.
- At HRT higher than 10 hours, the removal efficiency does not change significantly, HRT=10hr is counted as optimum.
- In the region of low HRT, the decreasing rate of particulate concentration of Ibuprofen is higher than that in the higher HRT region.

4.3.3 Effect of pH-case study 3

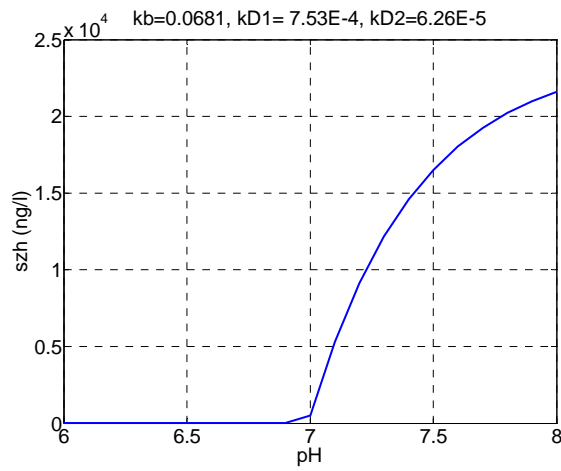
In this section, the effect of pH on removal of ionized compound was examined. pH was examined over the range of pH values from 6-8. Figure 4.30 displays this effect on removal of Ibuprofen for both the neutral and ionized forms of this compound in the solid and liquid phases. The biodegradation and sorption rates were presented in Figure 4.31.

At lower pH, there was a higher removal of the neutral form of ibuprofen (Figure 4.30a); and this is in good agreement with the literature that states in acidic condition, the ionized compounds behave like neutral compounds [41]. By increasing the pH, the concentration of the neutral form increased and the reduction in the biodegradation rate at higher pH supports this phenomenon (Figure 4.31a). On the other hand, with higher pH, there was better removal of the ionized form of ibuprofen (S_{zi}) (Figure 4.30a), but the trends in concentration were different in acidic and basic conditions as there was a sharp drop in concentration of S_{zi} in basic conditions. This was due to the structure of biodegradation process rate that includes the dissociation constant p_k , pH, etc (see case study 3 matrix model, Appendix F). The increase of biodegradation rate of S_{zi} supports this phenomenon (Figure 4.31b) as the soluble concentration of S_{zi} (4.30b) and biodegradation rate of S_{zi} (4.31b) mirror each other.

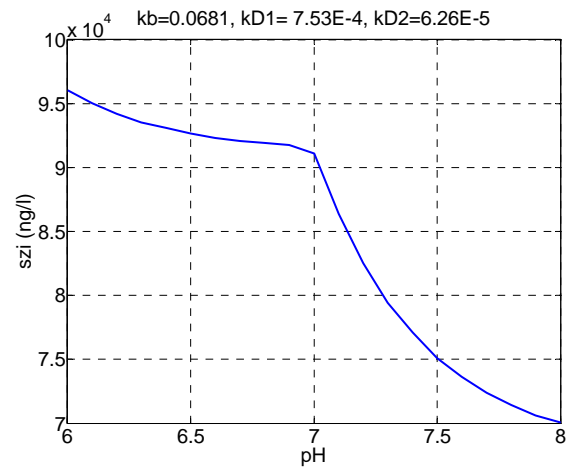
The concentration of compounds in the solid phase in the neutral form (X_{zb}) increased at higher pH values (Figure 4.30c), since the sorption rate increased at higher pH (Figure 4.31c). The concentration of the ionized form in the solid phase (X_{zc}) decreased at higher pH, but trends of reduction in acidic and basic condition were different (Figure 4.31d). The reduction of X_{zc} in basic conditions was sharper than that of acidic condition (Figure 4.30d). The reduction in sorption rate at higher pH supports that phenomenon (Figure 4.31d).

The following observations were drawn from the pH sensitivity analysis in this section:

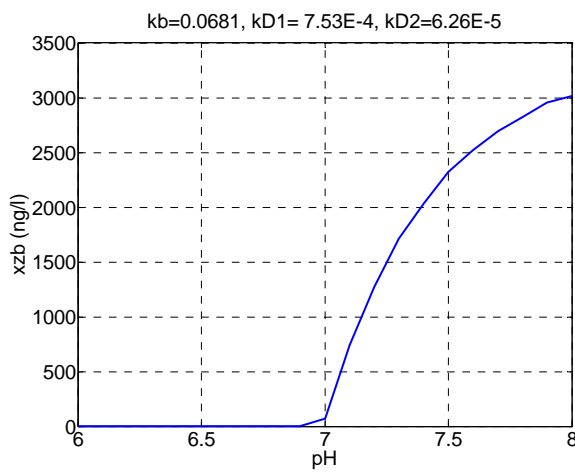
- Acidic condition provides better condition for removal of neutral form. On the other hand, basic condition provides suitable condition for removal of ionized form.
- Reduction of biodegradation rate for neutral form in acidic condition is sharper than that in basic condition (Figure 4.31a), and increasing rate in biodegradation rate of ionized form in basic condition is sharper than that in acidic condition (Figure 4.30b).
- Reduction rate in net sorption rate of ionized form in basic condition is sharper than acidic condition (Figure 4.31d), and increasing rate in net sorption of neutral form in basic condition is sharper than that in acidic condition (Figure 4.31c).



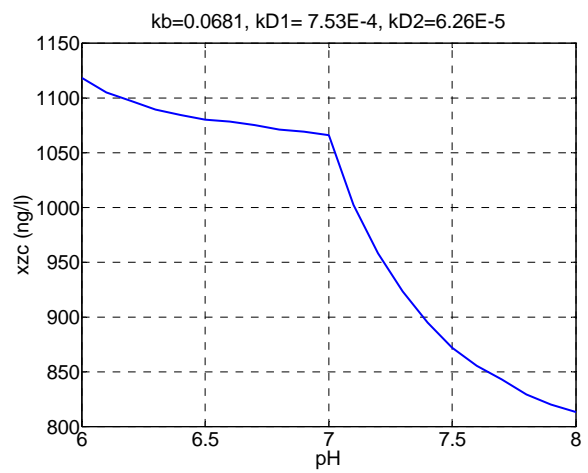
(a)



(b)

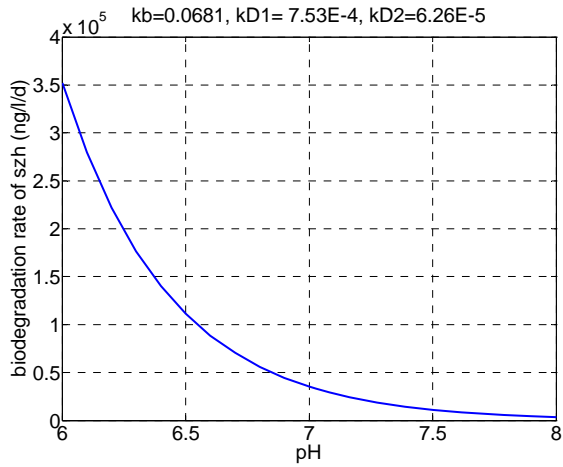


(c)

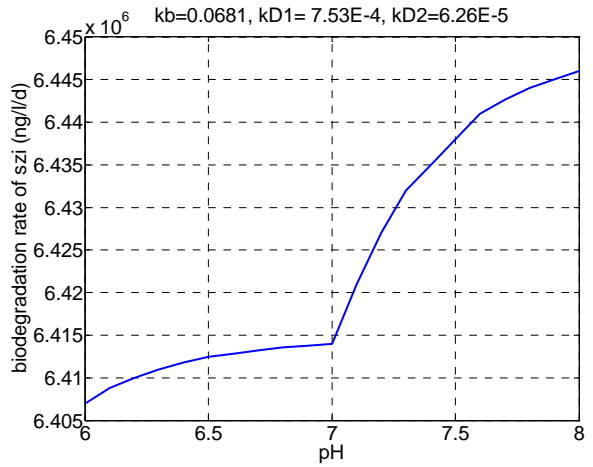


(d)

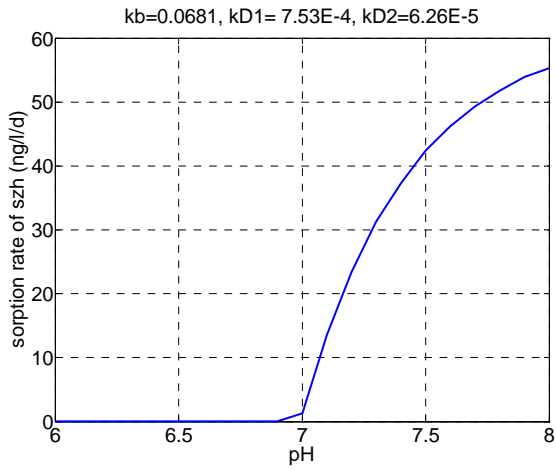
Figure 4.30 (a) S_{zh} , (b) S_{zi} , (c) X_{zb} , (d) X_{zc} in effluent flow versus pH, Influent conc. of $S_{zh}=24000\text{ng/l}$, $S_{zi}=4.3673E6\text{ng/l}$, $X_{zb}=X_{zc}=0$, HRT=12 hr, SRT=15 d



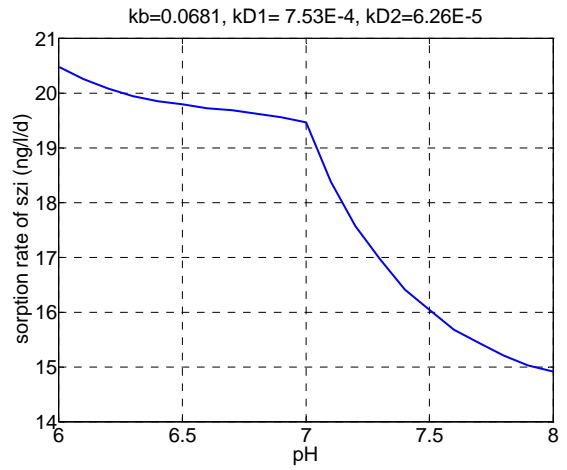
(a)



(b)



(c)



(d)

Figure 4.31 (a,b) Biodegradation and (c,d) Net sorption rate versus pH, HRT=12 hr, SRT=15 d

4.3.4 Chapter summary

In this chapter, the calibration employed for each case study was described. Following the calibration process, simulation results for each case study were reported. The comparison of each submodel against corresponding literature data (different from that used for calibration) was discussed.

Based on the sensitivity analysis reported in this section, the removal efficiency of XOCs was found to be sensitive to SRT, HRT, pH, kb and kd , although the fate model was more sensitive to kb and kd than to operational conditions. In wastewater treatment plants, varying the operational parameters, SRT, HRT, and pH imposes some costs to the plant. It is a fundamental engineering trade-off in WWTP between cost and removal efficiency. Depending on the allowable cost at the WWTP, the operation engineer can tune SRT, HRT and pH to improve removal efficiency. Additionally, based on various results shown on the sensitivity of the simulation outputs to the calibration parameters kb and kd , one can conclude that the results are considerably sensitive. This implies that although the integrated model of this thesis provides a novel framework for removing XOCs, a good source for these parameters is required.

CHAPTER 5

CONCLUSIONS AND RECOMMENDATIONS

5.1 Summary

A fate model was developed that can be used to better understand and optimize the removal of Xenobiotic Organic Compounds (XOCs) in combination with the removal of traditional pollutants in wastewater treatment plants. Through the modeling work, major mechanisms responsible for removal of XOCs in wastewater treatment were identified and integrated with an ASM1 model to create an uncalibrated model matrix. Activated sludge models (ASM) can differentiate between viable and non-viable biomass, so it was expected that ASM-based integrated fate models would be able to provide more accurate predictions of XOC fate over a range of operating conditions. Hence the development of an integrated fate and ASM model was employed in this research to have an improved estimate of the viable biomass.

Since specific groups of mechanisms were responsible for the removal of selected compounds, three different case studies were created for three different groups of compounds. Therefore, three different submodels were created and categorized within the fate model. Case Study 1 was categorized to express the removal of antibiotics like Sulfamethoxazole (SMX). Its removal mechanisms are biodegradation, sorption, and parent compound formation, with co-metabolism and competitive inhibition effects being inserted into the structure of the model. Removal mechanisms for Case Study 2, which is created for removing nonylphenol ethoxylates (NPEOs), are abiotic oxidative cleavage, hydrolysis, and biodegradation. The third case study includes removal of neutral and ionized XOCs through biodegradation and sorption.

Each submodel was calibrated separately for both conventional and trace compounds using available experimental data sets. The optimal model parameters for these data sets were obtained through a calibration process. The calibrated submodels were then integrated into the GPS-X modeling platform.

Using the model developer tool of the GPS-X software, the corresponding matrix components for each submodel (case study) were created. Each case study was simulated by implementing the corresponding layout and plant operational parameters within the GPS-X software. The validation process assessed the reliability of the model under the reported conditions. In this study, different data sets were used for the validation of the submodels; these results were discussed separately. From the

case studies, it was determined that the crucial controllable operational parameter for the target XOCs is the solids retention time (SRT), which has been identified in the literature. Hydraulic retention time (HRT), which is fixed by the process unit design volume and influent flow rate, is an example of a parameter that is relatively non-controllable. pH is another factor that mainly influences the removal of ionized compounds. The importance of the three aforementioned factors in removing XOCs was investigated via a sensitivity analysis in the GPS-X software. Other parameters in the proposed model, such as biodegradation and sorption rate coefficients (kb , kd) have been reported in the literature to span a range of values. Although values for these parameters were computed through the calibration process, a sensitivity analysis was performed separately for each case study to study the robustness of the simulation results.

The findings of this research can be summarized as follows:

- The removal efficiency of the SMX was found to be negative, because the conjugate was converted to SMX during the biotransformation process; this phenomenon compensates for biodegradation of SMX.
- The removal efficiency of XOCs was found to be sensitive to SRT, HRT, pH, kb and kd , although in most cases the fate model was more sensitive to kb and kd than to operational.
- Increases in SRT can enhance removal of all compounds that were studied in this research. Those compounds include SMX and its conjugate, NPEO, Ibuprofen (ionized compound) and Bisphenol-A (neutral compound)
- At SRT greater than 15 days, the removal efficiency in each case study does not change significantly, so 15 (days) can be reported as the optimal SRT.
- Higher HRT provides a good operational condition for removal of the compounds studied in this research. At HRT higher than 10-14 hours, the removal efficiency does not change significantly; HRT from 10 to 14 hr can be counted as optimum.
- Sensitivity analysis of three different cases showed that the fate model was more sensitive to biodegradation rate than to sorption rate.
- The study of pH effect in this thesis showed that for the ionized compound fate model, acidic condition provides better condition for removal of the neutral form. On the other hand, alkaline condition provides suitable condition for removal of the ionized form.

5.2 Recommendations

Although the integrated model of this thesis provides a novel framework for XOC fate simulation, recommendations for further study on the fate of XOCs compounds include the following:

- Various reliable sources of experimental data for both XOC and conventional compounds are important. The availability of this data for both conventional and trace compounds will lead to more robust and more accurate calibration and validation.
- There is a lack of information on XOCs transformation products in the aquatic systems that can impact the observed fate of the parent compounds in wastewater treatment. These products account for a broad range of compounds, including human conjugates, such as glucoronide, acetyl, sulphate; and other pharmaceuticals biotransformed via the parent compound. More experimental work is required to measure accurately the outcome of those compounds in wastewater treatment.
- Since a cometabolism mechanism is involved in the fate of most XOCs, the simultaneous measurement of primary substrate along with secondary substrate is required to better predict concentrations of trace organic compounds such as SMX and NPEO.

Bibliography

- [1] Barret, M., Patureau, D., Latrille, E., Carre`re, H., (2010). "A three-compartment model for micropollutants sorption in sludge: Methodological approach and insights." Water Research 44(2): 616-624.
- [2] Brooks, B.W., Foran, C.M., Richards, S.M., Weston, J., Turner, P.K., Stanley, J.K., Solomon, K.R., Slattery, M., La Point, T.W., (2003). "Aquatic ecotoxicology of fluoxetine" Toxicology Letters 142(3): 169-183.
- [3] Carballa, M., Omil, F., Juan, M. L. (2008). "Comparison of predicted and measured concentrations of selected pharmaceuticals, fragrances and hormones in Spanish sewage" Chemosphere 72(8): 1118-1123.
- [4] Carvalho, G., Novais, J.M., Pinheiro, H.M., Vanrolleghem, P.A., (2004). "Model development and application for surfactant biodegradation in an acclimatising activated sludge system." Chemosphere 54(10): 1495-1502.
- [5] Clara, M., Kreuzinger, N., Strenn, B., Gans, O., Kroiss, H., (2005). "The solids retention time--a suitable design parameter to evaluate the capacity of wastewater treatment plants to remove micropollutants." Water Research 39(1): 97-106.
- [6] Clara, M., Strenn, B., Kreuzinger, N. (2004). "Carbamazepine as a possible anthropogenic marker in the aquatic environment: investigations on the behaviour of Carbamazepine in wastewater treatment and during groundwater infiltration." Water Research 38(4): 947-954.
- [7] Clara, M., Strenn, B., Saracevic, E., Kreuzinger, N., (2004). "Adsorption of bisphenol-A, 17[beta]-estradiol and 17[alpha]-ethinylestradiol to sewage sludge." Chemosphere 56(9): 843-851.
- [8] Gaulke, L.S., Strand, S.E., Kalhorn, T.F., Stensel, H.D., (2009). "Estrogen Biodegradation Kinetics and Estrogenic Activity Reduction for Two Biological Wastewater Treatment Methods" Environmental Science & Technology 43(18): 7111-7116.
- [9] Göbel, A., McArdell, C.S., Joss, A., Siegrist, H., Giger, W., (2007) "Fate of sulfonamides, macrolides, and trimethoprim in different wastewater treatment technologies" Science of The Total Environment 372(2-3): 361-371.

- [10] Göbel, A., Thomsen, A., McArdell, C.S., Joss, A., Giger, W., (2005). "Occurrence and Sorption Behavior of Sulfonamides, Macrolides, and Trimethoprim in Activated Sludge Treatment" Environmental Science & Technology 39(11): 3981-3989.
- [11] Grady Jr, C. L., Daigger, G. T., Love, N. G., Filipe, C. D., Leslie Grady, C. P. (1999). Biological Wastewater Treatment, New York, Marcel Dekker.
- [12] Henze, M., Grady, C. P., Gujer, W., Marais, G. V. R., Matsuo, T. (1987). "A general model for single-sludge wastewater treatment systems" Water Research 21 (5): 505–515.
- [13] Henze, M., Gujer, W., Mino, T., van Loosdrecht, M. (2000). Activated Sludge Models ASM1, ASM2, ASM2d and ASM3. Scientific and Technical Report No 9. London, UK.
- [14] Jones, O. A. H., Voulvoulis, N., Lester, J. N. (2002). "Aquatic environmental assessment of the top 25 English prescription pharmaceuticals" Water Research 36(20): 5013-5022.
- [15] Joss, A., Andersen, H., Ternes, T., Richle, P. R., Siegrist, H. (2004). "Removal of Estrogens in Municipal Wastewater Treatment under Aerobic and Anaerobic Conditions: Consequences for Plant Optimization." Environmental Science & Technology 38(11): 3047-3055.
- [16] Joss, A., Keller, E., Alder, A. C., Göbel, A., McArdell, C. S., Ternes, T., Siegrist, H. (2005). "Removal of pharmaceuticals and fragrances in biological wastewater treatment" Water Research 39(14): 3139-3152.
- [17] Joss A., Zabczynski, S., Göbel, A., Hoffmann, B., Löffler, D., McArdell, C. S., Ternes, T.A., Thomsen, A., Siegrist, H. (2006). "Biological degradation of pharmaceuticals in municipal wastewater treatment: Proposing a classification scheme." Water Research 40(8): 1686-1696.
- [18] Joss, A. S., H.; Ternes, T. A. (2008). "Are we about to upgrade wastewater treatment for removing organic micropollutants" Water Sci. Technol. 57 (2): 251-255.
- [19] Karahan, Ö., Olmez-Hanci, T., Arslan-Alaton, I., Orhon, D., (2010). "Modelling biodegradation of nonylphenol ethoxylate in acclimated and non-acclimated microbial cultures" Bioresource Technology 101(21): 8058-8066.
- [20] Khan, S. J. and Ongerth, J. E., (2004). "Modelling of pharmaceutical residues in Australian sewage by quantities of use and fugacity calculations" Chemosphere 54(3): 355-367.
- [21] Kupper, T., Plagellat, C., Brändli, R. C., de Alencastro, L. F., Grandjean, D., Tarradellas, J. (2006). "Fate and removal of polycyclic musks, UV filters and biocides during wastewater treatment" Water Research 40(14): 2603-2612.

- [22] Langford, K. H. and K. V. Thomas (2009). "Determination of pharmaceutical compounds in hospital effluents and their contribution to wastewater treatment works." Environment International 35(5): 766-770.
- [23] Li, B. and Zhang, T., (2010). "Biodegradation and Adsorption of Antibiotics in the Activated Sludge Process" Environmental Science & Technology 44(9): 3468-3473.
- [24] Li, F., Yuasa, A., Obara, A., Mathews, A.P., (2005). "Aerobic batch degradation of 17-[beta] estradiol (E2) by activated sludge: Effects of spiking E2 concentrations, MLVSS and temperatures." Water Research 39(10): 2065-2075.
- [25] Lindblom, E., Press-Kristensen, K., Vanrolleghem, P. A., Mikkelsen, P. S., Henze, M., (2009). "Dynamic experiments with high bisphenol-A concentrations modelled with an ASM model extended to include a separate XOC degrading microorganism." Water Research 43(13): 3169-3176.
- [26] Lindblom, E., Gernaey, K., Henze, M., Mikkelsen, P. (2006). "Integrated modelling of two xenobiotic organic compounds" Water Sci. Technol. 54 (6-7): 213–221.
- [27] Maoz, A. and B. Chefetz (2010). "Sorption of the pharmaceuticals carbamazepine and naproxen to dissolved organic matter: Role of structural fractions." Water Research 44(3): 981-989.
- [28] Monteith, H., Andres, H., Snowling, S. and Schraa, O. (2008). "Modeling the Fate of Estrogenic Hormones in Municipal Wastewater Treatment" Proc. WEFTEC08: 3477-3495.
- [29] Ottmar, K. J., Colosi, L. M., Smith, J. A. (2010). "Sorption of statin pharmaceuticals to wastewater treatment biosolids, terrestrial soils, and freshwater sediment" J Environ Eng 136(3): 256–264.
- [30] Plósz, B. G., Leknes, H., Thomas, K. V. (2010). "Impacts of Competitive Inhibition, Parent Compound Formation and Partitioning Behavior on the Removal of Antibiotics in Municipal Wastewater Treatment" Environmental Science & Technology 44(2): 734-742.
- [31] Press-Kristensen, K. (2007). "Biodegradation of Xenobiotic Organic Compounds in Wastewater Treatment Plants" Institute of Environment & Resources. Lyngby, Denmark, The Technical University of Denmark. Ph.D.: 57.
- [32] Schwarzenbach, R.P., Gschwend, P.M., Imboden, D.M., (2003) , Environmental Organic Chemistry. New York, Wiley.

- [33] Racz, L., and Goel, R. (2009). "A Systematic Approach to Evaluate the Biodegradation Kinetics of Estrogens by Nitrifying Activated Sludge" Proc. WEFTEC09: 2571-2590.
- [34] Siegrist, H., Joss, A., Ternes, T. and Oehlmann, J. (2005). "Fate of EDCs in wastewater treatment and EU perspective on EDC regulation" Proc. WEFTEC05: 3142-3164.
- [35] Stuer-Lauridsen, F., Birkved, M., Hansen, L. P., Holten Lützhøft, H. C., Halling-Sørensen, B., (2000). "Environmental risk assessment of human pharmaceuticals in Denmark after normal therapeutic use" Chemosphere 40(7): 783-793.
- [36] Suárez, S., Carballa, M., Omil, F., Lema, J. M. (2008). "How are pharmaceutical and personal care products (PPCPs) removed from urban wastewaters?" Reviews in Environmental Science and Biotechnology 7(2): 125-138.
- [37] Suarez, S., Lema, J. M., Omil, F., (2010). "Removal of Pharmaceutical and Personal Care Products (PPCPs) under nitrifying and denitrifying conditions" Water Research 44(10): 3214-3224.
- [38] Tchobanoglous, G., Burton, F. L. and Stensel, H. D., (2004). Wastewater Engineering, Treatment, Disposal, Reuse, Metcalf & Eddy, Inc., McGraw-Hill Publishing Company Ltd.
- [39] Ternes, T. A., Herrmann, N., Bonerz, M., Knacker, T., Siegrist, H., Joss, A., (2004). "A rapid method to measure the solid-water distribution coefficient (K_d) for pharmaceuticals and musk fragrances in sewage sludge." Water Research 38(19): 4075-4084.
- [40] Ternes, T. A., Joss, A. (Eds.). (2006). "Human Pharmaceuticals, Hormones and Fragrances, The Challenge of Micropollutants in Urban Water Management" London, IWA Publishing.
- [41] Urase, T. and Kikuta, T., (2005). "Separate estimation of adsorption and degradation of pharmaceutical substances and estrogens in the activated sludge process" Water Research 39(7): 1289-1300.
- [42] Zabczynski S., Felis E., Ternes T.A., Miksch K., (2009). "Fate of PPCPs in sequencing batch reactor (SBR)" Water Research 2(3): 127-132.
- [43] Kim, J. Y., Ryu, K., Kim, E. J., Choe, W. S., Cha, G. C., Yoo, I. K. (2007). "Degradation of bisphenol A and nonylphenol by nitrifying activated sludge." Process Biochemistry 42(10): 1470-1474.
- [44] Yang, S. F., Lin, C. F., Yu-Chen Lin, A., Hong, P. K. (2012). "Fate of sulfonamide antibiotics in contact with activated sludge e Sorption and biodegradation." Water Research 46: 1301-1308.

- [45] Stevens-Garmon, J, Drewes, J.E., Khan, S.J., McDonald, J.A., Dickenson, E.R.V. (2011). "Sorption of emerging trace organic compounds onto wastewater sludge solids" Water Research 45: 3417-3426.
- [46] Hyland, K.C., Dickenson, E.R.V., Drewes, J.E. and Higgins, C.P. (2012). "Sorption of ionized and neutral emerging trace organic compounds onto activated sludge from different wastewater treatment configurations" Water Research 46: 1958-1968.
- [47] Smyth, Sh. A., (2012) "Occurrence and fate of pharmaceuticals and personal care products in municipal waste water treatment systems" Water science and Technology, Environment Canada
- [48] Leifer A., (1988) "The Kinetics of Environmental Aquatic Photo-chemistry: Theory and Practice" American Chemical Society, Washington D.C.
- [49] Metcalfe, C.D., Koenig, B.G., Bennie, D.T., Servos, M., Ternes, T.A., Hirsch, R. (2003) "Occurrence of neutral and acidic drugs in the effluents of Canadian sewage treatment plants" Environmental Toxicology and Chemistry 22: 2872-80.
- [50] Buser, H.R., T. Poiger, M.D. Muller (1999) "Occurrence and environmental behavior of the chiral pharmaceutical drug ibuprofen in surface waters and in wastewater" Environmental Science & Technology 33: 2529-35.
- [51] Bendz D., Paxeus, N.A., Ginn, T.R., Loge, F.J., (2005) "Occurrence and fate of pharmaceutically active compounds in the environment, a case study: Hoje River in Sweden" Journal of Hazardous Materials. 122: 195-204.
- [52] Clara, M., Strenn, B., Gans, O., Martinez, E., Kreuzinger, N. Kroiss, H., (2005) "Removal of selected pharmaceuticals, fragrances and endocrine disrupting compounds in a membrane bioreactor and conventional wastewater treatment plants" Water Research 39: 4797-807.
- [53] Castiglioni S., Bagnati, R., Fanelli, R., Pomati, F., Calamari, D., Zuccato, E., (2006) "Removal of pharmaceuticals in sewage treatment plants in Italy" Environmental Science & Technology. 40: 357-63.
- [54] Kasprzyk-Hordern B., Dinsdale, R.M., Guwy, A.J., (2009) "The removal of pharmaceuticals, personal care products, endocrine disruptors and illicit drugs during wastewater treatment and its impact on the quality of receiving waters"(vol 43, pg 363), Water Research. 44: 2076-2086.

- [55] Tixier C., Singer, H.P., Oellers, S., Muller, S.R., (2003) "Occurrence and fate of carbamazepine, clofibrac acid, diclofenac, ibuprofen, ketoprofen, and naproxen in surface waters" Environmental Science & Technology 37: 1061-8.
- [56] Andreozzi R., Raffaele M., Nicklas P., (2003) "Pharmaceuticals in STP effluents and their solar photodegradation in aquatic environment" Chemosphere. 50: 1319-30.
- [57] Packer, J.L., Werner, J.J., Latch, D.E., McNeill, K., Arnold, W.A., (2003) "Photochemical fate of pharmaceuticals in the environment: Naproxen, diclofenac, clofibrac acid, and ibuprofen. Aquatic Sciences", Environmental Science & Technology 65: 342-51.
- [58] Yamamoto, H., Nakamura, Y., Moriguchi, S., Honda, Y., Tamura, I., Hirata, Y., Honda, Y., Hayashi, A., Sekizawa, J. (2009) "Persistence and Partitioning of Eight Selected Pharmaceuticals in the Aquatic Environment: Laboratory Photolysis, Biodegradation, and Sorption Experiments" Water Research 43: 351-62
- [59] ECB (European Chemical Bureau), (2003) "Isopropylidenediphenol (Bisphenol A). European Union Risk Assessment Report, Institute for Health and Consumer Protection" European Commission. 302 pp.
- [60] Kjølholt, J., Nielsen, P., Stuer-Lauridsen, F., (2003) "Endocrine disrupting compounds and pharmaceuticals in wastewater" Environmental project No. 799, Danish Environmental Protection Agency, Denmark. 46 pp
- [61] Plo'sz, B. G., Leknes, H., Liltved, H., Thomas, K. V. (2009) "Dynamics in the occurrence and the fate of hormones and antibiotics in activated sludge wastewater treatment" Manuscript submitted to. Sci. Total Environ., STOTEN-D-09-01185
- [62] Horva'th, R. S. (1972)"Cometabolism of the herbicide 2,3,6-trichlorobenzoate by natural microbial populations" Bull. Environ. Contam. Toxicol., 7, 273-276.
- [63] Criddle, C. S. (1993) "The kinetics of cometabolism" Biotechnol. Bioeng., 41, 1048-1056.
- [64] Chang, H. L. and Alvarez-Cohen, L. (1995) "Model for the cometabolic biodegradation of chlorinated organics" Environ. Sci. Technol., 29 (9), 2357-2367
- [65] Kolpin, D. W., Furlong, E. T., Meyer, M. T., Thurman, E. M., Zaugg, S. D., Barber, L. B., Buxton, H. T. (2002) "Pharmaceuticals, hormones, and other organic wastewater contaminants in US streams, 1999-2000: A national reconnaissance" Environmental Science & Technology. 36: 1202-11.

- [66] Nakada, N., Shinohara, H., Murata, A., Kiri, K., Managaki, S., Sato, N., Takada, H. (2007) "Removal of selected pharmaceuticals and personal care products (PPCPs) and endocrine-disrupting chemicals (EDCs) during sand filtration and ozonation at a municipal sewage treatment plant" Water Research. 41: 4373-82
- [67] Halle C. (2009) "Biofiltration in Drinking Water Treatment: Reduction of Membrane Fouling and Biodegradation of Organic Trace Contaminants" [PhD Thesis]. Waterloo, Ontario, Canada: University of Waterloo.
- [68] Ying G.G., Kookana, R.S., Kumar, A., (2008) "Fate of estrogens and xenoestrogens in four sewage treatment plants with different technologies" Environmental Toxicology and Chemistry, 27: 87-94.
- [69] Ahel, M., Scully, F.E., Hoigne, J., Giger, W., (1994) "PHOTOCHEMICAL DEGRADATION OF NONYLPHENOL AND NONYLPHENOL POLYETHOXYLATES IN NATURAL-WATERS" Chemosphere 28: 1361-8.
- [70] Zhang, J., Yang, M., Zhang, Y., Chen, M., (2007) "Biotransformation of nonylphenol ethoxylates during sewage treatment under anaerobic and aerobic conditions" Environmental Science 20: 135–141.
- [71] Henze, M., Gujer, W., Mino, T., van Loosdrecht, M., (2000). "Activated Sludge Models ASM1, ASM2, ASM2d and ASM3". Scientific and Technical Report No 9. IWA Publishing, London, UK.
- [72] Orhon, D., Babuna, F.G., Karahan, O., (2009b) "Industrial Wastewater Treatment by Activated Sludge". IWA Publishing, London SW1H 0QS, UK, p. 400.
- [73] Scott, M.J., Jones, M.N., (2000) "The biodegradation of surfactants in the environment". Biochim. Biophys. Acta 1508, 235–251.
- [74] Zhang, J., Yang, M., Zhang, Y., Chen, M., (2008) "Biotransformation of nonylphenol ethoxylates during sewage treatment under anaerobic and aerobic conditions". J. Environ. Sci. 20, 135–141.
- [75] Pomiès, M., Choubert, J.M., Wisniewski, C., Coquery, M., (2012) "Modelling of micropollutant removal in biological wastewater treatments: A review". Science of the Total Environment 443, 733–748
- [76] TOXCHEM User's Manual version 3, (2006) "Modeling the fate of toxics in wastewater treatment", 1992 – 2006 Hydromantis, Inc.

- [77] Noñdler, k., Licha, T., Barbieri, M., Pe´rez, S., (2012) "Evidence for the microbially mediated abiotic formation of reversible and non-reversible sulfamethoxazole transformation products during denitrification", water research 46, 2131- 2139
- [78] JONES, F. W., WESTMORELAND, D. J., (1998) "Degradation of Nonylphenol Ethoxylates during the Composting of Sludges from Wool Scour Effluents", Environ. Sci. Technol. 32, 2623-2627
- [79] Giger, W., Brunner, P.H., Schaffner, C., (1984) "4-Nonylphenol in sewage sludge: accumulation of toxic metabolites from nonionic surfactants". Science, 225(4662):623–625
- [80] Osburn Q.W., Benedict, J. H., (1966) "Polyethoxylated alkyl phenols: relationship of structure to biodegradation mechanism". J Am Oil Chem Soc. 43:141–146.
- [81] Tanghe, T., Devriese, G., Verstraete, W., (1998) "Nonylphenol degradation in lab scale activated sludge units is temperature dependent" Water Res. 32:2889–2896.
- [82] Horva´th, R. S. (1972) "Cometabolism of the herbicide 2,3,6-trichlorobenzoate by natural microbial populations" Bull. Environ. Contam. Toxicol. 7, 273–276.
- [83] Byrns G., (2001) "The fate of xenobiotic organic compounds in wastewater treatment plants" Water Res; 35(10):2523–33.
- [84] Dionisi, D., Bornoroni, L., Mainelli, S., Majone, M., Pagnanelli, F., Papini, M.P., (2008) "Theoretical and experimental analysis of the role of sludge age on the removal of adsorbed micropollutants in activated sludge processes" Ind Eng Chem Res; 47(17):6775–82.
- [85] Alvarez-Cohen, L., McCarty P.L., (1991) "A cometabolic biotransformation model for halogenated aliphatic-compounds exhibiting product toxicity" Environ Sci Technol; 25(8): 1381–7.
- [86] Alvarez-Cohen, L., Speitel, G.E., (2001) "Kinetics of aerobic cometabolism of chlorinated solvents". Biodegradation; 12(2):105–26
- [87] Andersen, H.R., Hansen, M., Kjolholt, J., Stuer-Lauridsen, F., Ternes, T., Halling-Sorensen B., (2005) "Assessment of the importance of sorption for steroid estrogens removal during activated sludge treatment" Chemosphere; 61(1):139–46.
- [88] Artola-Garicano, E., Borkent, I., Damen, K., Jager, T., Vaes, W.H.J., (2003) "Sorption kinetics and microbial biodegradation activity of hydrophobic chemicals in sewage sludge: model and measurements based on free concentrations" Environ Sci Technol; 37(1):116–22.

- [89] Barret, M., Carrere, H., Delgadillo, L., Patureau, D., (2010a) "PAH fate during the anaerobic digestion of contaminated sludge: do bioavailability and/or cometabolism limit their biodegradation?" Water Res; 44(13):3797–806.
- [90] Barret, M., Carrere, H., Latrille, E., Wisniewski, C., Patureau, D., (2010b) "Micropollutant and sludge characterization for modeling sorption equilibria" Environ Sci Technol; 44(3): 1100–6.
- [91] Boeije, G., Schowanek, D., Vanrolleghem, P., (1998) "Adaptation of the SimpleTreat chemical fate model to single-sludge biological nutrient removal wastewater treatment plants". Water Sci Technol; 38(1):211–8.
- [92] Carballa, M., Omil, F., Lema, J.M., Llopart, M., Garcia-Jares, C., Rodriguez, I., Gomez, M., Ternes, T., (2004) "Behavior of pharmaceuticals, cosmetics and hormones in a sewage treatment plant" Water Res; 38(12):2918–26.
- [93] Carucci, A., Cappai, G., Piredda, M., (2006) "Biodegradability and toxicity of pharmaceuticals in biological wastewater treatment plants" J. Environ Sci Health A Tox Hazard Subst Environ Eng; 41(9):1831–42.
- [94] Choubert, J., Ruel, M., Esperanza, M., Budzinski, H., Miege, C., Lagarrigue, C., Coquery, M. (2011)"Limiting the emissions of micro-pollutants: what efficiency can we expect from wastewater treatment plants"? Water Sci Technol; 63(1):57–65.
- [95] Cowan, C.E., Larson, R.J., Feijtel, T.C.J., Rapaport, R.A. (1993) "An improved model for predicting the fate of consumer product chemicals in waste-water treatment plants" Water Res; 27(4):561–73.
- [96] Delgadillo-Mirquez, L., Lardon, L., Steyer, J.P., Patureau D., (2011) "A new dynamic model for bioavailability and cometabolism of micropollutants during anaerobic digestion" Water Res; 45(15):4511–21.
- [97] Dionisi, D., Bertin, L., Bornoroni, L., Capodicasa, S., Papini, M.P., Fava F., (2006) "Removal of organic xenobiotics in activated sludges under aerobic conditions and anaerobic digestion of the adsorbed species" J Chem. Technol. Biotechnol.; 81(9):1496–505.
- [98] Fernandez-Fontaina, E., Omil, F., Lema, J.M., Carballa M., (2012a) "Influence of nitrifying conditions on the biodegradation and sorption of emerging micropollutants" Water Res; 46(16):5434–44.

- [99] Fernandez-Fontaina, E., Pinho, I., Carballa, M., Omil, F., Lema, J.M., (2012b) "Biodegradation kinetic constants and sorption coefficients of micropollutants in membrane bioreactors" Biodegradation; 1-13.
- [100] Gobel, A., Thomsen, A., McArdell, C.S., Joss, A., Giger, W., (2005) "Occurrence and sorption behavior of sulfonamides, macrolides, and trimethoprim in activated sludge treatment" Environ. Sci. Technol.; 39(11):3981–9.
- [101] Gobel, A., McArdell, C.S., Joss, A., Siegrist, H., Giger, W., (2007) "Fate of sulfonamides, macrolides, and trimethoprim in different wastewater treatment technologies" Sci. Total Environ.; 372(2–3):361–71.
- [102] Gros, M., Petrović, M., Ginebreda, A., Barcelo, D., (2010) "Removal of pharmaceuticals during wastewater treatment and environmental risk assessment using hazard indexes" Environ Int; 36(1):15–26.
- [103] Halling-Sorensen, B., Nielsen, S.N., Lanzky, P.F., Ingerslev, F., Lutzhoft, H.C., Jorgensen S.E., (1998) "Occurrence, fate and effects of pharmaceutical substances in the environment—a review" Chemosphere; 36(2):357–94.
- [104] Hauduc, H., Gillot, S., Rieger, L., Ohtsuki, T., Shaw, A., Takács, I., Winkler, S. (2009) "Activated sludge modeling in practice: an international survey" Water Sci Technol; 60(8):1943–51.
- [105] Jacobsen, B.N., Arvin E., (1996) "Biodegradation kinetics and fate modelling of pentachlorophenol in bioaugmented activated sludge reactors" Water Res; 30(5):1184–94.
- [106] Jacobsen, B.N., Nyholm, N., Pedersen, B.M., Poulsen, O., Ostfeldt, P., (1993) "Removal of organic micropollutants in laboratory activated-sludge reactors under various operating conditions—sorption" Water Res; 27(10):1505–10.
- [107] Jia, A., Wan, Y., Xiao, Y., Hu, J.Y., (2012) "Occurrence and fate of quinolone and fluoroquinolone antibiotics in a municipal sewage treatment plant" Water Res; 46(2): 387–94.
- [108] Jones, O.A.H., Voulvoulis, N., Lester, J.N., (2005) "Human pharmaceuticals in wastewater treatment processes" Environ Sci Technol; 35(4):401–27.
- [109] Khunjar, W., Mackintosh, S., Skotnika-Pitak, J., Baik, S., Aga, D., Love, N., (2011) "Elucidating the relative roles of ammonia oxidizing and heterotrophic bacteria during the biotransformation of 17 alpha-ethinylestradiol and trimethoprim" Environ Sci Technol; 45(8):3605–12.

- [110] Kim, S., Eichhorn, P., Jensen, J.N., Weber, A.S., Aga, D.S., (2005) "Removal of antibiotics in wastewater: effect of hydraulic and solid retention times on the fate of tetracycline in the activated sludge process" Environ Sci Technol; 39(15):5816–23.
- [111] Kimura K., Hara, H., Watanabe, Y., (2010) "Elimination of selected pharmaceuticals by biosolids from municipal wastewater treatment plants: importance of modest pH change and degree of mineralization" Water Sci. Technol.; 62(5):1084–9.
- [112] Kreuzinger, N., Clara, M., Strenn, B., Kroiss, H., (2004) "Relevance of the sludge retention time (SRT) as design criteria for wastewater treatment plants for the removal of endocrine disruptors and pharmaceuticals from wastewater" Water Sci. Technol.; 50(5): 149–56.
- [113] Lee K.C., Rittmann B.E., Shi J.C., McAvoy D. (1998) "Advanced steady-state model for the fate of hydrophobic and volatile compounds in activated sludge" Water Environ Res; 70 (6):1118–31.
- [114] Limousin, G., Gaudet, J.P., Charlet, L., Szenknect, S., Barthès, V., Krimissa, M., (2007) "Sorption isotherms: a review on physical bases, modeling and measurement" Appl Geochem; 22(2):249–75.
- [115] Louvet, J.N., Giammarino, C., Potier, O., Pons, M.N., (2010) "Adverse effects of erythromycin on the structure and chemistry of activated sludge" Environ Pollut; 158(3):688–93.
- [116] Mackay, D., (1979) "Finding fugacity feasible" Environ Sci Technol; 13(10):1218–23.
- [117] Majewsky, M., Galle, T., Zwank, L., Fischer K., (2010) "Influence of microbial activity on polar xenobiotic degradation in activated sludge systems" Water Sci Technol; 62(3): 701–7.
- [118] Monteith, H.D., Parker, W.J., Bell, J.P., Melcer, H. (1995) "Modeling the fate of pesticides in municipal wastewater treatment" Water Environ Res; 67(6):964–70.
- [119] Munoz. I., Gomez-Ramos, M.J., Aguera, A., Garcia-Reyes, J.F., Molina-Diaz, A., Fernandez-Alba, A.R., (2009) "Chemical evaluation of contaminants in wastewater effluents and the environmental risk of reusing effluents in agriculture" TrAC Trends Anal Chem; 28(6): 676–94.
- [120] Ort, C., Gujer, W., (2006) "Sampling for representative micropollutant loads in sewer systems" Water Sci Technol; 54(6–7):169–76.

- [121] Ort, C., Lawrence, M., Rieckermann, J., Joss, A., (2010) "Sampling for pharmaceuticals and personal care products (PPCPs) and illicit drugs in wastewater systems: are your conclusions valid? A critical review" Environ Sci Technol; 44(16):6024–35.
- [122] Parker, W.J., Monteith, H.D., Bell, J.P., Melcer, H., Macberthouex, P., (1994) "Comprehensive fate model for metals in municipal waste-water treatment" J. Environ Eng. ASCE; 120(5): 1266–83.
- [123] Peev, M., Schonerklee, M., De Wever, H., (2004) "Modelling the degradation of low concentration pollutants in membrane bioreactors" Water Sci Technol; 50(5):209–18.
- [124] Plósz, B.G., Langford, K.H., Thomas, K.V., (2012) "An activated sludge modeling framework for xenobiotic trace chemicals (ASMX): assessment of diclofenac and carbamazepine" Biotechnol Bioeng; 109(11):2757–69.
- [125] Radjenovic, J., Petrovic, M., Barcelo, D., (2009) "Fate and distribution of pharmaceuticals in wastewater and sewage sludge of the conventional activated sludge (CAS) and advanced membrane bioreactor (MBR) treatment" Water Res; 43(3):831–41.
- [126] Rittmann, B.E., Tularak, P., Lee, K.C., Federle, T.W., Itrich, N.R., Kaiser, S.K., Shi, J., Drew C. McAvoy, D.C., (2001) "How adaptation and mass transfer control the biodegradation of linear alkylbenzene sulfonate by activated sludge" Biodegradation; 12(1):31–7.
- [127] Nöddler, K., Licha, T., Manuela, B., Pe´rez, S. (2012) "Evidence for the microbially mediated abiotic formation of reversible and non-reversible sulfamethoxazole transformation products during denitrification" Water Research; (46) 2131-2139
- [128] Siegrist, H., Alder, A., Gujer, W., Giger, W., (1989) "Behaviour and modelling of NTA degradation in activated sludge systems" Water Sci Technol; 21:315–24.
- [129] Rittmann, B.E., Lee, K.C., Shi, J., McAvoy, D.C., (2003) "Modeling nonsteady-state conditions and kinetics of mass transport for hydrophobic compounds in activated-sludge treatment" Water Environ Res; 75(3):273–80.
- [130] Cloutier, F., Jalby, G., Lessard, P., Vanrolleghem, P.A. (2008) "Dynamic modelling of heavy metals behavior in wastewater treatment plants" J Water Sci; 22(4):461–71.
- [131] Govind, R., Lai, L., Dobbs, R., (1991) "Integrated model for predicting the fate of organics in waste-water treatment plants" Environ. Prog., 10(1):13–23.

- [132] Melcer, H., Bell, J.P., Thompson, D.J., Yendt, C.M., Kemp, J., Steel, P., (1994) "Modeling volatile organic contaminants fate in waste-water treatment plants" J Environ Eng ASCE; 120(3):588–609
- [133] Verlicchi, P., Al Aukidy, M., Zambello, E., (2012)"Occurrence of pharmaceutical compounds in urban wastewater: removal, mass load and environmental risk after a secondary treatment—a review" Sci Total Environ; 429:123–55.
- [134] Dalton, H., Stirling, D.I., (1982) "Co-metabolism" Philos Trans R Soc Lond B Biol Sci; 297(1088): 481–96.
- [135] Struijs, J., Stoltenkamp, J., Vandemeent, D., (1991) "A spreadsheet-based box model to predict the fate of xenobiotics in a municipal waste-water treatment-plant" Water Res; 25(7): 891–900.
- [136] Xue, W., Wu, C., Xiao, K., Huang, X., Zhou, H., Tsuno, H., Tanaka, H. (2010) "Elimination and fate of selected micro-organic pollutants in a full-scale anaerobic/anoxic/aerobic process combined with membrane bioreactor for municipal wastewater reclamation" Water Res; 44(20): 5999–6010.
- [137] Zhao, J., Li, Y., Zhang, C., Zeng, Q., Zhou, Q., (2007) "Sorption and degradation of Bisphenol A by aerobic activated sludge" Journal of Hazardous Material; 155: 305-311
- [138] Athanasios, S., Constantinos, I., Vasiliki, C., Georgia, G., Nikolaos, S., (2010) "Removal of selected endocrine disrupters in activated sludge systems: Effect of sludge retention time on their sorption and biodegradation" Bioresource Technology; 101: 2090–2095
- [139] Jahan, K., Ordóñez, R., Ramachandran, R., Perlis, S., and Stern, M., (2008) "MODELING BIODEGRADATION OF NONYLPHENOL" Water, Air, & Soil Pollution; Volume 8: 395-404
- [140] Chang, B.V., Chiang, F., Yuan, S.Y., (2005) "Biodegradation of nonylphenol in sewage sludge" Chemosphere; 60: 1652–1659
- [141] Krogh, K.A., Halling-Sorensen, B., Mogensen, B.B., Vejrup, K.V., (2003) "Environmental properties and effects of nonionic surfactant adjuvants in pesticides: a review" Chemosphere; 50: 871–901

- [142] William Jones, F., Westmorel, D.J., (1998) "Degradation of Nonylphenol Ethoxylates during the Composting of Sludges from Wool Scour Effluents" Environ. Sci. Technol.; 32: 2623-2627
- [143] Staples, C.A., Williams, J. B., Blessing, R. L., Varineau, P., T., (1999) "MEASURING THE BIODEGRADABILITY OF NONYLPHENOL ETHER CARBOXYLATES, OCTYLPHENOL ETHER CARBOXYLATES, AND NONYLPHENOL" Chemosphere, Vol. 38, No. 9, 2029-2039
- [144] Carrera, J., Martin-Hernandez, M., Eugenia Suarez-Ojeda, M., Perez, J., (2011) "Modelling the pH dependence of the kinetics of aerobic p-nitrophenol biodegradation" Journal of Hazardous Materials; 186: 1947–1953
- [145] Smook, T.M., Zho, H., Zytner, R.G., (2008) "Removal of ibuprofen from wastewater: comparing biodegradation in conventional, membrane bioreactor, and biological nutrient removal treatment systems" Water Sci. Technol.; 57(1): 1–8.
- [146] Collado, N., Buttiglieri, G., Ferrando-Climent, L., Rodriguez-Mozaz, S., Barceló, D., Comas, J., Rodriguez-Roda, I., (2012) "Removal of ibuprofen and its transformation products: Experimental and simulation studies" Science of the Total Environment; 433: 296–301
- [147] Shimp, R.J., and Young, R.L., (1988) "Availability of Organic Chemicals for Biodegradation in Settled Bottom Sediments" Ecotoxicol Environ. Safety; 4, 31.
- [148] Abbasi, S., and Rittmann, B.E. (1994) "Role of Direct Biodegradation of Sorbed Organics in Active Sludge Treatment Process" Water Environ. Fed. 67th Annul. Conf. Exposition Chicago, Ill.
- [149] Larson, R., and Vashon, RD., (1983) "Adsorption and Biodegradation of Cationic Surfactants in Laboratory and Environmental Systems" Dev. Ind. Microbiol. 24, 425.
- [150] Castiglioni, S., Bagnati, R., Fanelli, R., Pomati, F., Calamari, D., Zuccato, E., (2006) "Removal of pharmaceuticals in sewage treatment plants in Italy" Environmental Science & Technology 40 (1), 357–363.
- [151] Sipma, J., Osuna, B., Collado N., Monclús, H., Ferrero, G., Comas, J., Rodriguez-Roda, I., (2010) "Comparison of removal of pharmaceuticals in MBR and activated sludge systems" Desalination 250; 653–659
- [152] Dionisi, D., Bertin, L., Bornoroni, L., Capodicasa, S., Petrangeli Papini, M., and Fava, F., (2006) "Removal of organic xenobiotics in activated sludges under aerobic conditions and

- anaerobic digestion of the adsorbed species" Journal of Chemical Technology and Biotechnology 81; 1496–1505
- [153] Kemp, J., Zytner, R.G., Sterne, L., Rittmann, B.E., (2002) "Measuring and modelling VOC biotransformation rates" Environ Technol; 23(5); 547–51
- [154] Draper, N. R. and Smith, H., (1981) "Applied regression analysis", John Wiley and Sons, Inc., New York.
- [155] Smith, L.H., McCarty, P.L. and Kitanidis, P.K., (1998) "Spreadsheet method for evaluation of biochemical reaction rate coefficients and their uncertainties by weighted nonlinear least-squares analysis of the integrated monod equation", Applied and Environmental Microbiology, 64(6); 2044-2050
- [156] Fauser, P., Vikelsøe, J., Sørensen, P. B., & Carlsen, L., (2003) "Phthalates, nonylphenols and LAS in an alternately operated wastewater treatment plant—fate modelling based on measured concentrations in wastewater and sludge" Water research; 37(6), 1288-1295
- [157] Tanaka, H., Sato, C., Komori, K., Yakou, Y., Tamamoto, H., Miyamoto, N., Higashitani, T., (2003), "Occurrence of endocrine disruptors in sewage and their behavior in sewage treatment plants in Japan" Environ. Sci; 10(1), 1-24
- [158] Jacobsen, B., and Guildal, T., (2000) "Novel aspects for management of xenobiotic compounds in wastewatertreatment plants linking theory, field studies, regulation, engineering, and experience" Water Science & Technology; 42(7-8), 315-322.
- [159] Buser, H. R., Poiger, T., & Müller, M. D., (1999) "Occurrence and environmental behavior of the chiral pharmaceutical drug ibuprofen in surface waters and in wastewater" Environmental science & technology, 33(15), 2529-2535.
- [160] Andersen, R.H., (2004) "Pollution of the aquatic environment by steroid estrogens" Ph.D. thesis, Department of Analytical Chemistry, The Danish University of Pharmaceutical Sciences, Denmark, 94 pp.
- [161] Daughton, C. G., & Ternes, T. A. (1999), "Pharmaceuticals and personal care products in the environment: agents of subtle change?" Environmental Health Perspectives; 107 (Suppl 6), 907.

Appendices

Appendix A

Uncalibrated Model Matrix

Model : PPCP	I:	1	2	3	4	5	6	7	8	9	10	11	12	13	14	15	16	17
GPS-X library: cniplib	Stoichiometry matrix															NPEO		
j	Rate	xbh	xba	xu	xs	xi	xnd	ss	snh	snd	sno	si	so	snn	salk	xii	Sza	Szb
	Unit	gCOD	gCOD	gCOD	gCOD	gCOD	gN	gCOD	gN	gN	gN	gCOD	gCOD	gN	Mole HCO ₃	gCOD	g/m ³	g/m ³
1	r1	1						-1/yh	-ibhn				-(1-yh)/yh		-ibhn/14			
2	r2	1						-1/yh	-ibhn		-(1-yh)/(2.86.yh)			(1-yh)/(2.86.yh)	(-ibhn/14)+((1-yh)/14.2.86.yh))			
3	r3	1						-1/yh			-ibhn		-(1-yh)/yh		-ibhn/14			
4	r4	1						-1/yh			-ibhn-(1-yh)/(2.86.yh)			(1-yh)/(2.86.yh)	(-ibhn/14)+((1-yh)/14.2.86.yh))			
5	r5	-1		fuh	1-fuh		ibhn-fuh.iuhn											
6	r6				-1			1										
7	r7						-1			1								
8	r8								1	-1					1/14			
9	r9								-ibhn-1/ya		1/ya		-(4.57-ya)/ya		(-ibhn/14)-1/(ya.7)			
10	r10		1	fua	1-fua		ibhn-fua.iuhn											
11	r11		-1														-(1-f _{INPEO})	α
12	r12																	1
13	r13	1											-(1-yh)/yh					-1
14	r14																	
15	r15																	
16	r16																	
17	r17																	
18	r18																	
19	r19																	
20	r20																	
21	r21																	
22	r22																	
23	r23																	
24	r24																	
25	r25																	
26	r26																	

18	19	20	21	22	23	24	25	26	27	28					
NPEO		SMX			Ibuprofen (Ionized compound)				BPA (Neutral compound)		Compi		Process rate equations:		Units
Szc	Szd	Szf	Szg	Xza	Szh	Xzb	Szi	Xzc	Szj	Xzd					
g/m ³	g/m ³	g/m ³	g/m ³	g/m ³	g/m ³	g/m ³	g/m ³	g/m ³	g/m ³	g/m ³					
												aerobic growth of heterotrophs on soluble substrate with ammonia as N source	muh.MssHET.MsoHET.MsnhGEN.salksatHET.xbh	gCOD/m3/d	
												anoxic growth of heterotrophs on soluble substrate with ammonia as N source	etah.muh.MssHET.inhibsoaxHET.MsnoHET.MsnhGEN.salksatHET.xbh	gCOD/m3/d	
												aerobic growth of heterotrophs on soluble substrate with nitrate as N source	muh.MssHET.MsoHET.inhibsnhHET.MsnoHET.salksatHET.xbh	gCOD/m3/d	
												anoxic growth of heterotrophs soluble substrate with nitrate as N source	etah.muh.MssHET.inhibsoaxHET.inhibsnhHET.MsnoHET.salksatHET.xbh	gCOD/m3/d	
												decay of heterotrophs	bh.xbh	gCOD/m3/d	
												hydrolysis of entrapped organics	kh.(subsatHET).(MsoHET + etah.inhibsoo2HET.MsnoHET).xbh	gCOD/m3/d	
												hydrolysis of entrapped organic nitrogen	r6.(xnd/(xs))	gCOD/m3/d	
												ammonification of soluble organic nitrogen	ka.snd.xbh	gN/m3/d	
												growth of autotrophs	mua.MsnhGEN.MsnhNIT.MsoNIT.salksatAUT.xba	gCOD/m3/d	
												decay of autotrophs	ba.xba	gCOD/m3/d	
1-α	f _{INPEO}											abiotic cleavage	K _{OCL} .Sza	gCOD/m3/d	
-1												hydrolysis of Sza	K _{hNPEO} .(Szc/xbh)/(K _{xNPEO} +Szc/xbh).xbh	gCOD/m3/d	
												growth on Szb	K _{bioNPEO} .Szb.(Ks)/(Ks+ss).so/(Koh+so).xbh	g/m3/d	
		-1										aerobic biotransformation of Szf	K _{1BioOx} .Szf.(Ks.η _{bio})/(Ks.η _{bio} +ss).so/(Koh+so).xbh	g/m3/d	
		1	-1									aerobic parent compound formation	K _{1DecOx} .Szg.(Ks.η _{1Dec})/(Ks.η _{1Dec} +ss).so/(Koh+so).xbh	g/m3/d	
		1		-1								aerobic desorption of Szf	K _{Des} .Szf.so/(Koh+so)	g/m3/d	
		1		-1								anoxic desorption of Szf	K _{Des} .Szf.Ko/(Koh+so)	g/m3/d	
		-1		1								aerobic sorption of Szf	K _{Des} .K _{1DOx} .Szf.so/(Koh+so).X _{ss}	g/m3/d	
		-1										anoxic biotransformation of Szf	K _{1BioAx} .Szf.(Ks.η _{bio})/(Ks.η _{bio} +ss).Ko/(Koh+so).xbh	g/m3/d	
		1	-1									anoxic parent compound formation	K _{1DecAx} .Szg.(Ks.η _{1Dec})/(Ks.η _{1Dec} +ss).Ko/(Koh+so).xbh	g/m3/d	
		-1		1								anoxic sorption of Szf	K _{Des} .K _{1DAx} .Szf.Ko/(Koh+so).X _{ss}	g/m3/d	
					-1	1						sorption of neutral form of compound (HA)	K _{1des} .K _{D1} .Szh.X _{ss}	g/m3/d	
					1	-1						Desorption of neutral form of compound (HA)	K _{1des} .Xzb	g/m3/d	
					-1							Biodegradation of neutral form of compound (HA)	K _{bio1} .(Szh+Szi).xbh.so/(Koh + so).(1/(10^(pH-pka)+1))	g/m3/d	
							-1	1				sorption of ionized form of compound (A ⁻)	K _{2des} .K _{D2} .Szi.X _{ss}	g/m3/d	
							1	-1				Desorption of ionized form of compound (A ⁻)	K _{2des} .Xzc	g/m3/d	
							-1					Biodegradation of ionized form of compound (A ⁻)	K _{bio2} .(Szh+Szi).xbh.so/(Koh + so).(1/(10^(pka-pH)+1))	g/m3/d	
									-1	1		sorption of neutral compound	K _{des3} .K _{d3} .Szj.X _{ss}	g/m3/d	
									1	-1		Desorption of neutral compound	K _{des3} .Xzd	g/m3/d	
									-1			Biodegradation of neutral compound	K _{bio3} .Szj.xbh.so/(koh + so)	g/m3/d	

Appendix A Cont'd: Internal variables of uncalibrated model (PPCP), ASM1 and Mantis Models

Internal variables:	Units	Description
<i>Aerobic Growth of Heterotrophs at DO Saturation</i>		
$r1_{sat} = \text{muh.MssHET.MsnhGEN.xbh}$	gCOD/m3/d	aerobic growth of heterotrophs at DO saturation
<i>Aerobic Growth of Autotrophs at DO Saturation</i>		
$r9_{sat} = \text{mua.MsnhGEN.MsnhNIT.xba}$	gCOD/m3/d	aerobic growth of autotrophs at DO saturation
<i>Actual Oxygen Uptake Rate (OUR)</i>		
$\text{our} = -\text{rso}$	gO2/m3/d	actual oxygen uptake rate
<i>Maximal Oxygen Uptake Rate</i>		
$\text{ourmax} = -(\text{coeffso}(1).\text{muh.MssHET.MsnhGEN.xbh} + \text{coeffso}(3).\text{muh.MssHET.inhibsnhHET.MsnoHET.xbh} + \text{coeffso}(9).\text{mua.MsnhGEN.MsnhNIT.xba})$	gO2/m3/d	maximal oxygen uptake rate (at DO saturation)
<i>Actual Nitrogen Utilization Rate (NUR)</i>		
$\text{nur} = -(\text{coeffsnh}(9).\text{r9})$	gN/m3/d	actual nitrogen utilization rate
<i>Maximal Nitrogen Utilization Rate</i>		
$\text{nurmax} = -(\text{coeffsnh}(9).\text{mua.MsnhGEN.MsnhNIT.xba})$	gN/m3/d	maximal nitrogen utilization rate (at DO saturation)
<i>Denitrification Rate</i>		
$\text{dnr} = -(\text{coeffsno}(2).\text{r2} + \text{coeffsno}(4).\text{r4})$	gN/m3/d	denitrification rate
<i>Saturation and Inhibition Functions</i>		
$\text{MsnhGEN} = \text{snh}/(\text{snh} + \text{knh})$	-	ammonia (as nutrient) saturation function
$\text{subsathET} = ((\text{xs}/(\text{xbh})) / ((\text{xs}/(\text{xbh})) + \text{kx}))$	-	slowly biodegradable substrate saturation function for hydrolysis
$\text{MssHET} = \text{ss}/(\text{ss} + \text{ksh})$	-	readily biodegradable substrate saturation function for heterotrophs
$\text{MsoHET} = \text{so}/(\text{so} + \text{koh})$	-	oxygen saturation function for heterotrophs
$\text{MsnoHET} = \text{sno}/(\text{sno} + \text{kno})$	-	nitrate saturation function for heterotrophs
$\text{Inhibsoo2HET} = \text{koh}/(\text{so} + \text{koh})$	-	oxygen inhibition function for heterotrophs - anaerobic conditions
$\text{InhibsoaxHET} = \text{kad}/(\text{so} + \text{kad})$	-	oxygen inhibition function for heterotrophs - anoxic conditions
$\text{inhibsnhHET} = \text{knh}/(\text{snh} + \text{knh})$	-	ammonia (as nutrient) inhibition function
$\text{MsnhNIT} = \text{snh}/(\text{snh} + \text{kna})$	-	ammonia saturation function for autotrophs
$\text{MsoNIT} = \text{so}/(\text{so} + \text{koa})$	-	oxygen saturation function for autotrophs
$\text{salksatHET} = \text{salk}/(\text{kalk} + \text{salk})$	-	alkalinity saturation function for heterotrophs
$\text{salksatAUT} = \text{salk}/(\text{kalka} + \text{salk})$	-	alkalinity saturation function for autotrophs

Appendix B

ASM1 Model

The International Association on Water Pollution Research and Control (IAWPRC) Task Group realized that due to the long solids retention times and low growth rates of the bacteria, the actual effluent substrate concentrations between different activated sludge treatment plants did not vary greatly. What significantly different were the levels of MLSS and electron acceptor (oxygen or nitrate). Thus the focus of the Activated Sludge Model No.1 (called *asm1* in GPS-X) is the prediction of the solids and electron acceptor.

The Task Group considered the trade-off between model accuracy and practicality. They identified the major biological processes occurring in the system and characterized these processes with the simplest rate expressions that could be used, resembling the real reactions.

The use of switching functions was made by the Task Group since some reactions depended on the type of electron acceptor present. These functions were of the form:

$$\frac{S_o}{K_{OH} + S_o} \quad (3.1)$$

$$\frac{K_{OH}}{K_{OH} + S_o} \quad (3.2)$$

In equation 3.1, at low concentration of dissolved oxygen (S_o), the parameter K_{OH} dominated the expression and approaches a value of zero, but for equation 3.2, the amount of that approaches unity. At high values of S_o , the parameter K_{OH} would be negligible and the expression approaches unity, and for the other equation, S_o is the dominant so the equation approaches zero. If the switching function was inverted, then the limits when S_o were high or low are reversed. A consequence of using switching functions of this form is that they are continuous functions unlike discontinuous on/off switches which are more difficult to simulate.

In the development of activated sludge modelling, the manner in which the quantity of organic matter is measured (BOD, COD or TOC) is inconsistent. The Task Group decided to use COD since mass balances can be carried out and since it has links to the electron equivalents in the organic substrate, biomass and electron acceptor.

The organic material is categorized according to a number of characteristics. First is the biodegradability of the material. The non-biodegradable organics pass through the system unchanged and can be further categorized according to their physical state (soluble or particulate), which is removed from the system by different pathways. The particulate material is generally removed with the waste activated sludge, while the soluble material leaves with the effluent. The biodegradable material is categorized as either readily or

slowly biodegradable. The Task Group treated the former as soluble material, while the latter was treated as particulate material (this is not strictly correct, but simplifies matters). The readily biodegradable organics may be utilized for cell maintenance or growth with a transfer of electrons to the acceptors. The particulate (slowly) biodegradable substrate is hydrolysed to readily biodegradable material, assuming no energy utilization and no corresponding use of electron acceptor.

Two types of biomass are modelled: 1) heterotrophic; and 2) autotrophic.

The heterotrophic biomass is generated by the growth on readily biodegradable substrate under aerobic or anoxic conditions and decays (including endogenous respiration, death, predation and lysis) under all conditions.

The nitrogenous material is categorized according to its biodegradability and physical state. The non-biodegradable material is modelled as a fraction of the non-biodegradable particulate COD, while the non-biodegradable soluble material is ignored. The biodegradable nitrogenous material is divided into ammonia (free and ionized), soluble organic and particulate organic is converted to ammonia by the heterotrophic biomass. The conversion of ammonia to nitrate by the autotrophs is assumed to take place in one step

Model : ASM1	I:	1	2	3	4	5	6	7	8	9	10	11	12	13
GPS-X library: cniplib	Stoichiometry matrix													
j	Rates	S _I	S _S	X _I	X _S	X _{BH}	X _{BA}	X _U	S _O	S _{NO}	S _{NH}	S _{ND}	X _{ND}	S _{ALK}
	Units:	gCOD	gCOD	gCOD	gCOD	gCOD	gCOD	gCOD	gCOD	gN	gN	gN	gN	Mole HCO ₃
1	r1		-1/yh			1			-(1-yh)/yh		-i _{XB}			-i _{XB} /14
2	r2		-1/yh			1				-(1-yh)/(2.86.yh)	-i _{XB}			[-(1-yh)/(14.2.86yh)]- i _{XB} /14
3	r3						1		-(4.57-ya)/ya	1/ya	-i _{XB} -1/ya			(i _{XB} /14)-(1/7ya)
4	r4				1-f _p	-1		f _p					i _{XB} -f _p i _{XP}	
5	r5				1-f _p		-1	f _p					i _{XB} -f _p i _{XP}	
6	r6										1	-1		1/14
7	r7		1		-1									
8	r8											1	-1	

N0.	Compi	Process rate equations:	Units
ρ_1	Aerobic growth of heterotrophs	$\mu_{mH} \cdot (S_S/K_S + S_S) \cdot (S_O/K_{OH} + S_O) \cdot X_{BH}$	gCOD/m3/d
ρ_2	Anoxic growth of heterotrophs	$\mu_{mH} \cdot (S_S/K_S + S_S) \cdot (K_{OH}/K_{OH} + S_O) \cdot (S_{NO}/K_{NO} + S_{NO}) \cdot \eta_g \cdot X_{BH}$	gCOD/m3/d
ρ_3	Aerobic growth of autotrophs	$\mu_{mA} \cdot (S_{NH}/K_{NH} + S_{NH}) \cdot (S_O/K_{OA} + S_O) \cdot X_{BA}$	gCOD/m3/d
ρ_4	Decay of heterotrophs	$B_H \cdot X_{BH}$	gCOD/m3/d
ρ_5	Decay of autotrophs	$B_A \cdot X_{BA}$	gCOD/m3/d
ρ_6	Ammonification	$K_a \cdot S_{ND} \cdot X_{BH}$	gN/m3/d
ρ_7	Hydrolysis of organic compounds	$K_H \cdot (X_S/X_{BH}) / (K_X + X_S/X_{BH}) \cdot [(S_O/K_{OH} + S_O) + \eta_h \cdot (K_{OH}/K_{OH} + S_O) \cdot (S_{NO}/K_{NO} + S_{NO})] \cdot X_{BH}$	gCOD/m3/d
ρ_8	Hydrolysis of organic N	$\rho_7 \cdot (X_{ND}/X_S)$	gCOD/m3/d

Appendix C

Mantis Model Matrix

Model : MANTIS	I:	1	2	3	4	5	6	7	8	9	10	11	12	13	14	15
GPS-X library: cniplib	Stoichiometry matrix															
j	Rate s	xbh	xba	xu	xs	xi	xnd	ss	snh	snd	sno	si	so	snn	salk	xii
	Unit s:	gCOD	gCOD	gCOD	gCOD	gCOD	gN	gCOD	gN	gN	gN	gCOD	gCOD	gN	Mole HCO ₃	gCOD
1	r1	1						-1/yh	-ibhn				-(1-yh)/yh		-ibhn/14	
2	r2	1						-1/yh	-ibhn		-(1-yh)/(2.86.yh)			(1-yh)/(2.86.yh)	(-ibhn/14)+((1-yh)/14.2.86.yh)	
3	r3	1						-1/yh			-ibhn		-(1-yh)/yh		-ibhn/14	
4	r4	1						-1/yh			-ibhn-(1-yh)/(2.86.yh)			(1-yh)/(2.86.yh)	(-ibhn/14)+((1-yh)/14.2.86.yh)	
5	r5	-1		fuh	1-fuh		Ibhn-fuh.iuhn									
6	r6				-1			1								
7	r7						-1			1						
8	r8								1	-1					1/14	
9	r9								-ibhn-1/ya		1/ya		-(4.57-ya)/ya		(-ibhn/14)-1/(ya.7)	
10	r10		1	fua	1-fua		Ibhn-fua.iuhn									

Compi	Process rate equations:	Units
aerobic growth of heterotrophs on soluble substrate with ammonia as N source	muh.MssHET.MsoHET.MsnhGEN.salksatHET.xbh	gCOD/m3/d
anoxic growth of heterotrophs on soluble substrate with ammonia as N source	etah.muh.MssHET.inhibsoaxHET.MsnoHET.MsnhGEN.salksatHET.xbh	gCOD/m3/d
aerobic growth of heterotrophs on soluble substrate with nitrate as N source	muh.MssHET.MsoHET.inhibsnhHET.MsnoHET.salksatHET.xbh	gCOD/m3/d
anoxic growth of heterotrophs soluble substrate with nitrate as N source	etah.muh.MssHET.inhibsoaxHET.inhibsnhHET.MsnoHET.salksatHET.xbh	gCOD/m3/d
decay of heterotrophs	bh.xbh	gCOD/m3/d
hydrolysis of entrapped organics	kh. (subsathET).(MsoHET + etah.inhibsoo2HET.MsnoHET).xbh	gCOD/m3/d
hydrolysis of entrapped organic nitrogen	r6.(xnd/(xs))	gCOD/m3/d
ammonification of soluble organic nitrogen	ka.snd.xbh	gN/m3/d
growth of autotrophs	mua.MsnhGEN.MsnhNIT.MsoNIT.salksatAUT.xba	gCOD/m3/d

Appendix D

Case Study 1 Matrix

Model : PPCP	I:	1	2	3	4	5	6	7	8	9	10	11	12	13	14	15	16	17
GPS-X library: cniplib	Stoichiometry matrix															NPEO		
j	Rates	xbh	xba	xu	xs	xi	xnd	ss	snh	snd	sno	si	so	snn	salk	xii	Sza	Szb
	Units:	gCOD	gCOD	gCOD	gCOD	gCOD	gN	gCOD	gN	gN	gN	gCOD	gCOD	gN	Mole HCO ₃	gCOD	g/m ³	g/m ³
1	r1	1						-1/yh	-ibhn				-(1-yh)/yh		-ibhn/14			
2	r2	1						-1/yh	-ibhn		-(1-yh)/(2.86.yh)			(1-yh)/(2.86.yh)	(-ibhn/14)+((1-yh)/14.2.86.yh))			
3	r3	1						-1/yh			-ibhn		-(1-yh)/yh		-ibhn/14			
4	r4	1						-1/yh			-ibhn-(1-yh)/(2.86.yh)			(1-yh)/(2.86.yh)	(-ibhn/14)+((1-yh)/14.2.86.yh))			
5	r5	-1		fuh	1-fuh		ibhn-fuh.iuhn											
6	r6				-1			1										
7	r7						-1			1								
8	r8								1	-1					1/14			
9	r9								-ibhn-1/ya		1/ya		-(4.57-ya)/ya		(-ibhn/14)-1/(ya.7)			
10	r10		1	fua	1-fua		ibhn-fua.iuhn											
11	r11		-1														0	0
12	r12																	0
13	r13	1											-(1-yh)/yh					0
14	r14																	
15	r15																	
16	r16																	
17	r17																	
18	r18																	
19	r19																	
20	r20																	
21	r21																	
22	r22																	
23	r23																	
24	r24																	
25	r25																	
26	r26																	

18	19	20	21	22	23	24	25	26	27	28					
NPEO		SMX and its metabolite		Ibuprofen (Ionized compound)				BPA (Neutral compound)		Compi			Process rate equations:		Units
Szc	Szd	Szf	Szg	Xza	Szh	Xzb	Szi	Xzc	Szj	Xzd					
g/m ³	g/m ³	g/m ³	g/m ³	g/m ³	g/m ³	g/m ³	g/m ³	g/m ³	g/m ³	g/m ³					
											aerobic growth of heterotrophs on soluble substrate with ammonia as N source	muh.MssHET.MsoHET.MsnhGEN.salksatHET.xbh	gCOD/m3/d		
											anoxic growth of heterotrophs on soluble substrate with ammonia as N source	etah.muh.MssHET.inhibsoaxHET.MsnoHET.MsnhGEN.salksatHET.xbh	gCOD/m3/d		
											aerobic growth of heterotrophs on soluble substrate with nitrate as N source	muh.MssHET.MsoHET.inhibsnhHET.MsnoHET.salksatHET.xbh	gCOD/m3/d		
											anoxic growth of heterotrophs soluble substrate with nitrate as N source	etah.muh.MssHET.inhibsoaxHET.inhibsnhHET.MsnoHET.salksatHET.xbh	gCOD/m3/d		
											decay of heterotrophs	bh.xbh	gCOD/m3/d		
											hydrolysis of entrapped organics	kh. (subsathET).(MsoHET + etah.inhibsoo2HET.MsnoHET).xbh	gCOD/m3/d		
											hydrolysis of entrapped organic nitrogen	r6.(xnd/(xs))	gCOD/m3/d		
											ammonification of soluble organic nitrogen	ka.snd.xbh	gN/m3/d		
											growth of autotrophs	mua.MsnhGEN.MsnhNIT.MsnoNIT.salksatAUT.xba	gCOD/m3/d		
											decay of autotrophs	ba.xba	gCOD/m3/d		
0	0										abiotic oxidative cleavage	K _{OCL} .Sza	gCOD/m3/d		
0											hydrolysis of Sza	K _{hNPEO} .(Szc/xbh/(K _{xNPEO} +Szc/xbh)).xbh	gCOD/m3/d		
											growth on Szb	K _{bioNPEO} .Szb.(Ks)/(Ks+ss).so/(Koh+so).xbh	g/m3/d		
		-1									aerobic biotransformation of Szf	K _{1BioOx} .Szf.(Ks.η _{bio})/(Ks.η _{bio} +ss).so/(Ko+so).xbh	g/m3/d		
		1	-1								aerobic parent compound formation	K _{1DecOx} .Szg.(Ks.η _{1Dec})/(Ks.η _{1Dec} +Ss).so/(Ko+so).xbh	g/m3/d		
		1		-1							aerobic desorption of Szf	K _{Des} .Szf. so/(Ko+so)	g/m3/d		
		1		-1							anoxic desorption of Szf	K _{Des} .Szf. Ko/(Ko+so)	g/m3/d		
		-1		1							aerobic sorption of Szf	K _{Des} .K _{1DOx} .Szf.so/(Ko+so). X _{ss}	g/m3/d		
		-1									anoxic biotransformation of Szf	K _{1BioAx} .Szf.(Ks.η _{bio})/(Ks.η _{bio} +Ss).Ko/(Ko+so).xbh	g/m3/d		
		1	-1								anoxic parent compound formation	K _{1DecAx} .Szg.(Ks.η _{1Dec})/(Ks.η _{1Dec} +Ss).Ko/(Ko+so).xbh	g/m3/d		
		-1		1							anoxic sorption of Szf	K _{Des} .K _{1DAx} .Szf.Ko/(Ko+so). X _{ss}	g/m3/d		
					0	0					sorption of neutral form of compound (HA)	K _{1des} .K _{D1} .Szh. X _{ss}	g/m3/d		
					0	0					Desorption of neutral form of compound (HA)	K _{1des} .Xzb	g/m3/d		
					0						Biodegradation of neutral form of compound (HA)	K _{bio1} .(Szh+Szi).xbh.so/(koh + so).(1/(10^(pH-pka)+1))	g/m3/d		
							0	0			sorption of ionized form of compound (A ⁻)	K _{2des} .K _{D2} .Szi. X _{ss}	g/m3/d		
							0	0			Desorption of ionized form of compound (A ⁻)	K _{2des} .Xzc	g/m3/d		
							0				Biodegradation of ionized form of compound (A ⁻)	K _{bio2} .(Szh+Szi).xbh.so/(koh + so).(1/(10^(pka-pH)+1))	g/m3/d		
									0	0	sorption of neutral compound	K _{des3} .K _{d3} .Szj. X _{ss}	g/m3/d		
									0	0	Desorption of neutral compound	K _{des3} .Xzd	g/m3/d		
									0		Biodegradation of neutral compound	K _{bio3} .Szj.xbh.so/(koh + so)	g/m3/d		

Appendix D Cont'd: Internal variables of Case Study 1

Internal variables:	Units	Description
<i>Aerobic Growth of Heterotrophs at DO Saturation</i>		
$r_{1sat} = \text{muh.MssHET.MsnhGEN.xbh}$	gCOD/m3/d	aerobic growth of heterotrophs at DO saturation
<i>Aerobic Growth of Autotrophs at DO Saturation</i>		
$r_{9sat} = \text{mua.MsnhGEN.MsnhNIT.xba}$	gCOD/m3/d	aerobic growth of autotrophs at DO saturation
<i>Actual Oxygen Uptake Rate (OUR)</i>		
$\text{our} = -\text{rso}$	gO2/m3/d	actual oxygen uptake rate
<i>Maximal Oxygen Uptake Rate</i>		
$\text{ourmax} = -(\text{coeffso}(1).\text{muh.MssHET.MsnhGEN.xbh} + \text{coeffso}(3).\text{muh.MssHET.inhibsnhHET.MsnoHET.xbh} + \text{coeffso}(9).\text{mua.MsnhGEN.MsnhNIT.xba})$	gO2/m3/d	maximal oxygen uptake rate (at DO saturation)
<i>Actual Nitrogen Utilization Rate (NUR)</i>		
$\text{nur} = -(\text{coeffsnh}(9).\text{r9})$	gN/m3/d	actual nitrogen utilization rate
<i>Maximal Nitrogen Utilization Rate</i>		
$\text{nurmax} = -(\text{coeffsnh}(9).\text{mua.MsnhGEN.MsnhNIT.xba})$	gN/m3/d	maximal nitrogen utilization rate (at DO saturation)
<i>Denitrification Rate</i>		
$\text{dnr} = -(\text{coeffsno}(2).\text{r2} + \text{coeffsno}(4).\text{r4})$	gN/m3/d	denitrification rate
<i>Saturation and Inhibition Functions</i>		
$\text{MsnhGEN} = \text{snh}/(\text{snh} + \text{knh})$	-	ammonia (as nutrient) saturation function
$\text{subsatHET} = ((\text{xs}/(\text{xbh})))/((\text{xs}/(\text{xbh})) + \text{kx})$	-	slowly biodegradable substrate saturation function for hydrolysis
$\text{MssHET} = \text{ss}/(\text{ss} + \text{ksh})$	-	readily biodegradable substrate saturation function for heterotrophs
$\text{MsoHET} = \text{so}/(\text{so} + \text{koh})$	-	oxygen saturation function for heterotrophs
$\text{MsnoHET} = \text{sno}/(\text{sno} + \text{kno})$	-	nitrate saturation function for heterotrophs
$\text{Inhibsoo2HET} = \text{koh}/(\text{so} + \text{koh})$	-	oxygen inhibition function for heterotrophs - anaerobic conditions
$\text{InhibsoaxHET} = \text{kad}/(\text{so} + \text{kad})$	-	oxygen inhibition function for heterotrophs - anoxic conditions
$\text{inhibsnhHET} = \text{knh}/(\text{snh} + \text{knh})$	-	ammonia (as nutrient) inhibition function
$\text{MsnhNIT} = \text{snh}/(\text{snh} + \text{kna})$	-	ammonia saturation function for autotrophs
$\text{MsoNIT} = \text{so}/(\text{so} + \text{koa})$	-	oxygen saturation function for autotrophs
$\text{salksatHET} = \text{salk}/(\text{kalk} + \text{salk})$	-	alkalinity saturation function for heterotrophs
$\text{salksatAUT} = \text{salk}/(\text{kalka} + \text{salk})$	-	alkalinity saturation function for autotrophs

Appendix D1: Case study 1_Considering aerobic parent compound transformation and aerobic biodegradation only for sensitivity analysis

Model : PPCP	I:	1	2	3	4	5	6	7	8	9	10	11	12	13	14	15	16	17
GPS-X library: cniplib	Stoichiometry matrix															NPEO		
j	Rates	xbh	xba	xu	xs	xi	xnd	ss	snh	snd	sno	si	so	snn	salk	xii	Sza	Szb
	Units:	gCOD	gCOD	gCOD	gCOD	gCOD	gN	gCOD	gN	gN	gN	gCOD	gCOD	gN	Mole HCO ₃	gCOD	g/m ³	g/m ³
1	r1	1						-1/yh	-ibhn				-(1-yh)/yh		-ibhn/14			
2	r2	1						-1/yh	-ibhn		-(1-yh)/(2.86.yh)			(1-yh)/(2.86.yh)	(-ibhn/14)+((1-yh)/14.2.86.yh))			
3	r3	1						-1/yh			-ibhn		-(1-yh)/yh		-ibhn/14			
4	r4	1						-1/yh			-ibhn-(1-yh)/(2.86.yh)			(1-yh)/(2.86.yh)	(-ibhn/14)+((1-yh)/14.2.86.yh))			
5	r5	-1		fuh	1-fuh		ibhn-fuh.iuhn											
6	r6				-1			1										
7	r7						-1			1								
8	r8								1	-1					1/14			
9	r9								-ibhn-1/ya		1/ya		-(4.57-ya)/ya		(-ibhn/14)-1/(ya.7)			
10	r10		1	fua	1-fua		ibhn-fua.iuhn											
11	r11		-1														0	0
12	r12																	0
13	r13	1											-(1-yh)/yh					0
14	r14																	
15	r15																	
16	r16																	
17	r17																	
18	r18																	
19	r19																	
20	r20																	
21	r21																	
22	r22																	
23	r23																	
24	r24																	
25	r25																	
26	r26																	

18	19	20	21	22	23	24	25	26	27	28				
NPEO		SMX			Ibuprofen (Ionized compound)			BPA (Neutral compound)		Compi		Process rate equations:		Units
Szc	Szd	Szf	Szg	Xza	Szh	Xzb	Szi	Xzc	Szj	Xzd				
g/m ³	g/m ³	g/m ³	g/m ³	g/m ³	g/m ³	g/m ₃	g/m ₃	g/m ³	g/m ³	g/m ³				
											aerobic growth of heterotrophs on soluble substrate with ammonia as N source	muh.MssHET.MsoHET.MsnhGEN.salksatHET.xbh	gCOD/m3/d	
											anoxic growth of heterotrophs on soluble substrate with ammonia as N source	etah.muh.MssHET.inhibsoaxHET.MsnoHET.MsnhGEN.salksatHET.xbh	gCOD/m3/d	
											aerobic growth of heterotrophs on soluble substrate with nitrate as N source	muh.MssHET.MsoHET.inhibsnhHET.MsnoHET.salksatHET.xbh	gCOD/m3/d	
											anoxic growth of heterotrophs soluble substrate with nitrate as N source	etah.muh.MssHET.inhibsoaxHET.inhibsnhHET.MsnoHET.salksatHET.xbh	gCOD/m3/d	
											decay of heterotrophs	bh.xbh	gCOD/m3/d	
											hydrolysis of entrapped organics	kh.(subsatHET).(MsoHET + etah.inhibsoo2HET.MsnoHET).xbh	gCOD/m3/d	
											hydrolysis of entrapped organic nitrogen	r6.(xnd/(xs))	gCOD/m3/d	
											ammonification of soluble organic nitrogen	ka.snd.xbh	gN/m3/d	
											growth of autotrophs	mua.MsnhGEN.MsnhNIT.MsoNIT.salksatAUT.xba	gCOD/m3/d	
											decay of autotrophs	ba.xba	gCOD/m3/d	
0	0										abiotic oxidative cleavage	K _{OCL} .Sza	gCOD/m3/d	
0											hydrolysis of Sza	K _{hNPEO} .(Szc/xbh/(K _{xNPEO} +Szc/xbh)).xbh	gCOD/m3/d	
											growth on Szb	K _{bioNPEO} .Szb.(Ks)/(Ks+ss).so/(Koh+so).xbh	g/m3/d	
		-1									aerobic biotransformation of Szf	K _{1BioOx} .Szf.(Ks.η _{bio})/(Ks.η _{bio} +ss).so/(Ko+so).xbh	g/m3/d	
		1	-1								aerobic parent compound formation	K _{1DecOx} .Szg.(Ks.η _{1Dec})/(Ks.η _{1Dec} +Ss).so/(Ko+so).xbh	g/m3/d	
		1		-1							aerobic desorption of Szf	K _{Des} .Szf. so/(Ko+so)	g/m3/d	
		-1		1							aerobic sorption of Szf	K _{Des} .K _{1DOx} .Szf.so/(Ko+so). X _{ss}	g/m3/d	
					0	0					sorption of neutral form of compound (HA)	K _{1BioAx} .Szf.(Ks.η _{bio})/(Ks.η _{bio} +Ss).Ko/(Ko+so).xbh	g/m3/d	
					0	0					Desorption of neutral form of compound (HA)	K _{1DecAx} .Szg.(Ks.η _{1Dec})/(Ks.η _{1Dec} +Ss).Ko/(Ko+so).xbh	g/m3/d	
					0						Biodegradation of neutral form of compound (HA)	K _{Des} .K _{1DAx} .Szf.Ko/(Ko+so). X _{ss}	g/m3/d	
							0	0			sorption of ionized form of compound (A ⁻)	K _{1des} .K _{D1} .Szh. X _{ss}	g/m3/d	
							0	0			Desorption of ionized form of compound (A ⁻)	K _{1des} .Xzb	g/m3/d	
							0				Biodegradation of ionized form of compound (A ⁻)	K _{bio1} .(Szh+Szi).xbh.so/(koh + so).(1/(10^(pH-pka)+1))	g/m3/d	
								0	0		sorption of neutral compound	K _{2des} .K _{D2} .Szi. X _{ss}	g/m3/d	
								0	0		Desorption of neutral compound	K _{2des} .Xzc	g/m3/d	
								0			Biodegradation of neutral compound	K _{bio2} .(Szh+Szi).xbh.so/(koh + so).(1/(10^(pka-pH)+1))	g/m3/d	

Appendix D1 Cont'd: Internal variables of Case Study 1

Internal variables:	Units	Description
<i>Aerobic Growth of Heterotrophs at DO Saturation</i>		
$r1_{sat} = \text{muh.MssHET.MsnhGEN.xbh}$	gCOD/m3/d	aerobic growth of heterotrophs at DO saturation
<i>Aerobic Growth of Autotrophs at DO Saturation</i>		
$r9_{sat} = \text{mua.MsnhGEN.MsnhNIT.xba}$	gCOD/m3/d	aerobic growth of autotrophs at DO saturation
<i>Actual Oxygen Uptake Rate (OUR)</i>		
$our = -r_{so}$	gO2/m3/d	actual oxygen uptake rate
<i>Maximal Oxygen Uptake Rate</i>		
$our_{max} = -(\text{coeffso}(1).\text{muh.MssHET.MsnhGEN.xbh} + \text{coeffso}(3).\text{muh.MssHET.inhibsnhHET.MsnoHET.xbh} + \text{coeffso}(9).\text{mua.MsnhGEN.MsnhNIT.xba})$	gO2/m3/d	maximal oxygen uptake rate (at DO saturation)
<i>Actual Nitrogen Utilization Rate (NUR)</i>		
$nur = -(\text{coeffsnh}(9).r9)$	gN/m3/d	actual nitrogen utilization rate
<i>Maximal Nitrogen Utilization Rate</i>		
$nur_{max} = -(\text{coeffsnh}(9).\text{mua.MsnhGEN.MsnhNIT.xba})$	gN/m3/d	maximal nitrogen utilization rate (at DO saturation)
<i>Denitrification Rate</i>		
$dnr = -(\text{coeffsno}(2).r2 + \text{coeffsno}(4).r4)$	gN/m3/d	denitrification rate
<i>Saturation and Inhibition Functions</i>		
$\text{MsnhGEN} = \text{snh}/(\text{snh} + \text{knh})$	-	ammonia (as nutrient) saturation function
$\text{subsathET} = ((\text{xs}/(\text{xbh})) / ((\text{xs}/(\text{xbh})) + \text{kx}))$	-	slowly biodegradable substrate saturation function for hydrolysis
$\text{MssHET} = \text{ss}/(\text{ss} + \text{ksh})$	-	readily biodegradable substrate saturation function for heterotrophs
$\text{MsoHET} = \text{so}/(\text{so} + \text{koh})$	-	oxygen saturation function for heterotrophs
$\text{MsnoHET} = \text{sno}/(\text{sno} + \text{kno})$	-	nitrate saturation function for heterotrophs
$\text{Inhibsoo2HET} = \text{koh}/(\text{so} + \text{koh})$	-	oxygen inhibition function for heterotrophs - anaerobic conditions
$\text{InhibsoaxHET} = \text{kad}/(\text{so} + \text{kad})$	-	oxygen inhibition function for heterotrophs - anoxic conditions
$\text{inhibsnhHET} = \text{knh}/(\text{snh} + \text{knh})$	-	ammonia (as nutrient) inhibition function
$\text{MsnhNIT} = \text{snh}/(\text{snh} + \text{kna})$	-	ammonia saturation function for autotrophs
$\text{MsoNIT} = \text{so}/(\text{so} + \text{koa})$	-	oxygen saturation function for autotrophs
$\text{salksatHET} = \text{salk}/(\text{kalk} + \text{salk})$	-	alkalinity saturation function for heterotrophs
$\text{salksatAUT} = \text{salk}/(\text{kalka} + \text{salk})$	-	alkalinity saturation function for autotrophs

Appendix E

Case Study 2 Matrix

Model : PPCP	I:	1	2	3	4	5	6	7	8	9	10	11	12	13	14	15	16	17
GPS-X library: cniplib	Stoichiometry matrix															NPEO		
j	Rates	xbh	xba	xu	xs	xi	xnd	ss	snh	snd	sno	si	so	snn	salk	xii	Sza	Szb
	Units:	gCOD	gCOD	gCOD	gCOD	gCOD	gN	gCOD	gN	gN	gN	gCOD	gCOD	gN	Mole HCO ₃	gCOD	g/m ³	g/m ³
1	r1	1						-1/yh	-ibhn				-(1-yh)/yh		-ibhn/14			
2	r2	1						-1/yh	-ibhn		-(1-yh)/(2.86.yh)			(1-yh)/(2.86.yh)	(-ibhn/14)+((1-yh)/14.2.86.yh))			
3	r3	1						-1/yh			-ibhn		-(1-yh)/yh		-ibhn/14			
4	r4	1						-1/yh			-ibhn-(1-yh)/(2.86.yh)			(1-yh)/(2.86.yh)	(-ibhn/14)+((1-yh)/14.2.86.yh))			
5	r5	-1		fuh	1-fuh		ibhn-fuh.iuhn											
6	r6				-1			1										
7	r7						-1			1								
8	r8								1	-1					1/14			
9	r9								-ibhn-1/ya		1/ya		-(4.57-ya)/ya		(-ibhn/14)-1/(ya.7)			
10	r10		1	fua	1-fua		ibhn-fua.iuhn											
11	r11		-1														-(1-f _{INPEO})	α
12	r12																	1
13	r13	1											-(1-yh)/yh					-1
14	r14																	
15	r15																	
16	r16																	
17	r17																	
18	r18																	
19	r19																	
20	r20																	
21	r21																	
22	r22																	
23	r23																	
24	r24																	
25	r25																	
26	r26																	

18	19	20	21	22	23	24	25	26	27	28			
NPEO		SMX			Ibuprofen (Ionized compound)				BPA (Neutral compound)		Compi	Process rate equations:	Units
Szc	Szd	Szf	Szg	Xza	Szh	Xzb	Szi	Xzc	Szj	Xzd			
g/m ³	g/m ³	g/m ³	g/m ³	g/m ³	g/m ³	g/m ³	g/m ³	g/m ³	g/m ³	g/m ³			
											aerobic growth of heterotrophs on soluble substrate with ammonia as N source	muh.MssHET.MsoHET.MsnhGEN.salksatHET.xbh	gCOD/m3/d
											anoxic growth of heterotrophs on soluble substrate with ammonia as N source	etah.muh.MssHET.inhibsoaxHET.MsnoHET.MsnhGEN.salksatHET.xbh	gCOD/m3/d
											aerobic growth of heterotrophs on soluble substrate with nitrate as N source	muh.MssHET.MsoHET.inhibsnhHET.MsnoHET.salksatHET.xbh	gCOD/m3/d
											anoxic growth of heterotrophs soluble substrate with nitrate as N source	etah.muh.MssHET.inhibsoaxHET.inhibsnhHET.MsnoHET.salksatHET.xbh	gCOD/m3/d
											decay of heterotrophs	bh.xbh	gCOD/m3/d
											hydrolysis of entrapped organics	kh. (subsathET).(MsoHET + etah.inhibsoo2HET.MsnoHET).xbh	gCOD/m3/d
											hydrolysis of entrapped organic nitrogen	r6.(xnd/(xs))	gCOD/m3/d
											ammonification of soluble organic nitrogen	ka.snd.xbh	gN/m3/d
											growth of autotrophs	mua.MsnhGEN.MsnhNIT.MsoNIT.salksatAUT.xba	gCOD/m3/d
											decay of autotrophs	ba.xba	gCOD/m3/d
1- α	f _{INPEO}										abiotic oxidative cleavage	K _{OCL} .Sza	gCOD/m3/d
-1											hydrolysis of Sza	K _{hNPEO} .(Szc/xbh/(K _{xNPEO} +Szc/xbh)).xbh	gCOD/m3/d
											growth on Szb	K _{bioNPEO} .Szb.(Ks)/(Ks+ss).so/(Koh+so).xbh	g/m3/d
		0									aerobic biotransformation of Szf	K _{1BioOx} .Szf.(Ks. η_{bio})/(Ks. η_{bio} +ss).so/(Ko+so).xbh	g/m3/d
		0	0								aerobic parent compound formation	K _{1DecOx} .Szg.(Ks. η_{1Dec})/(Ks. η_{1Dec} +Ss).so/(Ko+so).xbh	g/m3/d
		0		0							aerobic desorption of Szf	K _{Des} .Szf. so/(Ko+so)	g/m3/d
		0		0							anoxic desorption of Szf	K _{Des} .Szf . Ko/(Ko+so)	g/m3/d
		0		0							aerobic sorption of Szf	K _{Des} .K _{1DOx} .Szf.so/(Ko+so). X _{ss}	g/m3/d
		0									anoxic biotransformation of Szf	K _{1BioAx} .Szf.(Ks. η_{bio})/(Ks. η_{bio} +Ss).Ko/(Ko+so).xbh	g/m3/d
		0	0								anoxic parent compound formation	K _{1DecAx} .Szg.(Ks. η_{1Dec})/(Ks. η_{1Dec} +Ss).Ko/(Ko+so).xbh	g/m3/d
		0		0							anoxic sorption of Szf	K _{Des} .K _{1DAx} .Szf.Ko/(Ko+so). X _{ss}	g/m3/d
					0	0					sorption of neutral form of compound (HA)	K _{1des} .K _{D1} .Szh. X _{ss}	g/m3/d
					0	0					Desorption of neutral form of compound (HA)	K _{1des} .Xzb	g/m3/d
					0						Biodegradation of neutral form of compound (HA)	K _{bio1} .(Szh+Szi).xbh.so/(koh + so).(1/(10 ^{^(pH-pka)} +1))	g/m3/d
							0	0			sorption of ionized form of compound (A ⁻)	K _{2des} .K _{D2} .Szi. X _{ss}	g/m3/d
							0	0			Desorption of ionized form of compound (A ⁻)	K _{2des} .Xzc	g/m3/d
							0				Biodegradation of ionized form of compound (A ⁻)	K _{bio2} .(Szh+Szi).xbh.so/(koh + so).(1/(10 ^{^(pka-pH)} +1))	g/m3/d
									0	0	sorption of neutral compound	K _{des3} .K _{d3} .Szj. X _{ss}	g/m3/d
									0	0	Desorption of neutral compound	K _{des3} .Xzd	g/m3/d
									0		Biodegradation of neutral compound	K _{bio3} .Szj.xbh.so/(koh + so)	g/m3/d

Appendix F

Case Study 3 Matrix

Model : PPCP	I:	1	2	3	4	5	6	7	8	9	10	11	12	13	14	15	16	17
GPS-X library: cniplib	Stoichiometry matrix															NPEO		
j	Rates	xbh	xba	xu	xs	xi	xnd	ss	snh	snd	sno	si	so	snn	salk	xii	Sza	Szb
	Units:	gCOD	gCOD	gCOD	gCOD	gCOD	gN	gCO D	gN	gN	gN	gCOD	gCOD	gN	Mole HCO ₃	gCOD	g/m ³	g/m ³
1	r1	1						-1/yh	-ibhn				-(1-yh)/yh		-ibhn/14			
2	r2	1						-1/yh	-ibhn		-(1-yh)/(2.86.yh)			(1-yh)/(2.86.yh)	(-ibhn/14)+((1-yh)/14.2.86.yh))			
3	r3	1						-1/yh			-ibhn		-(1-yh)/yh		-ibhn/14			
4	r4	1						-1/yh			-ibhn-(1-yh)/(2.86.yh)			(1-yh)/(2.86.yh)	(-ibhn/14)+((1-yh)/14.2.86.yh))			
5	r5	-1		fuh	1-fuh		ibhn-fuh.iuhn											
6	r6				-1			1										
7	r7						-1			1								
8	r8								1	-1					1/14			
9	r9								-ibhn-1/ya		1/ya		-(4.57-ya)/ya		(-ibhn/14)-1/(ya.7)			
10	r10		1	fua	1-fua		ibhn-fua.iuhn											
11	r11		-1														0	0
12	r12																	0
13	r13	1											-(1-yh)/yh					0
14	r14																	
15	r15																	
16	r16																	
17	r17																	
18	r18																	
19	r19																	
20	r20																	
21	r21																	
22	r22																	
23	r23																	
24	r24																	
25	r25																	
26	r26																	

18	19	20	21	22	23	24	25	26	27	28					
NPEO		SMX			Ibuprofen (Ionized compound)				BPA (Neutral compound)		Compi		Process rate equations:		Units
Szc	Szd	Szf	Szg	Xza	Szh	Xzb	Szi	Xzc	Szj	Xzd					
g/m ³	g/m ³	g/m ³	g/m ³	g/m ³	g/m ³	g/m ³	g/m ³	g/m ³	g/m ³	g/m ³					
											aerobic growth of heterotrophs on soluble substrate with ammonia as N source	muh.MssHET.MsoHET.MsnhGEN.salksatHET.xbh	gCOD/m3/d		
											anoxic growth of heterotrophs on soluble substrate with ammonia as N source	etah.muh.MssHET.inhibsoaxHET.MsnoHET.MsnhGEN.salksatHET.xbh	gCOD/m3/d		
											aerobic growth of heterotrophs on soluble substrate with nitrate as N source	muh.MssHET.MsoHET.inhibsnhHET.MsnoHET.salksatHET.xbh	gCOD/m3/d		
											anoxic growth of heterotrophs soluble substrate with nitrate as N source	etah.muh.MssHET.inhibsoaxHET.inhibsnhHET.MsnoHET.salksatHET.xbh	gCOD/m3/d		
											decay of heterotrophs	bh.xbh	gCOD/m3/d		
											hydrolysis of entrapped organics	kh.(subsatHET).(MsoHET + etah.inhibsoo2HET.MsnoHET).xbh	gCOD/m3/d		
											hydrolysis of entrapped organic nitrogen	r6.(xnd/(xs))	gCOD/m3/d		
											ammonification of soluble organic nitrogen	ka.snd.xbh	gN/m3/d		
											growth of autotrophs	mua.MsnhGEN.MsnhNIT.MsoNIT.salksatAUT.xba	gCOD/m3/d		
											decay of autotrophs	ba.xba	gCOD/m3/d		
0	0										abiotic oxidative cleavage	K _{OCL} .Sza	gCOD/m3/d		
0											hydrolysis of Sza	K _{hNPEO} .(Szc/xbh/(K _{xNPEO} +Szc/xbh)).xbh	gCOD/m3/d		
											growth on Szb	K _{bioNPEO} .Szb.(Ks)/(Ks+ss).so/(Koh+so).xbh	g/m3/d		
		0									aerobic biotransformation of Szf	K _{1BioOx} .Szf.(Ks.η _{bio})/(Ks.η _{bio} +ss).so/(Ko+so).xbh	g/m3/d		
		0	0								aerobic parent compound formation	K _{1DecOx} .Szg.(Ks.η _{1Dec})/(Ks.η _{1Dec} +Ss).so/(Ko+so).xbh	g/m3/d		
		0		0							aerobic desorption of Szf	K _{Des} .Szf. so/(Ko+so)	g/m3/d		
		0		0							anoxic desorption of Szf	K _{Des} .Szf . Ko/(Ko+so)	g/m3/d		
		0		0							aerobic sorption of Szf	K _{Des} .K _{1DOx} .Szf.so/(Ko+so). X _{ss}	g/m3/d		
		0									anoxic biotransformation of Szf	K _{1BioAx} .Szf.(Ks.η _{bio})/(Ks.η _{bio} +Ss).Ko/(Ko+so).xbh	g/m3/d		
		0	0								anoxic parent compound formation	K _{1DecAx} .Szg.(Ks.η _{1Dec})/(Ks.η _{1Dec} +Ss).Ko/(Ko+so).xbh	g/m3/d		
		0		0							anoxic sorption of Szf	K _{Des} .K _{1DAX} .Szf.Ko/(Ko+so). X _{ss}	g/m3/d		
					-1	1					sorption of neutral form of compound (HA)	K _{1des} .K _{D1} .Szh. X _{ss}	g/m3/d		
					1	-1					Desorption of neutral form of compound (HA)	K _{1des} .Xzb	g/m3/d		
					-1						Biodegradation of neutral form of compound (HA)	K _{bio1} .(Szh+Szi).xbh.so/(koh + so).(1/(10^(pH-pka)+1))	g/m3/d		
							-1	1			sorption of ionized form of compound (A ⁻)	K _{2des} .K _{D2} .Szi. X _{ss}	g/m3/d		
							1	-1			Desorption of ionized form of compound (A ⁻)	K _{2des} .Xzc	g/m3/d		
							-1				Biodegradation of ionized form of compound (A ⁻)	K _{bio2} .(Szh+Szi).xbh.so/(koh + so).(1/(10^(pka-pH)+1))	g/m3/d		
									-1	1	sorption of neutral compound	K _{des3} .K _{d3} .Szj. X _{ss}	g/m3/d		
									1	-1	Desorption of neutral compound	K _{des3} .Xzd	g/m3/d		
									-1		Biodegradation of neutral compound	K _{bio3} .Szj.xbh.so/(koh + so)	g/m3/d		

Appendix G

Different XOCs along with Major References Including Some Parameter Variables and Experimental data

Different XOCs along with major references including some parameter variables and experimental data, [40]

Compound	Remarks and Major References
Antibiotics	
Ampicilin (AMP)	Li and Zhang 2010 (K_H , data)
Cefalexin (CLX)	Li and Zhang 2010 (K_H , K_{bio} , data)
Sulfamethoxazole (SMX)	Li and Zhang 2010 (K_H , K_{bio} , data), Suarez et al. 2010 (K_H , K_d), Plosz et al. 2009 (K_{bio} , K_d , data), Suarez et al. 2008 (K_H , K_d , K_{bio})
Sulfadiazine (SDZ)	Li and Zhang 2010 (K_H , K_{bio} , data)
Norfloxacin (NOR)	Li and Zhang 2010 (K_H , K_{bio} , data), Siegrist et al. 2005 (K_d , K_{bio})
Ciprofloxacin (CIP)	Li and Zhang 2010 (K_H , K_{bio} , data), Plosz et al. 2009 (K_{bio} , K_d , data)
Ofloxacin (OFL)	Li and Zhang 2010 (K_H , K_{bio} , data)
Tetracycline (TC)	Li and Zhang 2010 (K_H , data), Plosz et al. 2009 (K_{bio} , K_d , data)
Roxithromycin (ROX)	Li and Zhang 2010 (K_H , data), Suarez et al. 2010 (K_H , K_d), Joss et al. 2006 (K_{bio}), Suarez et al. 2008 (K_H , K_d , K_{bio})
Erythromycin (ERY)	Li and Zhang 2010 (K_H , data), Suarez et al. 2010 (K_H , K_d), Suarez et al. 2008 (K_H , K_d , K_{bio})

Azithromycin	Joss et al. 2006 (K_{bio} , K_d)
Clarithromycin	Joss et al. 2006 (K_{bio} , K_d , data)
(Anhydro-) erythromycin	Joss et al. 2006 (K_{bio} , K_d)
N ⁴ -acetyl-sulfamethoxazole	Joss et al. 2006 (K_{bio} , data)
Contrast agent	
Trimethoprim (TMP)	Li and Zhang 2010 (K_H , data), Suarez et al. 2010 (K_H , K_d), Suarez et al. 2008 (K_H , K_d)
Iopromide (IPM)	Joss et al. 2006 (K_{bio} , K_d , data), Suarez et al. 2008 (K_H , K_d , K_{bio})
ATH	Joss et al. 2006 (K_{bio})
DAMI	Joss et al. 2006 (K_{bio})
Diatrizoate	Joss et al. 2006 (K_{bio} , data)
Iohexol	Joss et al. 2006 (K_{bio})
Iomeprol	Joss et al. 2006 (K_{bio})
Iopamidol	Joss et al. 2006 (K_{bio})
Iothalamic acid	Joss et al. 2006 (K_{bio})

Ioxithalamic acid	Joss et al. 2006 (K_{bio})
Lipid regulator	
Bezafibrate (BZF)	Joss et al. 2006 (K_{bio} , data), Clara et al. 2004 (K_{bio} , data)
Clofibrinic acid	Joss et al. 2006 (K_{bio} , K_d)
Fenofibrinic acid	Joss et al. 2006 (K_{bio})
Gemfibrozil	Joss et al. 2006 (K_{bio} , K_d , data)
Statin Pharmaceuticals	
Atorvastatin	Ottmar et al. 2010 (K_d , data)
Simvastatin acid	Ottmar et al. 2010 (K_d , data)
Hormones	
17 α -ethinylestradiol (EE2)	Suarez et al. 2010 (K_H , K_d), Clara et al. 2004 (K_{bio} , data), Monteith et al. 2009 (K_H , K_d , K_{bio}), Clouzot et al. 2010 (K_{bio} , K_d , data), Racz et al. 2009 (K_H , K_d , K_{bio} , data), Gaulke et al. 2009 (K_{bio}), Clark et al. 2009 (K_{bio} , data), Suarez et al. 2008 (K_H , K_d , K_{bio})
17 β -estradiol (E2)	Suarez et al. 2010 (K_H , K_d), Clara et al. 2004 (K_{bio} , data), Racz et al. 2009 (K_H , K_d , K_{bio} , data), Monteith et al. 2009 (K_H , K_d , K_{bio}), Gaulke et al. 2009 (K_{bio} , data), Siegrist et al. 2005 (K_d , K_{bio}), Suarez et al. 2008 (K_H , K_d , K_{bio})

Estrone (E1)	Clara et al. 2004 (K_{bio} , data), Racz et al. 2009 (K_H , K_d , K_{bio} , data), Monteith et al. 2009 (K_H , K_d , K_{bio}), Gaulke et al. 2009 (K_{bio} , data), Suarez et al. 2008 (K_H , K_d , K_{bio})
Estriol (E3)	Clara et al. 2004 (K_{bio} , data), Racz et al. 2009 (K_H , K_{bio} , data)
Anti-depressants	
Fluoxetine (FLX)	Suarez et al. 2010 (K_H , K_d), Suarez et al. 2008 (K_H)
Citalopram (CTL)	Suarez et al. 2008 (K_H)
Anti-inflamatoires	
Ibuprofen (IBP)	Suarez et al. 2010 (K_H , K_d), Joss et al. 2006 (K_{bio} , K_d , data), Clara et al. 2004 (K_{bio} , data), Suarez et al. 2008 (K_H , K_d , K_{bio})
Naproxen (NPX)	Suarez et al. 2010 (K_H , K_d), Joss et al. 2006 (K_{bio} , K_d), Suarez et al. 2008 (K_H , K_{bio})
Diclofenac (DCF)	Suarez et al. 2010 (K_H , K_d), Joss et al. 2006 (K_{bio} , K_d), Clara et al. 2004 (K_{bio} , data), Suarez et al. 2008 (K_H , K_d , K_{bio})
Fenoprofen	Joss et al. 2006 (K_{bio} , K_d)
Indomethacin	Joss et al. 2006 (K_{bio} , K_d)

Paracetamol	Joss et al. 2006 (K_{bio} , K_d , data)
Fragrances (Musks)	
Galaxolide (HHCB)	Suarez et al. 2010 (K_H , K_d), Suarez et al. 2008 (K_H , K_d , K_{bio})
Tonalide (AHTN)	Suarez et al. 2010 (K_H , K_d), Suarez et al. 2008 (K_H , K_d , K_{bio})
Celestolide (ADBI)	Suarez et al. 2010 (K_H , K_d), Suarez et al. 2008 (K_H , K_d)
Other XOCs	
Fluorene	Barret et al. 2010 (K_{part} , K_{DCM} , data)
Phenanthrene	Barret et al. 2010 (K_{part} , K_{DCM} , data)
Anthracene	Barret et al. 2010 (K_{part} , K_{DCM} , data)
Fluoranthene	Barret et al. 2010 (K_{part} , K_{DCM} , data)
Pyrene	Barret et al. 2010 (K_{part} , K_{DCM} , data)
Benzo(a)anthracene	Barret et al. 2010 (K_{part} , K_{DCM} , data)
Chrysene	Barret et al. 2010 (K_{part} , K_{DCM} , data)
Benzo(b)fluoranthene	Barret et al. 2010 (K_{part} , K_{DCM} , data)

Benzo(k)fluoranthene	Barret et al. 2010 (K_{part} , K_{DCM} , data)
Benzo(a)pyrene	Barret et al. 2010 (K_{part} , K_{DCM} , data)
Dibenzo(a,h)anthracene	Barret et al. 2010 (K_{part} , K_{DCM} , data)
Benzo(g,h,i)perylene	Barret et al. 2010 (K_{part} , K_{DCM} , data)
Indeno(1,2,3,c,d)pyrene	Barret et al. 2010 (K_{part} , K_{DCM} , data)
Bisphenol-A (BPA)	Lindblom et al. 2009 (K_H , K_d , K_{bio} , data), Clara et al. 2004 (K_{bio} , data), Siegrist et al. 2005 (K_d , K_{bio})
Carbamazepine (CBZ)	Suarez et al. 2010 (K_H , K_d), Clara et al. 2004 (K_{bio} , data), Suarez et al. 2008 (K_H , K_d , K_{bio})
Diazepam (DZP)	Suarez et al. 2010 (K_H , K_d), Suarez et al. 2008 (K_H , K_d , K_{bio})
Piracetam	Joss et al. 2006 (K_{bio})
Nonylphenol ethoxylate (NPEO's)	Karahan et al. 2010(K_d , K_{bio} , data)

Appendix H

Degradation Rate Constant K_{bio} Observed in Batch Experiments with Activated Sludge

Degradation rate constant K_{bio} observed in batch experiments with activated sludge from nutrient removing wastewater treatment in municipal plants. The range indicates the 95% confidence interval obtained from two batch experiments (12 samples, taken over 48 hours). The sign ' \leq ' indicates that the lower limit was beyond experimental resolution. CAS: full-scale conventional activated sludge process, [17].

Group	Compound	K_{bio} for CAS LgSS⁻¹d⁻¹
Antibiotics	Azithromycin	≤ 0.1
	Clarithromycin	≤ 0.4
	(Anhydro-)erythromycin	≤ 0.1
	N ⁴ -Ac-sulfamethoxazole	5.9-6.7
	Roxithromycin	≤ 0.2
Antiphlogistics	Diclofenac	≤ 0.1
	Fenoprofen	10-14
	Ibuprofen	21-35
	Indomethacin	≤ 0.3
	Naproxen	1.0-1.9
	Paracetamol	58-80
Contrast Media	ATH	1.3-1.9
	DAMI	1.9-4.9
	Diatrizoate	≤ 0.1
	Iohexol	1.8-2.4
	Iomeprol	1.2-1.6
	Iopmidol	≤ 0.36
	Iopromide	1.6-2.5
	Iothalamic acid	≤ 0.24
Ioxithalamic acid	0.2-0.7	
Lipid regulators	Bezafibrate	2.1-3.0
	Clofibric acid	0.3-0.8
	Fenofibric acid	7.2-10.8
	Gemfibrozil	6.4-9.6
Nootropic	Piracetam	2.5-4.3

Appendix I

The Process Variables and The Compound Parameters for Case Study 1

Mantis model variables and parameters		Initial value in act. sludge	
COMPONENTS			
Inorganic Suspended Solids			
xii	inert inorganic suspended solids	41	g / m ³
Organic Variables			
si	soluble inert organic material	35	g COD / m ³
ss	readily biodegradable substrate	152	g COD / m ³
xi	particulate inert organic material	58	g COD / m ³
xs	slowly biodegradable substrate	163	g COD / m ³
xbh	active heterotrophic biomass	0	g COD / m ³
xba	active autotrophic biomass	0	g COD / m ³
xu	unbiodegradable particulate matter from cell decay	0	g COD / m ³
Dissolved Oxygen			
so	dissolved oxygen		g O ₂ / m ³
Nitrogen compounds			
snh	free and ionized ammonia	23.45	g N / m ³
snd	soluble biodegradable organic nitrogen	3	g N / m ³
xnd	particulate biodegradable organic nitrogen	9.27	g N / m ³
sno	nitrate and nitrite nitrogen	0	g N / m ³
snn	dissolved dinitrogen	0	g N / m ³
Alkalinity			
salk	alkalinity	7	mole / m ³
COMPOSITE VARIABLES			
Organic Matter (COD, BOD, TSS)			

scod	filtered COD	187	gCOD/m ³
xcod	particulate COD	221	gCOD/m ³
cod	total COD	408	gCOD/m ³
sbod	filtered carbonaceous BOD5	100.3	gO ₂ /m ³
xbod	particulate carbonaceous BOD5	107.6	gO ₂ /m ³
bod	total carbonaceous BOD5	207.9	gO ₂ /m ³
sbodu	filtered ultimate carbonaceous BOD	152	gO ₂ /m ³
xbodu	particulate ultimate carbonaceous BOD	163	gO ₂ /m ³
bodu	total ultimate carbonaceous BOD	315	gO ₂ /m ³
vss	volatile suspended solids	122.8	g/m ³
x	total suspended solids	163.8	g/m ³
Inorganic Matter			
xiss	inert inorganic suspended solids	41	g/m ³
Nitrogen compounds			
stkn	filtered TKN	26.5	gN/m ³
xtn	particulate TKN	13.2	gN/m ³
tn	total TKN	39.7	gN/m ³
tn	total nitrogen	39.7	gN/m ³
SMX compounds			
Szf	concentration of dissolved SMX parent compound	0.00021	g / m3
Szg	concentration of substance, biotransformed via the SMX parent compound	0.000467	g / m3
Xza	concentration of SMX parent	0	g / m3

	compound in solid phase		
Stoichiometric and kinetic parameters		at 20°C	Unit
Composite Variable Stoichiometry			
Organic Fractions			
icv	XCOD/VSS	1.48	gCOD/gVSS
fbod	BOD5/BODultimate ratio	0.66	-
Nutrient Fractions			
ibhn	N content of active biomass	0.068	g N / g COD
iuhn	N content of endogenous/inert mass	0.068	g N / g COD
Model Stoichiometry			
Active Heterotrophic Biomass			
yh	heterotrophic yield	0.666	gCOD/gCOD
fuh	heterotrophic endogenous fraction	0.08	gCOD/gCOD
Active Autotrophic Biomass			
ya	autotrophic yield	0.24	g COD/ g N
fua	autotrophic endogenous fraction	0.080	gCOD/gCOD
Kinetic			
muh	heterotrophic maximum specific growth rate	3.2	1/d
ksh	readily biodegradable substrate half saturation coefficient	5.00	gCOD/m ³
K _{Des}	desorption rate coefficient for SMX	0.1	1/d
K _{1DOx}	SMX aerobic solid-liquid sorption coefficient	2.914E-4	m ³ /gbiomass
K _{1DecOx}	SMX aerobic biotransformation rate coefficient	3.312E-2	m ³ /gbiomass/d
η _{1Dec}	SMX Correction factor for Ss inhibition on CLI formation	1.920	
K _{1BioOx}	SMX aerobic biotransformation rate for CLI	1.529E-3	m ³ /gbiomass/d
η _{bio}	correction factor for Ss inhibition on CLI biodegradation	2.886	
K _{1DAx}	SMX anoxic solid-liquid sorption coefficient	5.5E-4	m ³ /gbiomass
K _{1DecAx}	SMX anoxic biotransformation rate coefficient	3.823 E-2	m ³ /gbiomass/d
K _{1BioAx}	SMX anoxic biotransformation rate for CLI	1.529E-3	m ³ /gbiomass/d
K _s	half-saturation coefficient for Ss	10	g/m ³
koh	aerobic oxygen half saturation coefficient	0.2	gO ₂ /m ³
kad	anoxic oxygen half saturation coefficient	0.2	gO ₂ /m ³
etag	anoxic growth factor	0.50	-
kno	nitrate half saturation coefficient	0.100	gN/m ³
knh	ammonia (as nutrient) half saturation coefficient	0.05	gN/m ³
bh	heterotrophic decay rate	0.62	1/d

kalk	alkalinity half saturation coefficient	0.10	mole / m ³
mua	autotrophic maximum specific growth rate	0.90	1/d
kna	ammonia (as substrate) half saturation coefficient	0.70	gN/m ³
koa	oxygen half saturation coefficient	0.25	gO ₂ /m ³
ba	autotrophic decay rate	0.17	1/d
kalka	alkalinity half saturation coefficient for autotrophic growth	0.50	mole / m ³
Hydrolysis			
kh	maximum specific hydrolysis rate	3.00	1/d
kx	slowly biodegradable substrate half saturation coefficient	0.10	gCOD/gCOD
etah	anoxic hydrolysis factor	0.60	-
Ammonification			
ka	ammonification rate	0.080	m ³ /g COD/d

Appendix J

The Process Variables and The Compound Parameters for Case Study 2

Mantis model variables and parameters			
COMPONENTS			
Inorganic Suspended Solids		Initial value in act. sludge	Units
xii	inert inorganic suspended solids	69.4	g / m ³
Organic Variables			
si	soluble inert organic material	25	g COD / m ³
ss	readily biodegradable substrate	100	g COD / m ³
xi	particulate inert organic material	65	g COD / m ³
xs	slowly biodegradable substrate	310	g COD / m ³
xbh	active heterotrophic biomass	0	g COD / m ³
xba	active autotrophic biomass	0	g COD / m ³
xu	unbiodegradable particulate matter from cell decay	0	g COD / m ³
Dissolved Oxygen			
so	dissolved oxygen	0	g O ₂ / m ³
Nitrogen compounds			
snh	free and ionized ammonia	10	g N / m ³
snd	soluble biodegradable organic nitrogen	1.11	g N / m ³
xnd	particulate biodegradable organic nitrogen	24.5	g N / m ³
sno	nitrate and nitrite nitrogen	0	g N / m ³
snn	dissolved dinitrogen	0	g N / m ³
Alkalinity			
salk	alkalinity	7	mole / m ³
COMPOSITE VARIABLES			
Organic Matter (COD, BOD, TSS)			
scod	filtered COD	125	gCOD/m ³
xcod	particulate COD	204.5	gCOD/m ³
cod	total COD	500	gCOD/m ³
sbod	filtered carbonaceous BOD5	66	gO ₂ /m ³
xbod	particulate carbonaceous BOD5	204.6	gO ₂ /m ³
bod	total carbonaceous BOD5	270.6	gO ₂ /m ³
sbodu	filtered ultimate carbonaceous BOD	100	gO ₂ /m ³
xbodu	particulate ultimate carbonaceous BOD	310	gO ₂ /m ³
bodu	total ultimate carbonaceous BOD	410	gO ₂ /m ³
vss	volatile suspended solids	208.3	g/m ³
x	total suspended solids	277.8	g/m ³
Inorganic Matter			
xiss	inert inorganic suspended solids	69.4	g/m ³

Nitrogen compounds			
stkn	filtered TKN	11.1	gN/m ³
xtkn	particulate TKN	28.9	gN/m ³
tkn	total TKN	40	gN/m ³
tn	total nitrogen	40	gN/m ³
NPEO compounds			
Sza (C _{NPEO})	NPEO concentration in bulk liquid	114	g / m ³
Szb (SS _{NPEO})	readily biodegradable substrate of NPEO	0	g / m ³
Szc (SH _{NPEO})	slowly biodegradable portion of NPEO	0	g / m ³
Szd (SI _{NPEO})	non biodegradable portion of NPEO	0	g / m ³
Stoichiometric and kinetic parameters			Unit
Composite Variable Stoichiometry		at 20°C	
Organic Fractions			
icv	XCOD/VSS	1.48	gCOD/gVSS
fbod	BOD5/BODultimate ratio	0.66	-
Nutrient Fractions			
ibhn	N content of active biomass	0.068	g N / g COD
ihhn	N content of endogenous/inert mass	0.068	g N / g COD
Model Stoichiometry			
Active Heterotrophic Biomass			
yh	heterotrophic yield	0.666	gCOD/gCOD
fuh	heterotrophic endogenous fraction	0.08	gCOD/gCOD
Active Autotrophic Biomass			
ya	autotrophic yield	0.24	g COD/ g N
fua	autotrophic endogenous fraction	0.080	gCOD/gCOD
Kinetic			
muh	heterotrophic maximum specific growth rate	3.2	1/d
ksh	readily biodegradable substrate half saturation coefficient	5.00	gCOD/m ³
muh _{NPEO}	rate of heterotrophic growth on NPEO	4.3	1/d
k _{sNPEO}	half saturation coefficient for NPEO	25.0	gCOD/m ³
k _{bioNPEO}		0.2168±0.095	m ³ /gbiomass/d
koh	aerobic oxygen half saturation coefficient	0.2	gO ₂ /m ³
kad	anoxic oxygen half saturation coefficient	0.2	gO ₂ /m ³
etag	anoxic growth factor	0.50	-
kno	nitrate half saturation coefficient	0.100	gN/m ³
knh	ammonia (as nutrient) half saturation coefficient	0.05	gN/m ³
bh	heterotrophic decay rate	0.62	1/d
kalk	alkalinity half saturation coefficient	0.10	mole / m ³
mua	autotrophic maximum specific growth rate	0.90	1/d
kna	ammonia (as substrate) half saturation coefficient	0.70	gN/m ³

koa	oxygen half saturation coefficient	0.25	gO ₂ /m ³
ba	autotrophic decay rate	0.17	1/d
kalka	alkalinity half saturation coefficient for autotrophic growth	0.50	mole / m ³
Hydrolysis			
kh	maximum specific hydrolysis rate	3.00	1/d
K _x	slowly biodegradable substrate half saturation coefficient	0.10	gCOD/gCOD
K _{hNPEO}	hydrolysis rate coefficient of NPEO	1.3	1/d
K _{xNPEO}	half saturation coefficient for the hydrolysis of NPEO	0.0200	gCOD/gCOD
f _{iNPEO}	non-biodegradable fraction of NPEO	0.2	gCOD/gCOD
α	readily biodegradable fraction of NPEO produced through adsorption/oxidative cleavage	0.2	gCOD/gCOD
K _{OCL}	first-order adsorption/oxidative cleavage coefficient	250.0	1/d
f _{es}	fraction of metabolic products	0.2	gCOD/gCOD
etah	anoxic hydrolysis factor	0.60	-
Ammonification			
ka	ammonification rate	0.080	m ³ /g COD/d

Appendix K

The Process Variables and The Compound Parameters for Case Study 3

Mantis model variables and parameters		Initial value in act. sludge	
COMPONENTS			
Inorganic Suspended Solids			
xii	inert inorganic suspended solids	59.7	g / m ³
Organic Variables			
si	soluble inert organic material	21.5	g COD / m ³
ss	readily biodegradable substrate	86	g COD / m ³
xi	particulate inert organic material	55.9	g COD / m ³
xs	slowly biodegradable substrate	266.6	g COD / m ³
xbh	active heterotrophic biomass	0	g COD / m ³
xba	active autotrophic biomass	0	g COD / m ³
xu	unbiodegradable particulate matter from cell decay	0	g COD / m ³
Dissolved Oxygen			
so	dissolved oxygen		g O ₂ / m ³
Nitrogen compounds			
snh	free and ionized ammonia	10	g N / m ³
snd	soluble biodegradable organic nitrogen	1.11	g N / m ³
xnd	particulate biodegradable organic nitrogen	25.1	g N / m ³
sno	nitrate and nitrite nitrogen	0	g N / m ³
snn	dissolved dinitrogen	0	g N / m ³
Alkalinity			
salk	alkalinity	7	mole / m ³
COMPOSITE VARIABLES			
Organic Matter (COD, BOD, TSS)			
scod	filtered COD	107.5	gCOD/m ³
xcod	particulate COD	322.5	gCOD/m ³
cod	total COD	430	gCOD/m ³

sbod	filtered carbonaceous BOD5	56.8	gO_2/m^3
xbod	particulate carbonaceous BOD5	176	gO_2/m^3
bod	total carbonaceous BOD5	232.7	gO_2/m^3
sbodu	filtered ultimate carbonaceous BOD	86	gO_2/m^3
xbodu	particulate ultimate carbonaceous BOD	266.6	gO_2/m^3
boddu	total ultimate carbonaceous BOD	352.6	gO_2/m^3
vss	volatile suspended solids	179.2	g/m^3
x	total suspended solids	239.9	g/m^3
Inorganic Matter			
xiss	inert inorganic suspended solids	59.7	g/m^3
Nitrogen compounds			
stkn	filtered TKN	11.1	gN/m^3
xtkn	particulate TKN	28.9	gN/m^3
tkn	total TKN	40	gN/m^3
tn	total nitrogen	40	gN/m^3
Neutral and ionized compounds			
Szh	concentration of neutral dissolved Ibuprofen	0.024	g / m^3
Szi	concentration of ionized Ibuprofen	4.3673	g / m^3
Xzb	concentration of neutral particulate Ibuprofen	0	g / m^3
Xzc	concentration of ionized particulate Ibuprofen	0	g / m^3
Szj	concentration of neutral dissolved Bisphenol-A	0.024	g / m^3
Xzd	concentration of neutral particulate Bisphenol-A	0	g / m^3
Stoichiometric and kinetic parameters		at 20°C	Unit
Composite Variable Stoichiometry			
Organic Fractions			

icv	XCOD/VSS	1.8	gCOD/gVSS
fbod	BOD5/BODultimate ratio	0.66	-
Nutrient Fractions			
ibhn	N content of active biomass	0.068	g N / g COD
iuhn	N content of endogenous/inert mass	0.068	g N / g COD
Model Stoichiometry			
Active Heterotrophic Biomass			
Yh	heterotrophic yield	0.666	gCOD/gCOD
fuh	heterotrophic endogenous fraction	0.08	gCOD/gCOD
Active Autotrophic Biomass			
ya	autotrophic yield	0.24	g COD/ g N
fua	autotrophic endogenous fraction	0.080	gCOD/gCOD
Kinetic			
muh	heterotrophic maximum specific growth rate	3.2	1/d
ksh	readily biodegradable substrate half saturation coefficient	5.00	gCOD/m ³
K _{bio1} , K _{bio2}	Biodegradation coefficient for neutral and ionized form of compound	0.1943	m ³ /gbiomass/d
K _{D1}	sorption partition coefficient for neutral form	3.23E-4	m ³ /gbiomass
K _{D2}	sorption partition coefficient for ionized form	1.96E-5	
K _{1des}	desorption rate coefficient for neutral form	0.1	1/d
K _{2des}	desorption rate coefficient for ionized form	0.1	1/d
pH		7	
pKa		4.74	
K _{bio3}	Biodegradation coefficient for Bisphenol A	0.0502	m ³ /gbiomass/d
K _{3des}	desorption rate coefficient for neutral compound (Bisphenol-A)	0.1	m ³ /d
K _{D3}	neutral (Bisphenol A) partitioning coefficient	4.935E-4	m ³ /gbiomass
K _s	half-saturation coefficient for S _s	10	g/m ³
koh	aerobic oxygen half saturation coefficient	0.2	gO ₂ /m ³

kad	anoxic oxygen half saturation coefficient	0.2	gO ₂ /m ³
etag	anoxic growth factor	0.50	-
kno	nitrate half saturation coefficient	0.100	gN/m ³
knh	ammonia (as nutrient) half saturation coefficient	0.05	gN/m ³
bh	heterotrophic decay rate	0.62	1/d
kalk	alkalinity half saturation coefficient	0.10	mole / m ³
mua	autotrophic maximum specific growth rate	0.90	1/d
kna	ammonia (as substrate) half saturation coefficient	0.70	gN/m ³
koa	oxygen half saturation coefficient	0.25	gO ₂ /m ³
ba	autotrophic decay rate	0.17	1/d
kalka	alkalinity half saturation coefficient for autotrophic growth	0.50	mole / m ³
Hydrolysis			
kh	maximum specific hydrolysis rate	3.00	1/d
kx	slowly biodegradable substrate half saturation coefficient	0.10	gCOD/gCOD
etah	anoxic hydrolysis factor	0.60	-
Ammonification			
ka	ammonification rate	0.080	m ³ /g COD/d

Appendix L

Types of Libraries within The GPS-X

Six libraries are available for GPS-X:

- Carbon – Nitrogen (CNLIB)
- Carbon – Nitrogen – Industrial Pollutant (CNIPLIB)
- Carbon – Nitrogen – Phosphorus (CNIPLIB)
- Carbon – Nitrogen – Phosphorous – Industrial Pollutant (CNIPLIB)
- Advanced – Carbon – Nitrogen (CN2LIB)
- Advanced – Carbon – Nitrogen – Industrial Pollutant (CN2IPLIB)

Table L1. Carbon – Nitrogen – Industrial Pollutant Library (CNIPLIB)			
No.	State Variable	GPS-X Symbols	Units
1	Soluble inert organics	si	gCOD/m ³
2	Readily biodegradable (soluble substrate)	ss	gCOD/m ³
3	Particulate inert organics	xi	gCOD/m ³
4	Slowly biodegradable (Stored, particulate) substrate	xs	gCOD/m ³
5	Active heterotrophic biomass	xbh	gCOD/m ³
6	Active autotrophic biomass	xba	gCOD/m ³
7	Unbiodegradable particulate from cell decay	xu	gCOD/m ³
8	Cell internal storage product	xsto	gCOD/m ³
9	Dissolved oxygen	so	gO ₂ /m ³
10	Nitrate and nitrite N	sno	gN/m ³
11	Free and ionized ammonia	snh	gN/m ³
12	Soluble biodegradable organic nitrogen (in ss)	snd	gN/m ³
13	Particulate biodegradable organic nitrogen (in xs)	xnd	gN/m ³
14	Dinitrogen	snn	gN/m ³
15	Alkalinity	salk	Mole/ m ³
16	Inert inorganic suspended solids	xii	g/m ³
17	Soluble component “a”	Sza	notset
18	Soluble component “b”	Szb	notset
19	Soluble component “c”	Szc	notset
20	Soluble component “d”	Szd	notset
21	Soluble component “e”	Sze	notset
22	Soluble component “f”	Szf	notset
23	Soluble component “g”	Szg	notset
24	Soluble component “h”	Szh	notset
25	Soluble component “i”	Szi	notset
26	Soluble component “j”	Szj	notset
27	Soluble component “k”	Szk	notset
28	Soluble component “l”	Szl	notset
29	Soluble component “m”	Szm	notset
30	Soluble component “n”	Szn	notset
31	Soluble component “o”	Szo	notset

32	Particulate component “a”	Xza	notset
33	Particulate component “b”	Xzb	notset
34	Particulate component “c”	Xzc	notset
35	Particulate component “d”	Xzd	notset
36	Particulate component “e”	Xze	notset
37	Particulate component “f”	Xzf	notset
38	Particulate component “g”	Xzg	notset
39	Particulate component “h”	Xzh	notset
40	Particulate component “i”	Xzi	notset
41	Particulate component “j”	Xzj	notset
42	Particulate component “k”	Xzk	notset
43	Particulate component “l”	Xzl	notset
44	Particulate component “m”	Xzm	notset
45	Particulate component “n”	Xzn	notset
46	Particulate component “o”	Xzo	notset

Table L2. Nomenclature for the Jacobsen et al. 1996 matrix model		
X_A	Active nonspecific biomass	ML^{-3}
X_I	Inactive, organic particulate matter	ML^{-3}
X_S	Degradable organic particulate matter	ML^{-3}
X_I	Active specific biomass for SOC degradation	ML^{-3}
X_{SI}	Sorbed form of specific compound	ML^{-3}
SI	Dissolved form of specific compound	ML^{-3}
S	Degradable dissolved primary substrate	ML^{-3}
S_{O_2}	Concentration of dissolved oxygen	ML^{-3}
k_{La}	Liquid-air transfer rate	T^{-1}
μ_m	Maximum specific biomass growth rate	T^{-1}
k_{S,X_A}	Half saturation constant for X_A	ML^{-3}
k_{hyd}	Specific hydrolysis rate	T^{-1}
k_x	Half saturation for in monod equation	ML^{-3}

b_{X_A}	Specific biomass loss rate for X_A	T^{-1}
$k_{S,X1,S}$	Half saturation constant for biomass X_1 degrading S	ML^{-3}
$k_{bio,m,S1}$	Maximum specific S1 biodegradation rate constant	$M_{S1}M_{X1} T^{-1}$
b_{X_1}	Specific biomass loss rate for X_1	T^{-1}
$S_{O2, sat}$	Saturation concentration of dissolved oxygen	ML^{-3}
$S_{O2, set}$	Set point concentration of dissolved oxygen	ML^{-3}
Y	Biomass growth yield coefficient	$M_X M_S^{-1}$
f_i	Fraction	